X-633-65-332

NASA TM X-55364

SOLAR SIMULATION RESEARCH

AUGUST 1965

NASA

GODDARD SPACE FLIGHT CENTER

GREENBELT, MARYLAND

X-633-65-332

SOLAR SIMULATION RESEARCH

Charles H. Duncan

John Flemming

Daniel Gallagher

William Gdula*

Danny Lester*

Malcolm Lillywhite*

Roy McIntosh*

James Murray*

Stanley Neuder

James J. Webb

RADIOMETRY GROUP

THERMAL SYSTEMS BRANCH

SPACECRAFT TECHNOLOGY DIVISION

AUGUST 1965

*Taag Designs, Inc. employee at GSFC - Contract No. NAS5-2382

SOLAR SIMULATION RESEARCH

ABSTRACT

Research oriented toward improvement of measurement techniques of solar simulators, support equipment, and solar cells has resulted in measurement accuracy capabilities as follows:

1. Spectral irradiance — ±10%
2. Total irradiance — ±2.5%
3. Uniformity and stability — ±0.5%
4. Spectral response (detectors, solar cells) — ±3.0%

Two solar simulators are in use which have the following characteristics:

	Spectrolab A-1200	Spectrolab X-25L
1. Total irradiance —	18-200 mw cm^{-2}	80-155 mw cm^{-2}
2. Uniformity (1cm.x1cm. detector)—	±10%	±1.7%
3. Stability (24 hour) —	±0.5%	±0.5%
4. Collimation (half angle) —	1-3/4°	2°
5. Spectrum —	Unfiltered xenon	Filtered xenon
6. Target volume —	48" dia x 96" depth	12" dia x 12" depth
7. Vacuum —	10^{-7} Torr	10^{-11} Torr
8. Thermal shroud —	LN_2 — 250°C	LN_2 — 250°C

Research to develop an improved source for solar simulators is conducted using an experimental pressure arc chamber and a vortex stabilized radiation source. Preliminary results using Argon indicate an advantage could be obtained by using equal numbers of xenon and argon lamps in a solar simulator in which each lamp illuminates the total volume.

CONTENTS

PREFACE

This volume represents some of the work which has been performed by the Radiometry Group of the Thermal Systems Branch. The work reported here was supported by NASA HQ Work Unit numbers 124-09-05-06 (Solar Simulation Studies) and 123-33-01-01 (Solar Cell Calibration Techniques). This volume is devoted primarily to work performed under the Solar Simulation Studies project. These papers were given at the Third NASA HQ Solar Simulation Conference held at GSFC on July 14 and 15, 1965 and will also appear in the Proceedings of that Conference.

SOLAR SIMULATION RESEARCH

by

Charles H. Duncan

Radiometry Group

Thermal Systems Branch

Spacecraft Technology Division

SOLAR SIMULATION RESEARCH

by

Charles H. Duncan

Radiometry Group

Thermal Systems Branch

Spacecraft Technology Division

ABSTRACT

The basic mission of the Group is defined as "certification, calibration, improvement, operation, and maintenance of solar simulators, simulator components, solar cells, and related instrumentation." Major facilities in the Group include: (1) Spectrolab A-1200 solar simulator; (2) Radiometry Research Simulator; (3) Pressure arc chamber; and (4) Vortex-stabilized-radiation-source. Measurements of spectral irradiance, spectral radiance, total intensity, uniformity of total irradiance, ultra-violet effects, and ozone effects are made by the Group. Plans for the future include the establishment of a Calibrations Laboratory to calibrate all equipment in terms of primary standards and the evaluation of an instrumentation to remeasure the air mass zero solar spectral irradiance to an absolute accuracy of ±10%.

SOLAR SIMULATION RESEARCH

I. MISSION

The Radiometry Group, formerly Solar Simulation Group, of the Thermal Systems Branch, Spacecraft Technology Division consists of twelve people whose basic mission can be defined as:

"Certification, calibration, improvement, operation, and maintenance of solar simulators, simulator components, solar cells, and related instrumentation."

The Group is funded by NASA HQ under two tasks: 124-09-05-06 (Solar Simulation Studies) and 123-33-01-01 (Solar Cell Calibration Techniques).

The Group has two solar simulators, the Spectrolab A-1200 and the Spectrolab X-25L; two experimental arc chambers; and, support instrumentation to measure spectral irradiances, total intensity, spectral response of detectors and solar cells, spectral transmission of filters, ozone, and ultra-violet irradiance effects on materials.

II. FACILITIES

(1) Spectrolab A-1200 Solar Simulator

This facility was tested and accepted at the contractor's plant on 6 August 1964. Final installation on site at GSFC was delayed because of the vacuum chamber installation by the Bethlehem Corporation, Easton, Penn. The vacuum chamber was completed on 3 December 1964 and the final installation by Spectrolab began on 8 December 1964. The installation was installed, checked for conformance to specifications and accepted on 18 December 1964. The beam diameter furnished was 120 cm diameter by 240 cm deep. The uniformity obtainable with a 10 cm x 10 cm array of solar cells was ±8% and with a 1 cm x 1 cm solar cell ±10%. The intensity obtainable was 140 mw cm^{-2} with eleven 2500 watt

Osram xenon lamps. All of the specifications were met or were exceeded at the initial installation. Two additional contracts have been let to Spectrolab to improve the uniformity and spectral distribution of the system.

(2) Radiometry Research Simulator

This facility consists of a General Electric ultra-high vacuum system and a Spectrolab X-25L solar simulator. The initial performance of both systems was within specifications. This facility which simulates outer space conditions to a high degree of accuracy will be used to calibrate detectors, solar cells, materials, and equipment which will be used either inside the large simulator or for satellite experiments. The present six inch diameter window of the vacuum system will be replaced by a twelve inch diameter window to allow the use of the full beam of the X-25L.

(3) Arc Facilities

(A) Pressure Science, Inc. Pressure Arc Chamber

This facility which is used for basic arc studies and lamp development has the capability of pressure ranges inside the chamber from 10^{-5} Torr to 5000 psig. The concentrations and ratios of six gases inside the chamber can be varied as desired. In addition, impurities can be introduced into the chamber. The electrode configuration can also be varied. The maximum power is limited by the power supply which is a Christie 6500 watt x-series type.

(B) Plasmadyne Vortex Stabilized Radiation Source

This facility is being used to determine the feasibility of these sources for solar simulators. The power capability is 25 KW, the pressure variations possible are 50 psig to 250 psig. The facility is equipped with a recirculating

device and can be used to study the effects of ratios and concentrations of four gases or less. Electrode lifetime has been a problem and some work is in progress to improve the design of the electrodes. This equipment was originally purchased to obtain some independent checks on the results published by Plasmadyne Corporation.

(C) Grant to American University

A grant of $12,000 for a six month effort has been made to American University and Dr. Alan D. Morris for work to determine the basic laws governing arc operation and performance. This Grant will be renewed for at least twelve additional months. This Grant was made to obtain theoretical support for the arc studies being performed by the Group. The Grant number is: NGR 09-003-007.

III. MEASUREMENTS

(1) Spectral Irradiance and Spectral Radiance

A Leiss double monochromator with an integrating sphere is used to measure spectral irradiances. When spectral radiances are measured the integrating sphere is removed. The integrating sphere used is four inches in diameter, has two openings 140° apart, the entrance port is one inch in diameter and the exit port is 1/8" wide x 1/2" long. The sphere is made of aluminum which is first coated with evaporated aluminum, then coated with MgO. The aluminum is evaporated under the MgO coating in order to reflect any radiation which may not be reflected by the MgO coating. The detectors used at the exit slit are: (1) RCA 1P-28 with S-5 response for the wavelength region 250 nm - 650 nm; (2) RCA 7102 with S-1 response for the wavelength region 500 nm - 1100 nm; and (3) Eastman Kodak Pbs detector for the wavelength region 700 nm - 2600 nm.

The signals are amplified with a Brower Laboratories, Inc.(Westboro, Massachusetts) Model 129 amplifier and are either recorded on a Photovolt strip chart recorder or magnetic tape. The data logging system to record the data onto magnetic tape was manufactured by Control Equipment Corporation of Needham Heights, Massachusetts. A computer program to process the data has been written. The program computes the spectral distribution on a point to point basis, the percent of the total energy between 250 nm and 2500 nm contained in 10 nm bandwidths from 250 nm to 1100 nm and 100 nm bandwidths from 1100 nm to 2500 nm. The deviations from the values for the air mass zero solar irradiance is computed for each of these bands. The air mass zero solar irradiance is also divided into 100 parts, each containing 1 percent of the solar energy between 250 nm and 2500 nm. The computer also calculates the percent of energy in each of these bands and the deviations from the solar irradiance. The spectral absorptivities of various materials can be incorporated into the program and a value is calculated for the absorptivity of the material using the spectral irradiance of the source measured.

Figure 1 is a typical plot obtained from the 10 nm and 100 nm percent of total energy calculations, Figure 2 is the deviations from air mass zero solar irradiance for these valves, and Figure 3 is the deviations per 1% energy bandwidths for the same source. The source was an Osram 2500 watt xenon lamp operated at 2720 watts (85 amps at 32 volts). Table I is a reproduction of the computer printout for the Osram lamp. Table II is a tabulation of the absorptivities of various materials obtained from the computer program. The valves of spectral absorptivity for gold, silver, and aluminum were taken from the AIP Handbook and the valves from the other materials were obtained from Jack Triolo, Head, Optical Measurements Group, Thermal Systems Branch.

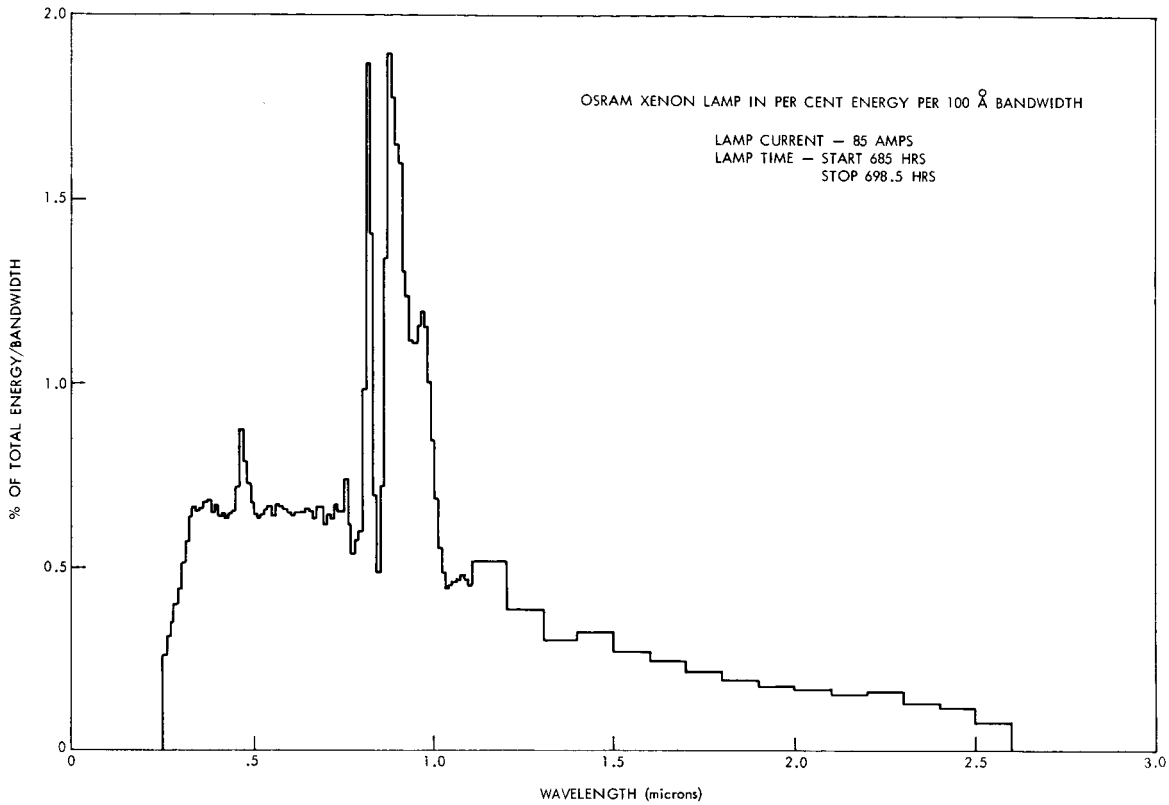

Figure 1 — Spectral Irradiance - Xenon

(2) Total Intensity

Total intensity is measured by either an Eppley Normal Incidence Pyrheliometer or by an Eppley Thermopile. Two normal incidence pyrheliometers were purchased from Eppley which had been calibrated for levels of 100 mw cm^{-2}. When these two were used to measure the intensity of the same uniform source, a difference of 10% was noted. The pyrheliometer which gave the lower value for intensity was recalibrated at Table Mountain, California in 1964 using the Angstrom Compensation Pyrheliometer as a reference. This recalibration indicated the pyrheliometer calibration constant gave values which were low by 9%. The new calibration constant was accepted as correct for levels near

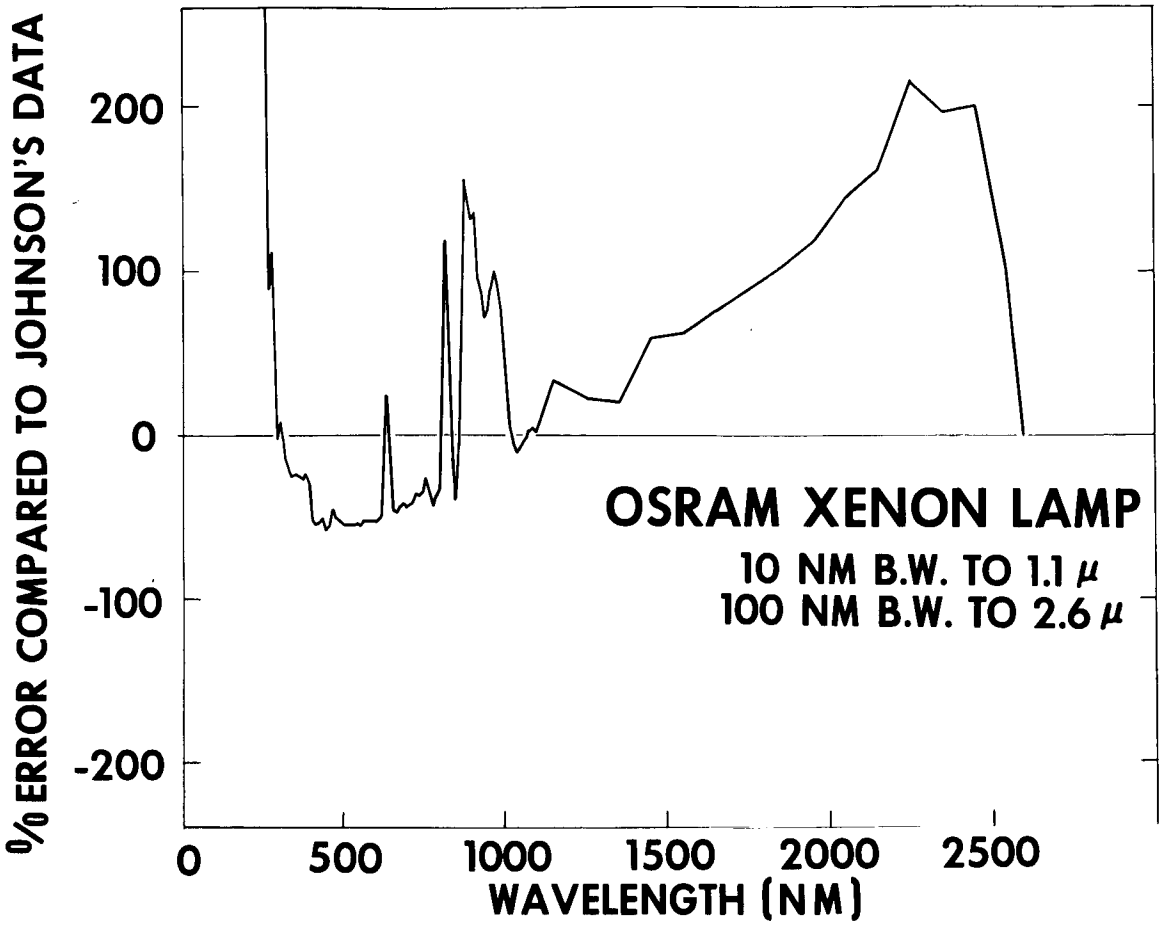

Figure 2 — Deviations from Air Mass Zero Solar Irradiance - Xenon

100 mw cm^{-2} and was later used to compare the readings from all the total intensity sensors in the Group which had been furnished with calibration constants. This work indicated that errors as large as 70% were possible if the calibration constants furnished with the detectors were used. New calibration constants were established for all the detectors in the Group based on the pyrheliometer calibration at Table Mountain.

The pyrheliometer is used to set the intensity levels of the A-1200 Spectrolab solar simulator. One test has been made which compared the intensity

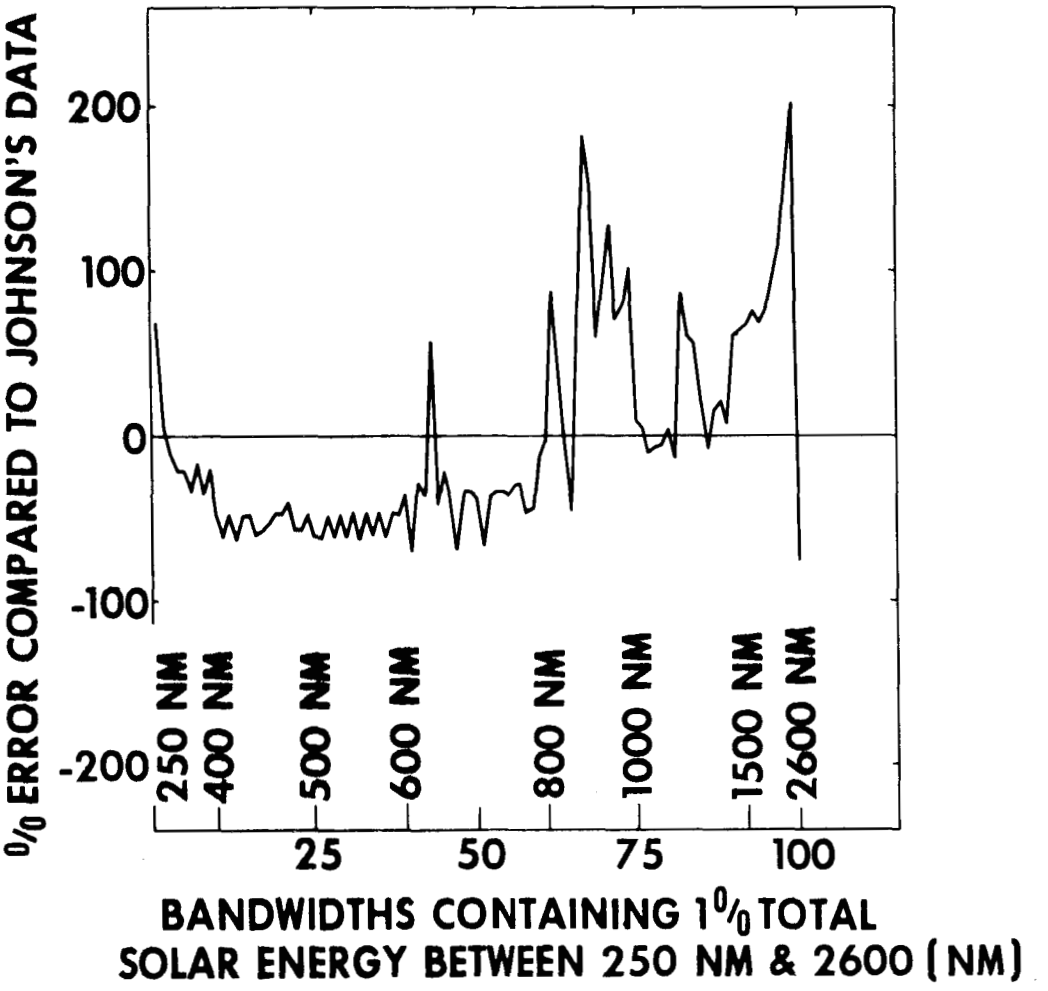

Figure 3 — Deviations per 1% Energy Bandwidths

as measured by the pyrheliometer to the intensity measured thermally by a grooved black plate detector furnished by Robert Kidwell, Head, Temperature Control Section, Thermal Systems Branch. This method is accurate to ±5%, the pyrheliometer accuracy is about ±5%. The results of this test indicated a difference of intensity values for the two methods to be from ±1% to ±4%. This agreement was well within the tolerances of the two methods. The Group is planning to purchase an Angstrom Compensation Pyrheliometer and some of the new high intensity total irradiance standards to improve the accuracy of measurements in this area.

Table I

The following pages represent the computer printout for the Osram xenon lamp at 2720 watts. Figures 1, 2, and 3 were plotted from this data.

WAVELENGTH INTERVAL CONTAINING 1% OF THE TOTAL SOLAR ENERGY LYING BETWEEN 250NM AND 2500NM		PERCENTAGE OF THE TOTAL TEST LAMP ENERGY BETWEEN 250NM AND 2500NM WITHIN THE INTERVAL	PERCENT ERROR OF TEST LAMP DISTRIBUTION WITH REFERENCE TO THE SOLAR DISTRIBUTION
250.0	296.7	1.675	67.485
296.7	316.3	1.048	4.757
316.3	330.5	0.886	-11.426
330.5	342.4	0.788	-21.249
342.4	353.9	0.658	-34.194
353.9	365.1	0.795	-20.496
365.1	375.8	0.687	-31.293
375.8	387.1	0.786	-21.373
387.1	397.9	0.664	-33.638
397.9	406.0	0.512	-48.768
406.0	413.2	0.511	-48.980
413.2	420.2	0.517	-48.435
420.2	427.6	0.375	-62.483
427.6	435.0	0.508	-49.162
435.0	442.2	0.516	-48.495
442.2	448.6	0.395	-60.500
448.6	454.8	0.420	-58.050
454.8	461.0	0.463	-53.684
461.0	467.2	0.532	-46.808
467.2	473.5	0.532	-46.848
473.5	479.7	0.430	-57.034
479.7	486.3	0.584	-41.555
486.3	492.9	0.430	-56.973
492.9	499.4	0.384	-61.617
499.4	506.3	0.520	-48.003
506.3	513.2	0.382	-61.805
513.2	520.2	0.512	-48.841
520.2	527.2	0.388	-61.240
527.2	534.1	0.522	-47.796
534.1	540.9	0.396	-60.431
540.9	547.7	0.399	-60.066
547.7	554.6	0.517	-48.347
554.6	561.6	0.392	-60.781
561.6	568.7	0.540	-46.012
568.7	575.7	0.403	-59.737
575.7	582.8	0.533	-46.702
582.8	589.9	0.396	-60.378
589.9	597.0	0.522	-47.754
597.0	604.4	0.451	-54.855
604.4	611.9	0.646	-35.382
611.9	619.6	0.327	-67.270
619.6	627.3	1.038	3.778
627.3	635.2	1.568	56.808
635.2	643.3	0.588	-41.237
643.3	651.4	0.788	-21.204
651.4	659.7	0.312	-68.942
659.7	668.0	0.633	-36.667
668.0	676.5	0.669	-33.142

Table I (Continued)

676.5	685.2	0.666	-33.418
685.2	694.1	0.304	-69.617
694.1	703.1	0.643	-35.741
703.1	712.1	0.626	-37.402
712.1	721.5	0.663	-33.704
721.5	731.0	0.665	-33.492
731.0	740.7	0.645	-35.503
740.7	750.6	0.702	-29.835
750.6	760.6	0.711	-28.865
760.6	771.0	0.541	-45.942
771.0	781.8	0.564	-43.532
781.8	792.7	0.583	-41.726
792.7	803.9	0.696	-30.393
803.9	815.3	2.476	147.601
815.3	827.1	1.410	40.363
827.1	839.2	0.699	-30.131
839.2	851.7	0.791	-20.713
851.7	864.7	0.997	-0.295
864.7	878.1	2.664	166.430
878.1	891.7	2.613	161.279
891.7	906.0	2.424	142.422
906.0	920.8	1.956	95.648
920.8	935.9	1.745	74.474
935.9	951.7	1.704	70.397
951.7	968.2	1.814	81.421
968.2	985.1	2.192	119.169
985.1	1003.0	1.230	23.025
1003.0	1021.9	1.145	14.488
1021.9	1041.4	0.923	-7.669
1041.4	1061.8	0.934	-6.604
1061.8	1083.2	0.963	-3.656
1083.2	1106.2	1.107	10.653
1106.2	1131.7	0.892	-10.334
1131.7	1157.2	1.355	35.457
1157.2	1182.7	1.735	73.527
1182.7	1210.2	1.672	67.199
1210.2	1242.1	1.381	38.092
1242.1	1273.9	1.005	0.466
1273.9	1307.2	1.017	1.699
1307.2	1346.8	1.218	21.806
1346.8	1386.4	1.239	23.589
1386.4	1432.0	1.446	44.582
1432.0	1480.7	1.717	71.731
1480.7	1536.1	1.605	60.524
1536.1	1595.7	1.593	59.327
1595.7	1666.9	1.745	74.462
1666.9	1747.0	1.664	66.421
1747.0	1840.6	2.061	106.101
1840.6	1952.3	2.052	105.191
1952.3	2087.9	2.432	143.228
2087.9	2264.1	2.900	189.992
2264.1	0.	0.284	-71.577

Table I (Continued)

INTERVAL (IN NMS)	TEST LAMP ENERGY PERCENT TOTAL PER 10NM WAVELENGTH INTERVAL	SOLAR ENERGY PERCENT TOTAL	WAVELENGTH (IN NMS)	PERCENT ERROR
10.0	0.259	0.072	255.0	257.95
10.0	0.311	0.166	265.0	87.52
10.0	0.349	0.166	275.0	110.78
10.0	0.400	0.290	285.0	37.90
10.0	0.444	0.456	295.0	-2.47
10.0	0.511	0.476	305.0	7.26
10.0	0.567	0.590	315.0	-3.89
10.0	0.635	0.746	325.0	-14.82
10.0	0.661	0.828	335.0	-20.21
10.0	0.650	0.870	345.0	-25.24
10.0	0.659	0.870	355.0	-24.22
10.0	0.676	0.922	365.0	-26.70
10.0	0.683	0.942	375.0	-27.48
10.0	0.645	0.859	385.0	-24.94
10.0	0.666	0.942	395.0	-29.31
10.0	0.636	1.346	405.0	-52.74
10.0	0.645	1.429	415.0	-54.89
10.0	0.628	1.357	425.0	-53.74
10.0	0.646	1.336	435.0	-51.65
10.0	0.649	1.564	445.0	-58.50
10.0	0.716	1.615	455.0	-55.67
10.0	0.874	1.605	465.0	-45.52
10.0	0.785	1.595	475.0	-50.76
10.0	0.725	1.522	485.0	-52.35
10.0	0.673	1.522	495.0	-55.78
10.0	0.648	1.450	505.0	-55.31
10.0	0.637	1.429	515.0	-55.41
10.0	0.646	1.439	525.0	-55.12
10.0	0.655	1.470	535.0	-55.42
10.0	0.666	1.460	545.0	-54.42
10.0	0.641	1.439	555.0	-55.47
10.0	0.674	1.408	565.0	-52.16
10.0	0.670	1.429	575.0	-53.13
10.0	0.662	1.408	585.0	-52.99
10.0	0.652	1.398	595.0	-53.36
10.0	0.644	1.336	605.0	-51.81
10.0	0.652	1.305	615.0	-50.05
10.0	1.038	1.284	625.0	-19.18
10.0	1.568	1.253	635.0	25.15
10.0	1.033	1.232	645.0	-16.15
10.0	0.654	1.212	655.0	-46.03
10.0	0.633	1.201	665.0	-47.28
10.0	0.669	1.170	675.0	-42.86
10.0	0.666	1.139	685.0	-41.55

Table I (Continued)

10.0	0.617	1.108	695.0	-44.27
10.0	0.647	1.118	705.0	-42.17
10.0	0.634	1.067	715.0	-40.59
10.0	0.673	1.056	725.0	-36.33
10.0	0.655	1.036	735.0	-36.74
10.0	0.653	1.004	745.0	-35.01
10.0	0.745	1.004	755.0	-25.85
10.0	0.617	0.963	765.0	-35.88
10.0	0.533	0.932	775.0	-42.76
10.0	0.579	0.922	785.0	-37.14
10.0	0.600	0.901	795.0	-33.40
10.0	0.989	0.880	805.0	12.35
10.0	1.875	0.859	815.0	118.20
10.0	1.410	0.849	825.0	66.01
10.0	0.699	0.818	835.0	-14.59
10.0	0.486	0.797	845.0	-39.10
10.0	0.725	0.777	855.0	-6.71
10.0	1.343	0.756	865.0	77.66
10.0	1.899	0.746	875.0	154.72
10.0	1.782	0.735	885.0	142.44
10.0	1.651	0.715	895.0	131.09
10.0	1.603	0.683	905.0	134.60
10.0	1.310	0.673	915.0	94.63
10.0	1.257	0.663	925.0	89.72
10.0	1.134	0.652	935.0	73.80
10.0	1.125	0.632	945.0	78.17
10.0	1.176	0.611	955.0	92.47
10.0	1.217	0.601	965.0	102.60
10.0	1.170	0.601	975.0	94.74
10.0	1.022	0.570	985.0	79.46
10.0	0.861	0.559	995.0	53.90
10.0	0.699	0.538	1005.0	29.81
10.0	0.563	0.528	1015.0	6.63
10.0	0.493	0.518	1025.0	-4.83
10.0	0.455	0.507	1035.0	-10.31
10.0	0.458	0.497	1045.0	-7.85
10.0	0.467	0.487	1055.0	-4.05
10.0	0.476	0.476	1065.0	-0.09
10.0	0.484	0.466	1075.0	3.83
10.0	0.477	0.456	1085.0	4.69
10.0	0.456	0.445	1095.0	2.42
100.0	0.529	0.392	1150.0	34.67
100.0	0.389	0.314	1250.0	24.08
100.0	0.306	0.253	1350.0	21.30
100.0	0.330	0.205	1450.0	50.80
100.0	0.275	0.168	1550.0	63.84
100.0	0.247	0.139	1650.0	78.26
100.0	0.220	0.115	1750.0	91.67
100.0	0.196	0.096	1850.0	103.96
100.0	0.180	0.082	1950.0	119.75
100.0	0.172	0.069	2050.0	147.27
100.0	0.156	0.059	2150.0	164.41
100.0	0.162	0.051	2250.0	219.96
100.0	0.130	0.043	2350.0	199.86
100.0	0.115	0.038	2450.0	200.94

Table I (Continued)

THE DATA GIVEN BELOW IN THREE GROUPS OF THREE COLUMNS ARE THE SPECTRAL ENERGY DISTRIBUTION OF THE LAMP UNDER TEST GIVEN IN TERMS OF THE PERCENT OF THE TOTAL ENERGY BETWEEN 250NM AND 2600NM WHICH LIES WITHIN A GIVEN WAVELENGTH INTERVAL. COLUMN ONE GIVES THE PERCENT OF THE TOTAL ENERGY WITHIN THE INTERVAL. COLUMN TWO GIVES THE CENTER WAVELENGTH OF THE INTERVAL. COLUMN THREE GIVES THE SHORT WAVELENGTH LIMIT OF THE INTERVAL.

0.04499	251.	250.	0.05085	253.	252.	0.05398	255.	254.
0.05394	257.	256.	0.05571	259.	258.	0.05795	261.	260.
0.06088	263.	262.	0.06301	265.	264.	0.06393	267.	266.
0.06502	269.	268.	0.06634	271.	270.	0.06796	273.	272.
0.06974	275.	274.	0.07147	277.	276.	0.07391	279.	278.
0.07691	281.	280.	0.07990	283.	282.	0.08244	285.	284.
0.08013	287.	286.	0.08044	289.	288.	0.08734	291.	290.
0.09039	293.	292.	0.09990	295.	294.	0.08802	297.	296.
0.08873	299.	298.	0.09341	301.	300.	0.09826	303.	302.
0.10302	305.	304.	0.10728	307.	306.	0.10933	309.	308.
0.10898	311.	310.	0.11028	313.	312.	0.11271	315.	314.
0.11595	317.	316.	0.11936	319.	318.	0.12252	321.	320.
0.12535	323.	322.	0.12754	325.	324.	0.12922	327.	326.
0.13033	329.	328.	0.13133	331.	330.	0.13238	333.	332.
0.13346	335.	334.	0.13325	337.	336.	0.13053	339.	338.
0.12875	341.	340.	0.12913	343.	342.	0.12959	345.	344.
0.13071	347.	346.	0.13201	349.	348.	0.13296	351.	350.
0.13268	353.	352.	0.13151	355.	354.	0.13076	357.	356.
0.13124	359.	358.	0.13255	361.	360.	0.13395	363.	362.
0.13513	365.	364.	0.13638	367.	366.	0.13764	369.	368.
0.13814	371.	370.	0.13774	373.	372.	0.13718	375.	374.
0.13618	377.	376.	0.13411	379.	378.	0.13140	381.	380.
0.12870	383.	382.	0.12760	385.	384.	0.12827	387.	386.
0.12913	389.	388.	0.13003	391.	390.	0.13237	393.	392.
0.13610	395.	394.	0.13600	397.	396.	0.13161	399.	398.
0.12763	401.	400.	0.12627	403.	402.	0.12682	405.	404.
0.12751	407.	406.	0.12802	409.	408.	0.12800	411.	410.
0.12767	413.	412.	0.12734	415.	414.	0.13023	417.	416.
0.13141	419.	418.	0.12768	421.	420.	0.12556	423.	422.
0.12506	425.	424.	0.12455	427.	426.	0.12474	429.	428.
0.12597	431.	430.	0.12756	433.	432.	0.13011	435.	434.
0.13234	437.	436.	0.12984	439.	438.	0.12690	441.	440.
0.12697	443.	442.	0.12705	445.	444.	0.13145	447.	446.
0.13650	449.	448.	0.13917	451.	450.	0.13932	453.	452.
0.14101	455.	454.	0.14567	457.	456.	0.15075	459.	458.
0.16653	461.	460.	0.16653	463.	462.	0.17349	465.	464.
0.19190	467.	466.	0.17593	469.	468.	0.18236	471.	470.
0.17324	473.	472.	0.13974	475.	474.	0.13813	477.	476.
0.15190	479.	478.	0.16081	481.	480.	0.15106	483.	482.
0.13919	485.	484.	0.13339	487.	486.	0.14094	489.	488.
0.15057	491.	490.	0.13876	493.	492.	0.12000	495.	494.
0.12794	497.	496.	0.12989	499.	498.	0.13094	501.	500.
0.13057	503.	502.	0.12967	505.	504.	0.12878	507.	506.
0.12788	509.	508.	0.12711	511.	510.	0.12697	513.	512.
0.12734	515.	514.	0.12771	517.	516.	0.12808	519.	518.
0.12846	521.	520.	0.12883	523.	522.	0.12920	525.	524.
0.12957	527.	526.	0.12994	529.	528.	0.13032	531.	530.
0.13069	533.	532.	0.13109	535.	534.	0.13149	537.	536.
0.13190	539.	538.	0.13230	541.	540.	0.13271	543.	542.
0.13311	545.	544.	0.13352	547.	546.	0.13392	549.	548.
0.13202	551.	550.	0.12629	553.	552.	0.12429	555.	554.
0.12753	557.	556.	0.13077	559.	558.	0.13389	561.	560.
0.13529	563.	562.	0.13508	565.	564.	0.13486	567.	566.
0.13464	569.	568.	0.13443	571.	570.	0.13421	573.	572.
0.13399	575.	574.	0.13373	577.	576.	0.13341	579.	578.
0.13308	581.	580.	0.13276	583.	582.	0.13243	585.	584.
0.13209	587.	586.	0.13170	589.	588.	0.13127	591.	590.
0.13083	593.	592.	0.13040	595.	594.	0.12996	597.	596.
0.12953	599.	598.	0.32192	603.	600.	0.32177	608.	605.
0.32442	613.	610.	0.32730	618.	615.	0.38197	623.	620.
0.65581	628.	625.	0.53849	633.	630.	0.72658	638.	635.
0.58763	643.	640.	0.44567	648.	645.	0.34229	653.	650.
0.31158	658.	655.	0.31497	663.	660.	0.31836	668.	665.
0.32561	673.	670.	0.34297	678.	675.	0.34527	683.	680.
0.32055	688.	685.	0.30383	693.	690.	0.31364	698.	695.
0.32595	703.	700.	0.31782	708.	705.	0.30816	713.	710.
0.32550	718.	715.	0.33747	723.	720.	0.33905	728.	725.
0.33003	733.	730.	0.32500	738.	735.	0.31997	743.	740.
0.33277	748.	745.	0.36887	753.	750.	0.37091	758.	755.

Table I (Continued)

0.33544	763.	760.	0.28201	768.	765.	0.25057	773.	770.
0.27488	778.	775.	0.28879	783.	780.	0.29051	788.	785.
0.29223	793.	790.	0.30778	798.	795.	0.38828	803.	800.
0.60064	808.	805.	0.89374	813.	810.	0.98164	818.	815.
0.81390	823.	820.	0.59573	828.	825.	0.40645	833.	830.
0.29024	838.	835.	0.24127	843.	840.	0.24429	848.	845.
0.30531	853.	850.	0.41924	858.	855.	0.57780	863.	860.
0.76520	868.	865.	0.92896	873.	870.	0.97014	878.	875.
0.91472	883.	880.	0.86776	888.	885.	0.83030	893.	890.
0.82088	898.	895.	0.82561	903.	900.	0.77773	908.	905.
0.67214	913.	910.	0.63789	918.	915.	0.64645	923.	920.
0.61088	928.	925.	0.57535	933.	930.	0.55251	938.	935.
0.56031	943.	940.	0.56515	948.	945.	0.57051	953.	950.
0.59739	958.	955.	0.60908	963.	960.	0.60775	968.	965.
0.59798	973.	970.	0.57162	978.	975.	0.53124	983.	980.
0.49085	988.	985.	0.45047	993.	990.	0.41008	998.	995.
0.36970	1003.	1000.	0.32931	1008.	1005.	0.29422	1013.	1010.
0.26890	1018.	1015.	0.25244	1023.	1020.	0.24033	1028.	1025.
0.22941	1033.	1030.	0.22567	1038.	1035.	0.22790	1043.	1040.
0.23014	1048.	1045.	0.23237	1053.	1050.	0.23461	1058.	1055.
0.23684	1063.	1060.	0.23908	1068.	1065.	0.24132	1073.	1070.
0.24251	1078.	1075.	0.24054	1083.	1080.	0.23846	1088.	1085.
0.23203	1093.	1090.	0.22399	1098.	1095.	0.21768	1103.	1100.
0.20137	1108.	1105.	0.19005	1113.	1110.	0.17874	1118.	1115.
0.17230	1123.	1120.	0.17340	1128.	1125.	0.17717	1133.	1130.
0.18559	1138.	1135.	0.21837	1143.	1140.	0.27085	1148.	1145.
0.32334	1153.	1150.	0.35641	1158.	1155.	0.36775	1163.	1160.
0.35995	1168.	1165.	0.35092	1173.	1170.	0.33752	1178.	1175.
0.32413	1183.	1180.	0.31073	1188.	1185.	0.29675	1193.	1190.
0.28213	1198.	1195.	0.26746	1203.	1200.	0.25805	1208.	1205.
0.25687	1213.	1210.	0.25867	1218.	1215.	0.25632	1223.	1220.
0.24393	1228.	1225.	0.22563	1233.	1230.	0.20733	1238.	1235.
0.18904	1243.	1240.	0.17789	1248.	1245.	0.17445	1253.	1250.
0.17051	1258.	1255.	0.16556	1263.	1260.	0.16060	1268.	1265.
0.15565	1273.	1270.	0.15069	1278.	1275.	0.14574	1283.	1280.
0.14256	1288.	1285.	0.14251	1293.	1290.	0.14384	1298.	1295.
0.14516	1303.	1300.	0.14649	1308.	1305.	0.14781	1313.	1310.
0.14914	1318.	1315.	0.15047	1323.	1320.	0.15179	1328.	1325.
0.15312	1333.	1330.	0.15444	1338.	1335.	0.15563	1343.	1340.
0.15566	1348.	1345.	0.15467	1353.	1350.	0.15368	1358.	1355.
0.15336	1363.	1360.	0.15391	1368.	1365.	0.15467	1373.	1370.
0.15544	1378.	1375.	0.15620	1383.	1380.	0.15696	1388.	1385.
0.15773	1393.	1390.	0.15849	1398.	1395.	0.15926	1403.	1400.
0.16002	1408.	1405.	0.16079	1413.	1410.	0.16155	1418.	1415.
0.16231	1423.	1420.	0.16308	1428.	1425.	0.16459	1433.	1430.
0.16498	1438.	1435.	0.16610	1443.	1440.	0.16679	1448.	1445.
0.17244	1453.	1450.	0.17810	1458.	1455.	0.18245	1463.	1460.
0.18088	1468.	1465.	0.17470	1473.	1470.	0.16652	1478.	1475.
0.16235	1483.	1480.	0.15617	1488.	1485.	0.14999	1493.	1490.
0.14382	1498.	1495.	0.28087	1505.	1500.	0.28216	1515.	1510.
0.29489	1525.	1520.	0.29434	1535.	1530.	0.28318	1545.	1540.
0.27171	1555.	1550.	0.26024	1565.	1560.	0.25753	1575.	1570.
0.26120	1595.	1590.	0.25941	1595.	1590.	0.25652	1605.	1600.
0.24262	1615.	1610.	0.24473	1625.	1620.	0.24640	1635.	1630.
0.24564	1645.	1640.	0.25197	1655.	1650.	0.25585	1665.	1660.
0.25194	1675.	1670.	0.24240	1685.	1680.	0.23453	1695.	1690.
0.23056	1705.	1700.	0.22882	1715.	1710.	0.22708	1725.	1720.
0.22534	1735.	1730.	0.22356	1745.	1740.	0.22083	1755.	1750.
0.21719	1765.	1760.	0.21355	1775.	1770.	0.20991	1785.	1780.
0.20628	1795.	1790.	0.20264	1805.	1800.	0.19900	1815.	1810.
0.19692	1825.	1820.	0.19700	1835.	1830.	0.19770	1845.	1840.
0.19840	1855.	1850.	0.19862	1865.	1860.	0.19510	1875.	1870.
0.19130	1885.	1880.	0.18650	1895.	1890.	0.18151	1905.	1900.
0.18067	1915.	1910.	0.18019	1925.	1920.	0.17970	1935.	1930.
0.17921	1945.	1940.	0.17872	1955.	1950.	0.17823	1965.	1960.
0.17838	1975.	1970.	0.17941	1985.	1980.	0.18070	1995.	1990.
0.36260	2010.	2000.	0.35645	2030.	2020.	0.34431	2050.	2040.
0.33217	2070.	2060.	0.32003	2090.	2080.	0.31062	2110.	2100.
0.30534	2130.	2120.	0.30149	2150.	2140.	0.30750	2170.	2160.
0.33572	2190.	2180.	0.35851	2210.	2200.	0.34265	2230.	2220.
0.32692	2250.	2240.	0.30419	2270.	2260.	0.28423	2290.	2280.
0.27246	2310.	2300.	0.26612	2330.	2320.	0.26010	2350.	2340.
0.25500	2370.	2360.	0.25046	2390.	2380.	0.24577	2410.	2400.
0.24069	2430.	2420.	0.22006	2450.	2440.	0.20059	2470.	2460.
0.23632	2490.	2480.						

Table II

Absorptivities of Materials obtained from Computer Program

Material	Solar	Osram Xenon	Osram* Xenon with P.E. 7C Filter	A-1200 Solar Simulator	X-25L, S.S.	Argon 600psig
Gold	19.7%	12.6%	11.8%	15.8%	18.6%	17.8%
Silver	4.98	4.90	2.76	4.22	3.85	7.19
Aluminum	7.75	7.08	6.94	8.23	7.44	7.65
Titanium Oxide-Silicate	19.7	22.5	19.6	17.4	19.7	24.0
Titanium Oxide-Silicone	19.0	21.0	18.4.	17.9	18.5	23.1
Zinc Oxide-Silicate	23.4	28.4	25.2	21.9	23.7	28.6
Zinc Oxide-Silicone	21.2	23.0	20.6	20.2	21.0	25.5
3M Velvet Black	97.2	97.2	97.2	97.2	97.2	97.2
CAT-A-lac Black	94.8	94.8	94.8	94.9	94.8	94.7
CAT-A-lac White (12 coats)	17.6	20.9	18.0	16.1	17.7	22.1
Leafing Aluminum	28.3	27.6	27.6	28.4	28.0	28.3

*The transmission of this filter is shown in Figure 4, and the spectral irradiance for the data shown is Figure 5.

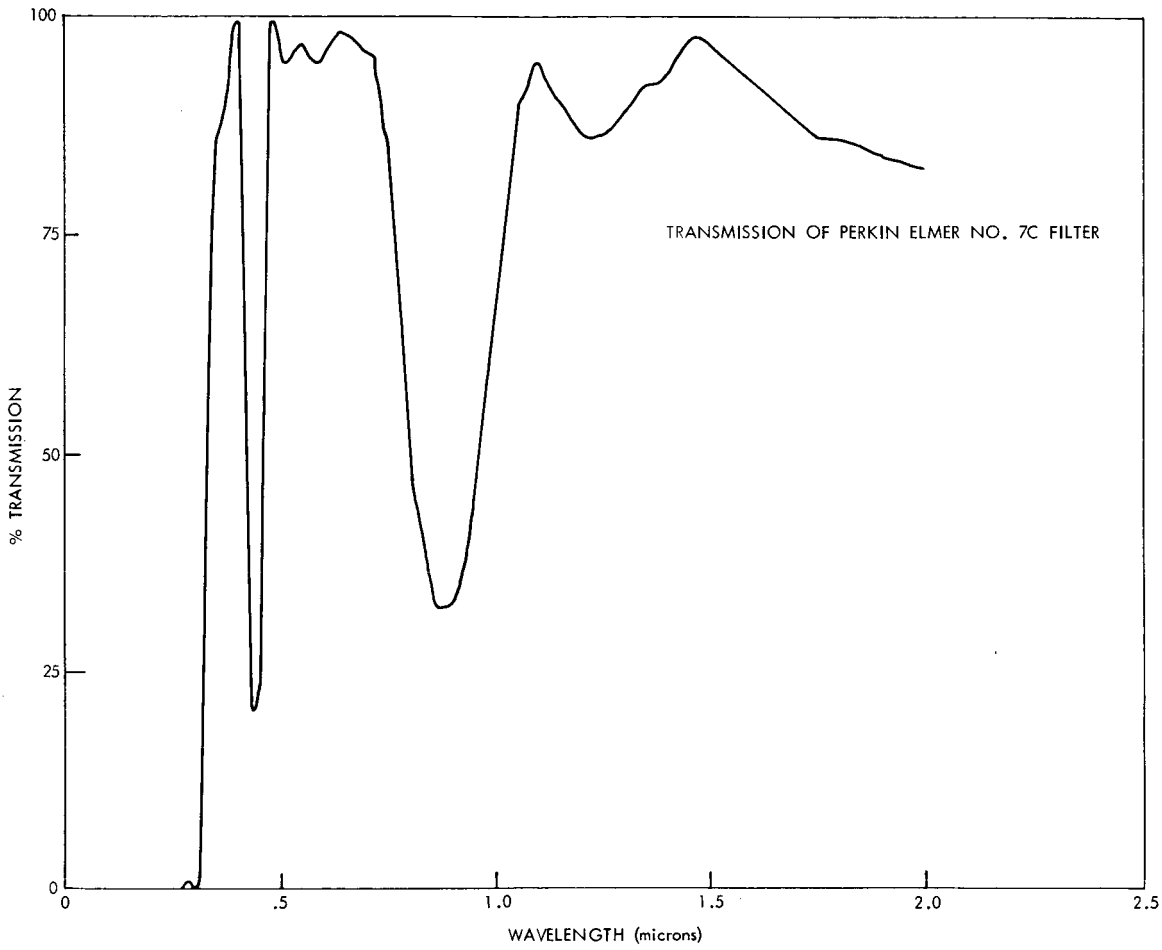

Figure 4 — Spectral Transmission of P.E. Filter

(3) Uniformity of Total Intensity

The uniformity of total intensity is measured by a 1 cm x 1 cm N/P silicon solar cell with 1/4Ω loading. The solar cell is used because of its rapid response time and also because the spectral distribution within the test volume of the simulator remains constant with position. The accuracy of these measurements (relative) is ±1%. The solar cell will be replaced soon by either a Hy-Cal pyrheliometer or by a Reeder 1 cm diameter thermopile. The effects of vacuum, temperature, and ultra-violet radiation on these detectors is being determined at present.

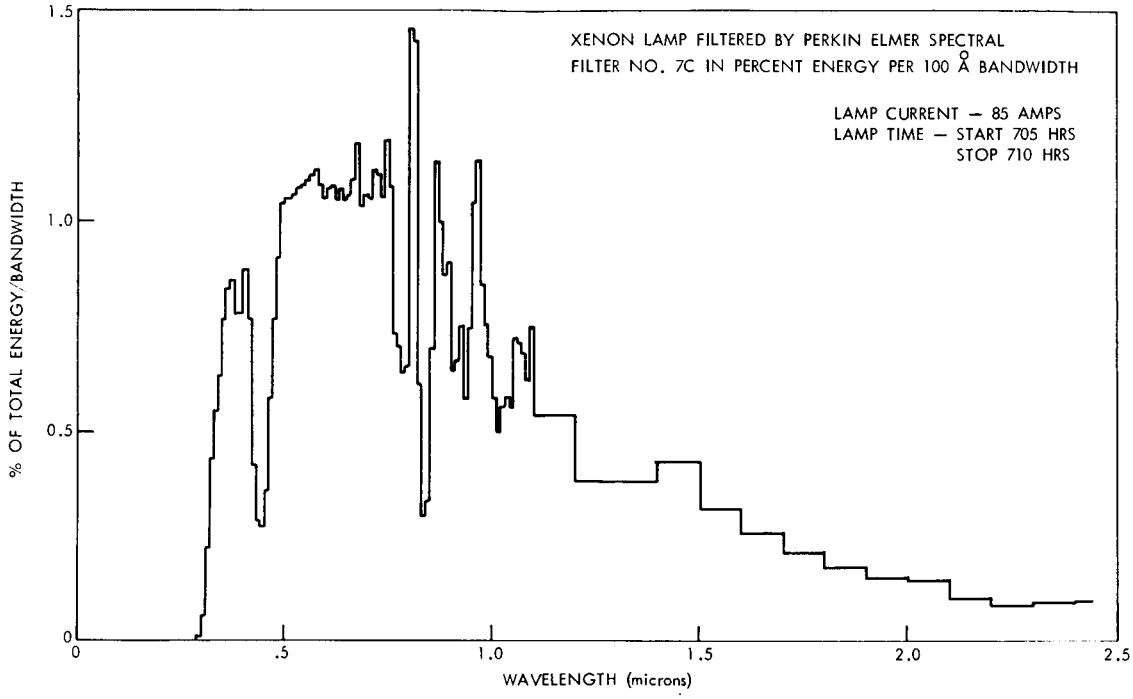

Figure 5 — Spectral Irradiance of Xenon and P.E. Filter

(4) Ultra-violet Irradiance

The quantity of ultra-violet radiation from several sources has been measured using a filter technique. This work was originally begun on a request from another Group which was performing some ultra-violet degradation studies on materials. This Group wished an accurate, cheap, and simple way to measure the ultra-violet irradiance. This work has been extended to determine the effect of lamp operation time on the ultra-violet irradiance and also to determine the effects of ultra-violet irradiance on the materials used on the total radiation detectors and the aluminized optical components of the solar simulator.

(5) Ozone

The amounts of oxone generated by compact arc lamps and by the solar simulator when air was used for cooling have been measured. The levels

inside the lamp housing were 10 parts per million by volume maximum and in the laboratory at a point 5 feet from the lamp housing 5-8 parts per hundred million by volume. This ozone generation was eliminated by filling the lamp housing with nitrogen and continuously flushing the system with GN_2 during simulator operation. The elimination of ozone reduces the degradation of the aluminum surfaces inside the lamp housing and also allows more of the ultra-violet irradiance to be transferred to the test volume of the simulator.

IV. FUTURE PLANS

(1) Calibrations Laboratory

A calibrations laboratory to calibrate all the instruments used by the Group on a periodic basis is being set up. All calibrations of equipment, detectors, etc. will be traceable to primary standards maintained by the National Bureau of Standards. This laboratory will also perform calibrations of detector spectral sensitivity, spectral response, and spectral transmissions of interference and neutral density filters. The effects of temperature, humidity, pressure, ultra-violet radiation, and electrical loading on the detectors and equipment will be determined. The effects of ultra-violet radiation on the filter transmission characteristics will be measured also.

A Barnes Engineering 1000°C black body radiation source and a Leeds and Northrup automatic optical pyrometer have been obtained to support the effort in this area.

An Eppley Mark IV Spectral Radiometer has been ordered and will be calibrated for use as a spectral monitor for the A-1200 solar simulator during satellite tests.

(2) Satellite Experiment

Equipment will be purchased, calibrated to an absolute accuracy of ±10%, and evaluated for suitability to remeasure the air mass zero solar spectral irradiance from a satellite. The improved standard of spectral irradiance developed by NBS under the current NASA contract will be used to calibrate the equipment.

The equipment package will be tested in the Radiometry Research Simulator and also will be used to determine the spectral irradiances of both the A-1200 and X-25L solar simulators.

One instrument which measures in the wavelength region from 2000A to 4500A has been purchased from ITT of Fort Wayne, Indiana. This is an electronic scanning spectrometer. The radiation incident upon the entrance slit is dispersed across the face of an image dissector camera tube by a McPherson grating monochromator. The spectrum on the face of the tube can be scanned either 100 or 1000 times per second. The effective aperature of the system is f/5; the dispersion, 130 A/mm.; the camera tube has a S-21 response; and, the minimum radiant sensitivity at 4000A is 10^{-6} watt cm^{-2} A^{-1}. This camera tube can resolve 130 elements per mm at 50% modulation hence the spectral resolution obtainable is about 1A. This instrument was used to examine the spectral irradiance of the plasmadyne VSRS and gave the first indication of the large ripple in irradiance associated with this arc. This instrument will be tested in both solar simulators to identify the effects of vacuum and temperature upon the calibrations. The possibility of using this instrument in a satellite experiment, balloon experiment, or airplane experiment will be determined. The instrument will also be tested for suitability for use as a spectral monitor for the A-1200 solar simulator.

THERMAL VACUUM SOLAR SIMULATOR

Malcolm Lillywhite*

James Murray*

Danny Lester*

Radiometry Group

Thermal Systems Branch

Spacecraft Technology Division

*Taag Designs, Inc. employee at GSFC.

THERMAL VACUUM SOLAR SIMULATOR

Malcolm Lillywhite

James Murray

Danny Lester

Radiometry Group

Thermal Systems Branch

Spacecraft Technology Division

ABSTRACT

A thermal vacuum solar simulator with the following specifications is in operation:

1. Uniformity of ±10% over 48 inch x 96 inch test volume with 1 cm^2 detector
2. Total irradiance of 200 mw cm^{-2} variable to 18 mw cm^{-2}
3. 10^{-8} torr
4. Collimation of 1° half angle
5. Stability of <±1/2%
6. Spectrum of xenon modified by optics
7. LN_2 to +250°C shroud temperatures

Future improvements include:

1. Uniformity of ±5% over total volume; ±2% over smaller volumes
2. Total irradiance of 250 mw cm^{-2} maximum
3. Spectral match to ±10% to ±25% of air mass zero solar irradiance

The solar simulator has been used to test IMP "D", "AEB", and the Oklahoma University active temperature control module. The simulator met or exceeded

all of the specifications; has been modified by GSFC for improved performance; and, contracts have been placed to Spectrolab, Inc., Sylmar, California for improvements to uniformity and spectral matching to air mass zero solar irradiance. Operational performance of the system has been very satisfactory to date.

THERMAL VACUUM SOLAR SIMULATOR

INTRODUCTION

The thermal vacuum solar simulator is used to test spacecraft coatings, materials, solar cells, and thermal models of spacecraft. The primary purpose of the system is to study the problems of thermal balance and active temperature control of spacecraft. The system consists of a space simulator (thermal vacuum system) fabricated by Bethlehem Corporation, Easton, Pa. and a A-1200 solar simulator fabricated by Spectrolab, Inc., North Hollywood, California. The system has been in operation since 18 December 1964 and has undergone a thorough series of calibration and stability tests. IMP-D, AEB, and the Oklahoma University active temperature control unit have been tested. The system has operated satisfactorily during each of these tests.

The Spectrolab A-1200 solar simulator met or exceeded all contract specifications when delivered on 18 December 1964. The specifications for the solar simulator are included as Appendix I.

System Description

The vacuum chamber is in the shape of a cyclinder (10') ten feet in diameter and (15') in axis length mounted with its axis horizontal (see Figure 1). A vacuum in the 10^{-8} Torr range can be attained in two hours with a test sample in place. The chamber has a shroud with temperature capabilities ranging from 73°K (liquid nitrogen) to 530°K (heating). Approximately one hour is required for the chamber to cycle 200°K.

The solar simulator optical system, shown in Figure 2, consists of three basic parts; 1. a vertically mounted silo containing the lamp module array and

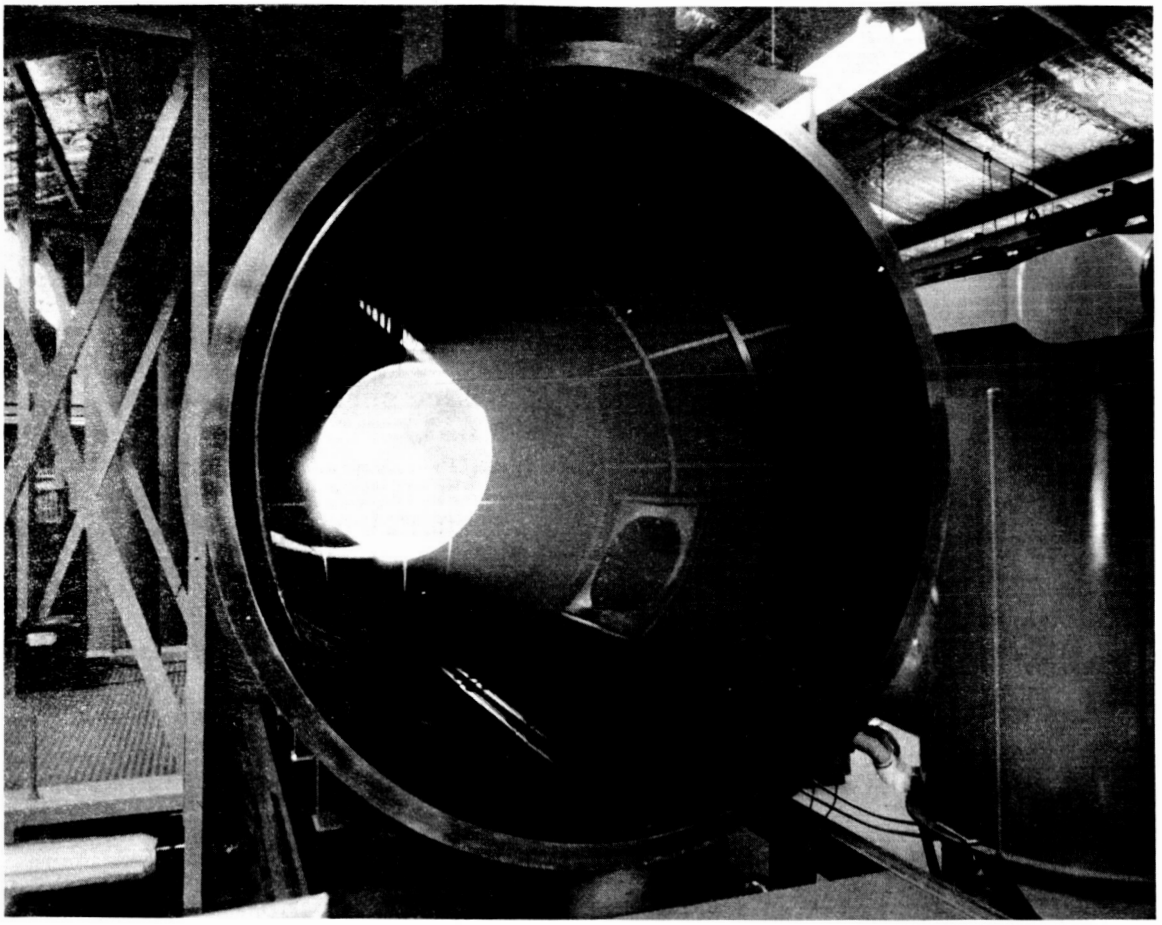

Figure 1—View of Simulator

related optics which operate at atmospheric pressure; 2. the field, projection, and vacuum seal lens assembly, and 3. the collimating mirror mounted inside the vacuum chamber.

The lamp modules consist of an Osram xenon 2.5 KW compact arc lamp mounted inside an aconic collector. The collector is electro-formed nickel, Kanogen treated, and evaporated with aluminum. The array is made of nineteen module units, each illuminating the entire test volume. The collectors focus the emitted energy at the field lens. A 34" octagonal, water cooled turning

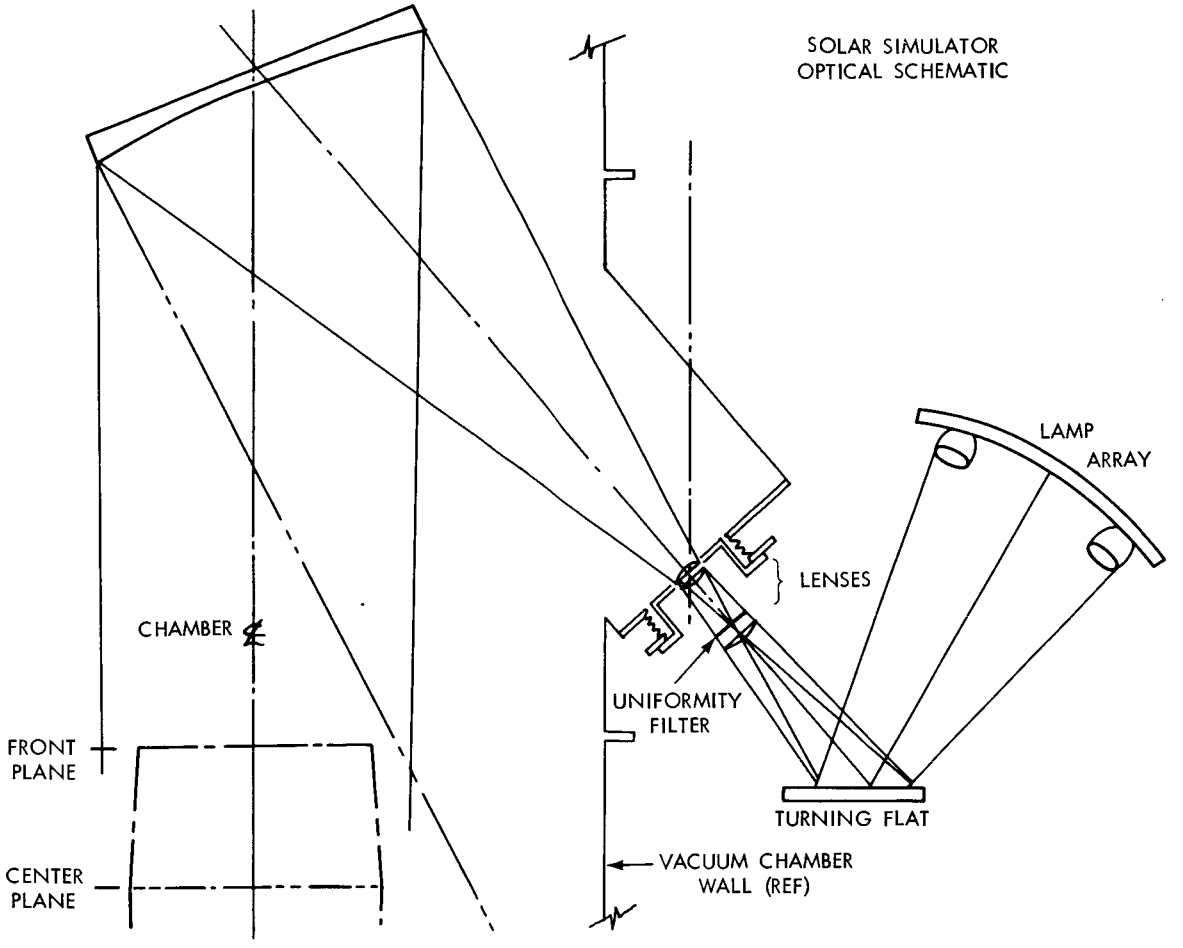

Figure 2—Solar Simulator Optical Schematic

flat is used to bring the energy into the vacuum system. The energy passes through an uniformity filter. This component is a source of some problems discussed in detail below. The transmission of the filter varies as a function of radial distance to produce a uniform beam at this point. The two projection lenses are used to form an image for the collimator. One of these lenses is used as the vacuum seal lense with a Dow Corning 916 silastic hot vulcanized gasket. This gasket has been used successfully for (400) four hundred hours and appears to be able to withstand the heat in this area. All lenses are made

of optical grade quartz. The collimating mirror is a (60") sixty inch aluminum off-axis parabola spun cast, component which is Kanogen treated and coated with evaporated aluminum and SiOx.

The silo and components are cooled by the circulation of gaseous nitrogen through a heat exchanger. Additional cooling is provided to areas of intense radiation by water circulation. Nitrogen is introduced into the system continuously during operation to minimize ozone generation by the arc sources.

The entire system is monitored by a console which is shown in Figure 3. This console displays information about individual module operation (e.g., voltage, current, elapsed time, etc.). The temperatures of optical and electronic components are monitored continuously during operation. This makes it possible to isolate and correct problems that may occur during testing and to observe any general trend of degradation of optical components. A detailed description of the electronic system is included as Appendix II.

Operational Characteristics

The solar simulation system met or exceeded all contract specifications when it was installed at GSFC on 18 December 1964. A list of the test requirements is given in Table I. The following three months were spent testing and calibrating the system. The results of this effort are shown in Table II. It should be pointed out that all specifications are compatible with each other (i.e., all specifications hold true for the limits of any other category).

The total irradiance or intensity has been measured with two detectors: 1. an Eppley pyrheliometer and 2. a black grooved plate detector (α = .99, ϵ = 1.04 (effective) ±1%). The pyrheliometer is used outside the chamber monitoring through a quartz port, the transmission of this port is shown in Figure 4. The

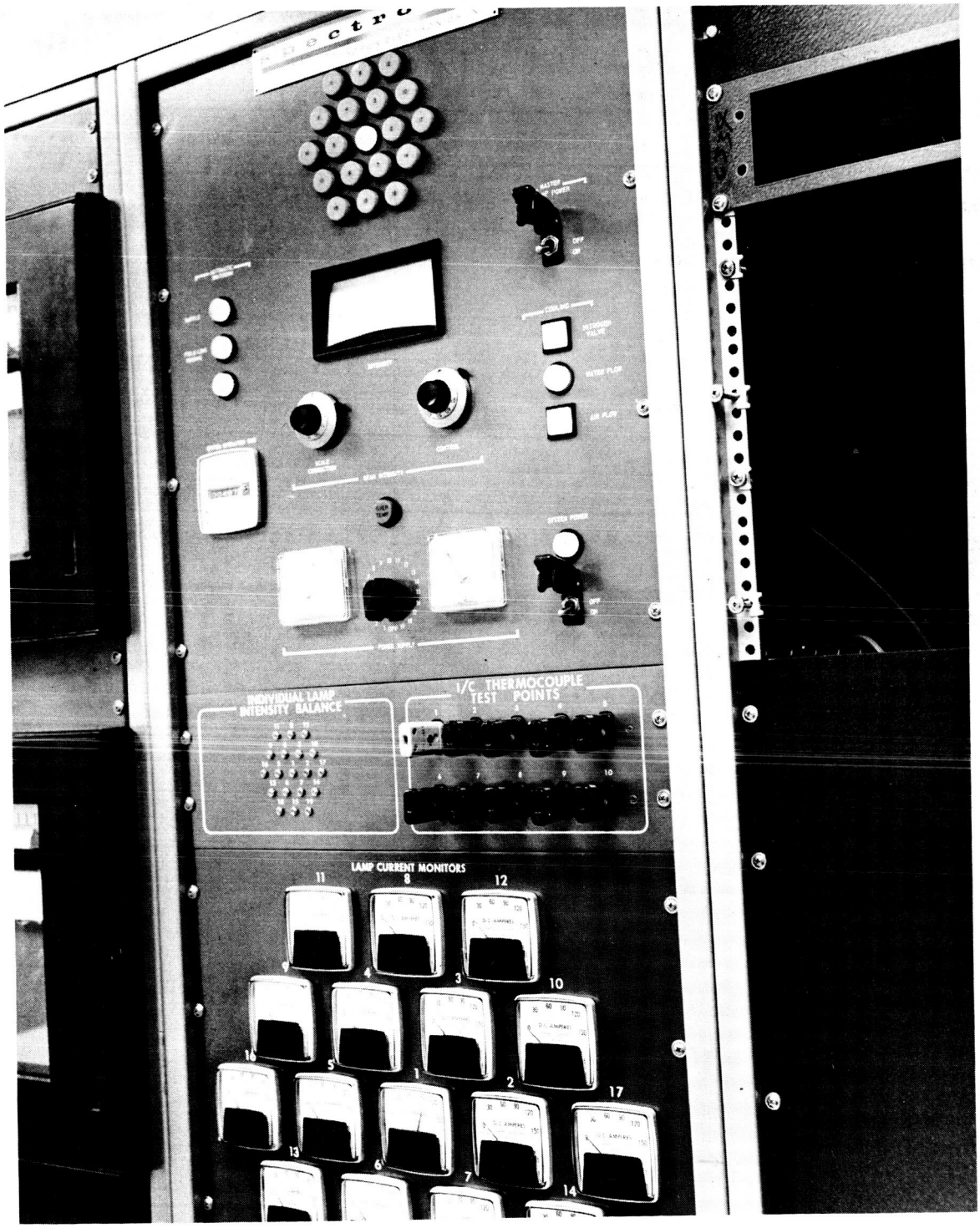

Figure 3—Control Console

Table I

SOLAR SIMULATOR ACCEPTANCE TEST SPECIFICATIONS

MEASUREMENT	SPECIFIED	CONDITIONS
TARGET AREA SIZE	~110 cm DIA. CIRCLE	
RADIANT FLUX DENSITY	MIN. 50 mw/cm^2 MAX. 40 mw/cm^2	VARIABLE
TEMPORAL VARIATIONS IN RADIANT FLUX	1 % RMS	< .1 SECOND
	±1 %	< 1 HOUR
	±2 %	> 24 HOURS
UNIFORMITY OF RADIANT FLUX DENSITY	±10 %	10 x 10 cm SOLAR CELL DETECTOR ARRAY
COLLIMATION ANGLE	2° HALF ANGLE	95 % TOTAL ENERGY IN ANGLE
SPECTRAL DISTRIBUTION	UNCORRECTED XENON SPECTRA	
BLACK SPACE SIMULATION	< 3 % TOTAL	i.e. REREFLECTED ENERGY

Table II

MEASURED PERFORMANCE SPECIFICATIONS FOR SOLAR SIMULATOR

MEASUREMENT	SPECIFICATION	CONDITIONS	MEASUREMENT ERROR
TARGET AREA SIZE	48"-52" ELLIPSE 7' DEEP ≅ 88 cu. ft.	VARIABLE (TO 24"-26" ELLIPSE)	
RADIANT FLUX DENSITY	1.5 SOLAR CONSTANT	VARIABLE .1 - 1.5 SOLAR CONSTANT	± 2% INSTRUMENT ERROR ± 3% OF CALIBRATION
TEMPORAL VARIATIONS IN RADIANT FLUX DENSITY	SHORT TERM ± 2% $\frac{\text{PEAK}}{\text{AVG.}}$	NORMAL	
	< 1% $\frac{\text{TOTAL RMS}}{\text{AVG.}}$	60 cps AND HARMONICS	
	LONG TERM 400 HOURS	DEGRADATION OF COMPONENTS	
LAMP WARM-UP TIME	30 MIN.	TO COMPLETELY STABILIZE ARC	
UNIFORMITY OF RADIANT FLUX DENSITY	± 10 %	1 cm x 1 cm SOLAR CELL DETECTOR LOADED FOR LINEARITY ($\frac{1}{4}\wedge$)	± 1% REPEATABILITY
COLLIMATION ANGLE	$1\frac{1}{2}^\circ$ HALF ANGLE FULL ARRAY	PIN HOLE DEVICE	$\frac{1}{2}^\circ$ MAX.-MIN. ARRAY SIZE
SPECTRAL DISTRIBUTION	UNCORRECTED XENON SPECTRA		±10% RELATIVE ±15% ABSOLUTE
BLACK SPACE SIMULATION EFFECT	5 % OF TOTAL IRRADIANT ENERGY	TEST AREA SHROUD	± 100 %
	RADIATION OF A 73°K BLACK BODY	WALL SHROUD	
	RADIATION OF A ~40°K BLACK BODY	COLLIMATING MIRROR	
TESTING TIME DURATION	100 HOURS 400 HOURS	- PREVIOUSLY TESTED - EXPECTED CAPABILITY	MAINTAINING ALL SPECIFICATIONS

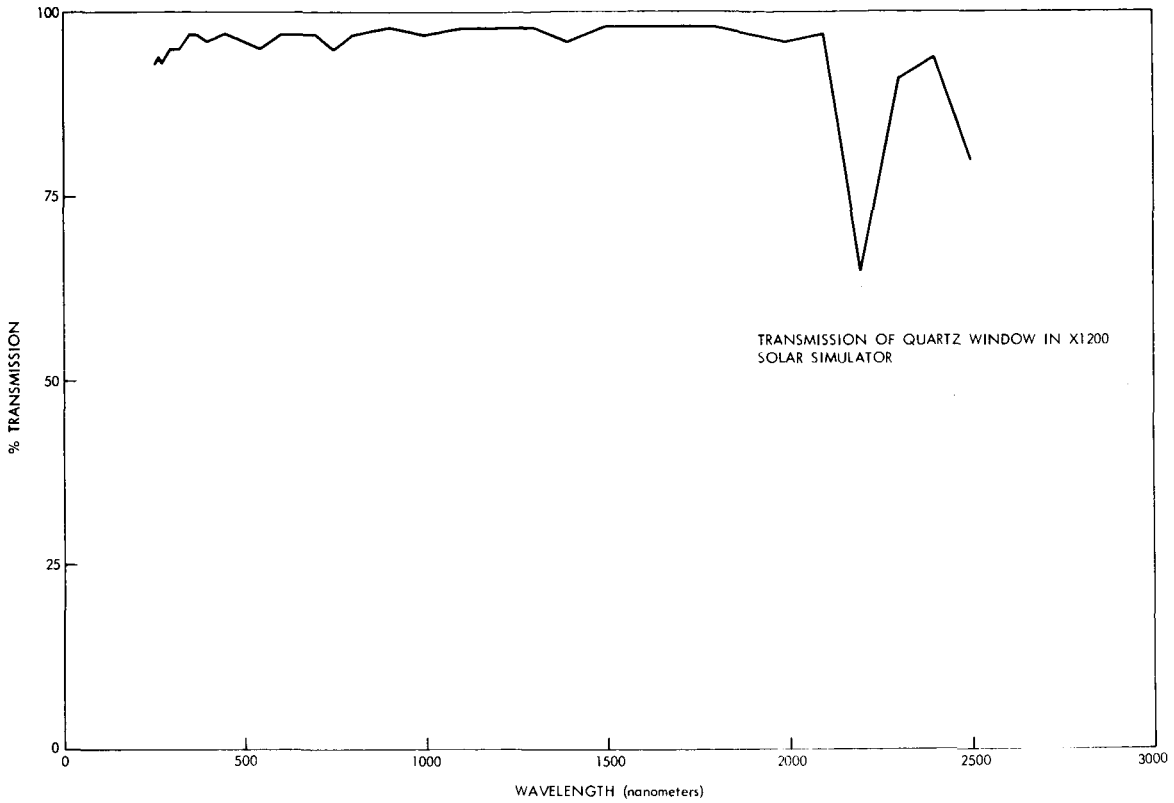

Figure 4—Spectral Transmission of Port

black plate is used inside the vacuum chamber. These detectors have relatively slow time constants. A comparison of the results of this type of measurement is given in Table III.

The temporal variations of irradiance in the target area (stability) are considered to be symmetrical and therefore do not effect the uniformity but merely shift the entire uniformity pattern. This is attributed to power supply regulation characteristics; however, the RMS variation is less than 1% - which is quite acceptable for thermal balance measurements.

The uniformity of irradiance with spatial variation has a maximum deviation from the average of ±10% using a 1 cm x 1 cm solar cell as a detector. Uniformity

Table III

RESULTS OF SOLAR SIMULATOR RADIANT FLUX DENSITY CALIBRATION TEST

(TESTED UNDER COLD-WALL VACUUM CONDITIONS)

ENERGY LEVEL SETTING MEASURED BY EPPLEY PYRHELIOMETER	IN VACUUM MEASUREMENT USING A BLACK GROOVED PLATE THERMO-DETECTOR					
MEASURED ERROR ±2% RANDOM	CALCULATED ABSOLUTE TEMP. SCALE ±2% RANDOM		MEASURED ABSOLUTE TEMP. SCALE		% ERROR	
FRACTION OF SOLAR CONSTANT	T	T^4	T	T^4	T	T^4
.21	253° K	4.09×10^9	254° K	4.16×10^9	+ 40%	1.7%
.52	317° K	10.09×10^9	325° K	11.15×10^9	+ 2.21%	10.5%
1.00	373° K	19.31×10^9	380° K	20.85×10^9	+1.88%	8.0%
1.05	378° K	20.41×10^9	382° K	21.29×10^9	+1.06%	4.3%
1.34	402° K	26.11×10^9	410° K	28.25×10^9	+1.99%	8.2%
1.56	418° K	30.52×10^9	427° K	33.24×10^9	+2.15%	8.9%

of ±8% has been obtained using a 10 cm x 10 cm array of solar cells. The scanning device gives the exact position and size of hot spots or small localized deviations from the average. These hot spots do not exceed the ±10% deviation from the average. Figure 5 shows the scanning device. The use of a solar cell as a detector has certain inherent disadvantages. These are spectral response, temperature effects, and electrical loading. The most serious of these is the spectral range covered by the solar cell. The spectral irradiance of this simulator is constant throughout the test volume which allows a solar cell to be used for this measurement. The linearity of the solar cell i.e., output vs. irradiant energy is obtained by loading the cell with a one quarter (1/4) ohm resistor.

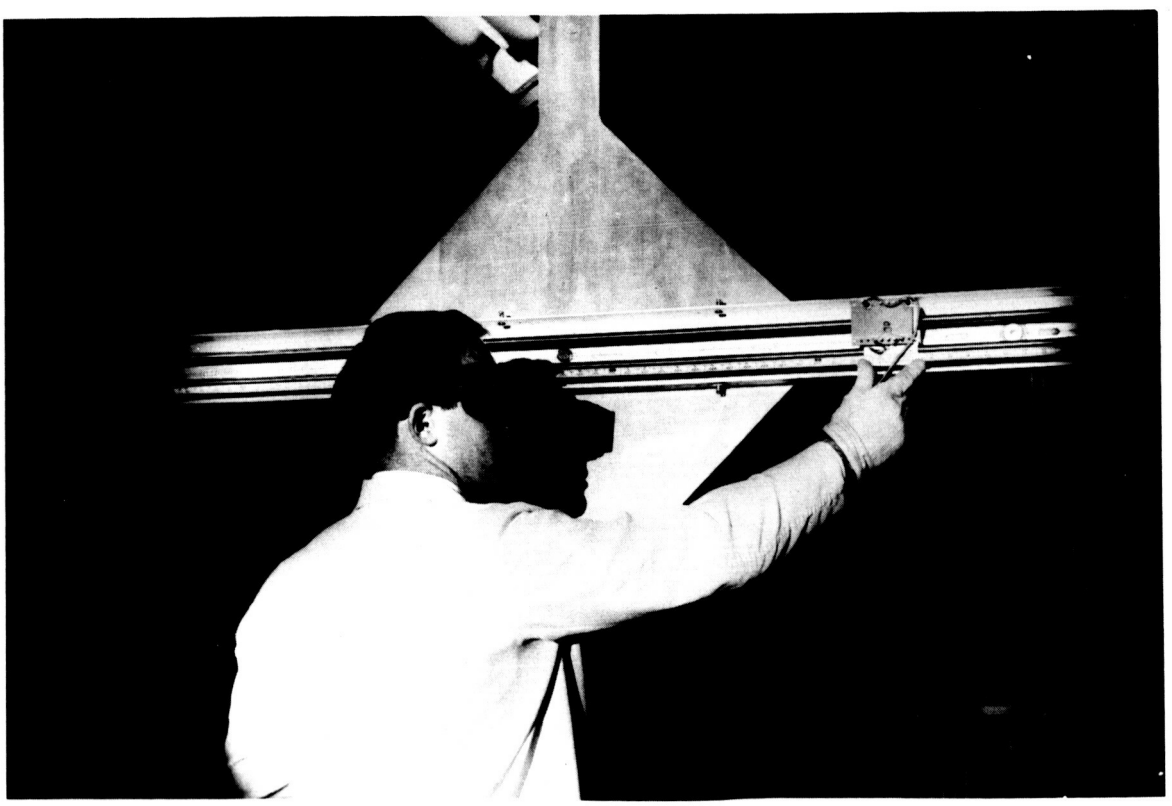

Figure 5—Uniformity Scanner

This ensures against saturation current levels being attained by the solar cell at these energy levels. A typical continuous uniformity scan for four radial positions, horizontal, vertical and diagonals is shown in Figure 6.

Spectral irradiance is measured during an extended test every 100 hours or when any optical change or adjustment is made. The measurement is taken through a quartz port at the rear of the test volume. The measurement is made with the Leiss Instrumentation[1]. A typical spectral distribution is shown in Figure 7. This measurement was made during the IMP-D test. Appendix III is the computer printout of this data. The present spectral distribution is low in the ultraviolet and visible regions excessive in the infrared.

The black space simulation ability of the various shrouds with respect to the incident irrandiance in the system is of concern to the thermal balance of a

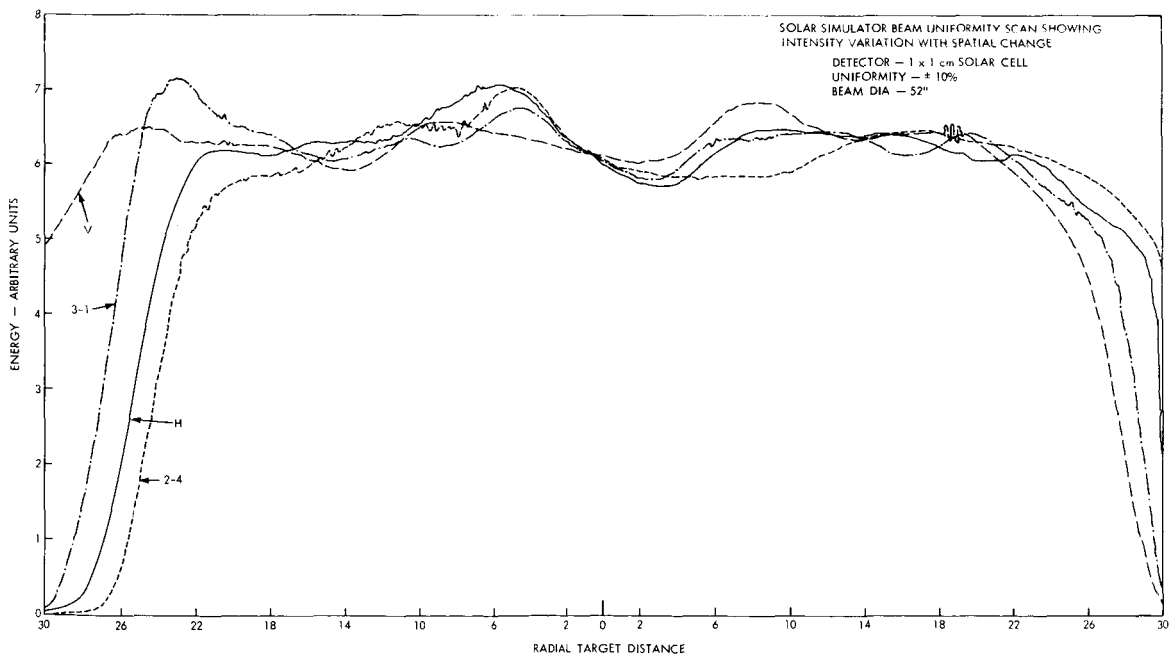

Figure 6—Uniformity Scans

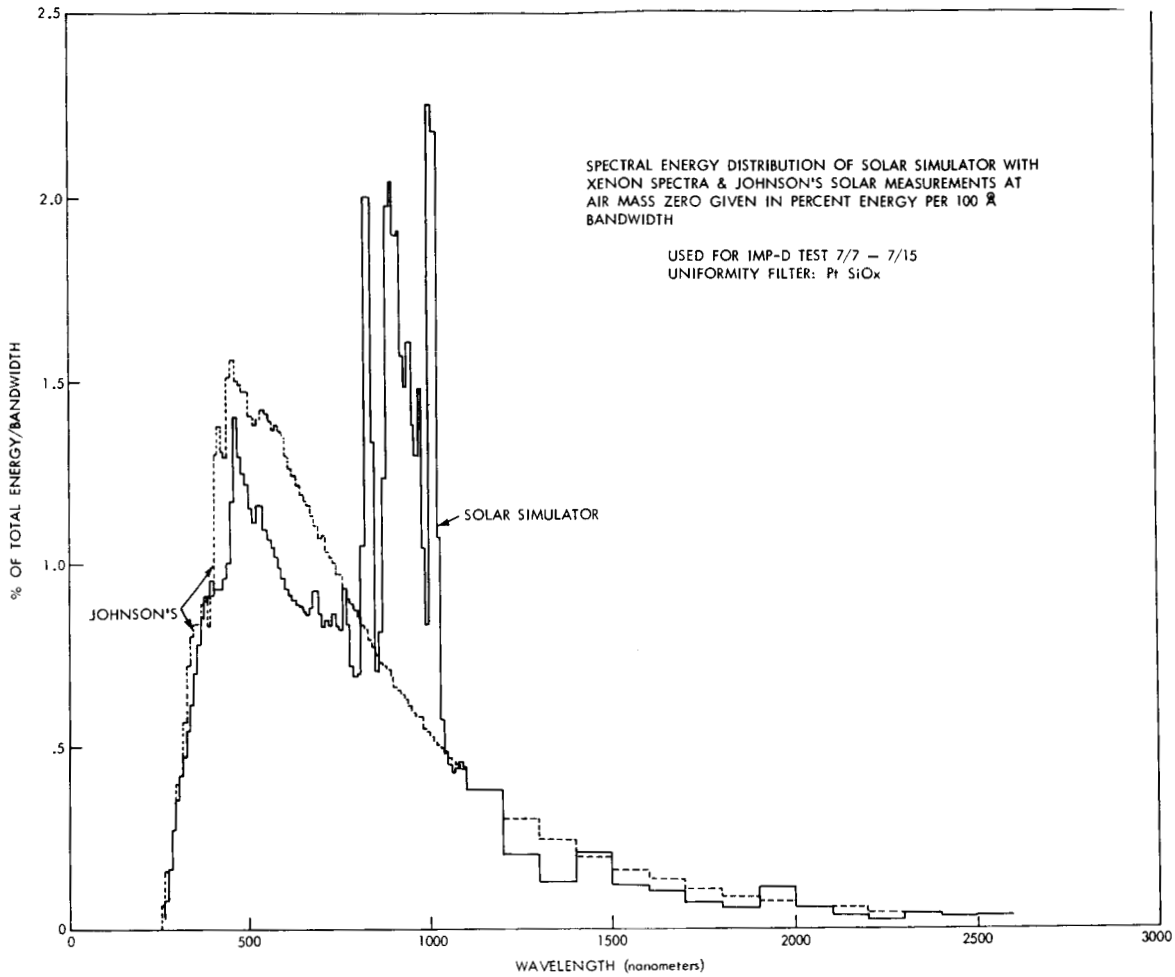

Figure 7—Spectral Irradiance of Simulator

spacecraft. The effect due to the efficiency (or inefficiency) of the shroud as a black space is difficult to predict with any degree of accuracy because of the physical construction and corresponding reflective characteristics of the shroud. Measurements taken indicate that as a function of spatial change, with a test sample in place, the reflected irradiance has varied from 0% to 8% of incident irradiance. This effect, in the past, has been treated as a compensating factor to account for overheating of samples by estimating effective values;

however these values are not constant. The conditions change with the shape of the spacecraft (i.e., shadows cast on shroud) and its position in the test volume. An effort is now underway to obtain reliable data with which to predict more accurately the effect of the black space simulation efficiency on the thermal balance of a spacecraft.

Maintainance and Test Operation

The operation of the solar simulation system during a test situation consists primarily of checking the monitoring instrumentation of various components periodically. The temperature of optical and electronic components are monitored continuously and checked every half hour during operation and are compared with previously determined normal operating temperatures for equivalent conditions. Individual lamp module current and voltage arc also monitored. If a lamp should fail during a test it can be replaced either by turning on another lamp or replacement of the lamp. (Eleven lamps produce one solar constant.) A system for height adjustment of lamps (SHAL) has been fabricated which simulates the optical characteristics of the solar simulator silo. This system allows a new lamp module to be adjusted for maximum output and desired uniformity outside of the system and replaced in its respective position without terminating operation of the solar simulator during a test.

The maintenance operations are performed between test runs. This involves checking lamp module current monitors and their power supply adjustments and checking for any damaged or degraded optics. The effects of degradation is a primary problem. The expected lifetime of the system's various optical components is stated below:

2.5 KW Xenon Lamps 800 hrs (replacement)

Aluminized Aconic Collectors	400 hrs (realuminized)
Aluminized Turning Flat	300 hrs (realuminized)
Uniformity Filter	250 hrs (replacement)
Black Paints	1000 hrs (repainted)

Degradation affects the total irradiance and the spectral irradiance of the test volume. The spectral irradiance of the system, with more than 400 hrs. operating time accumulated, is shown in Figure 8.

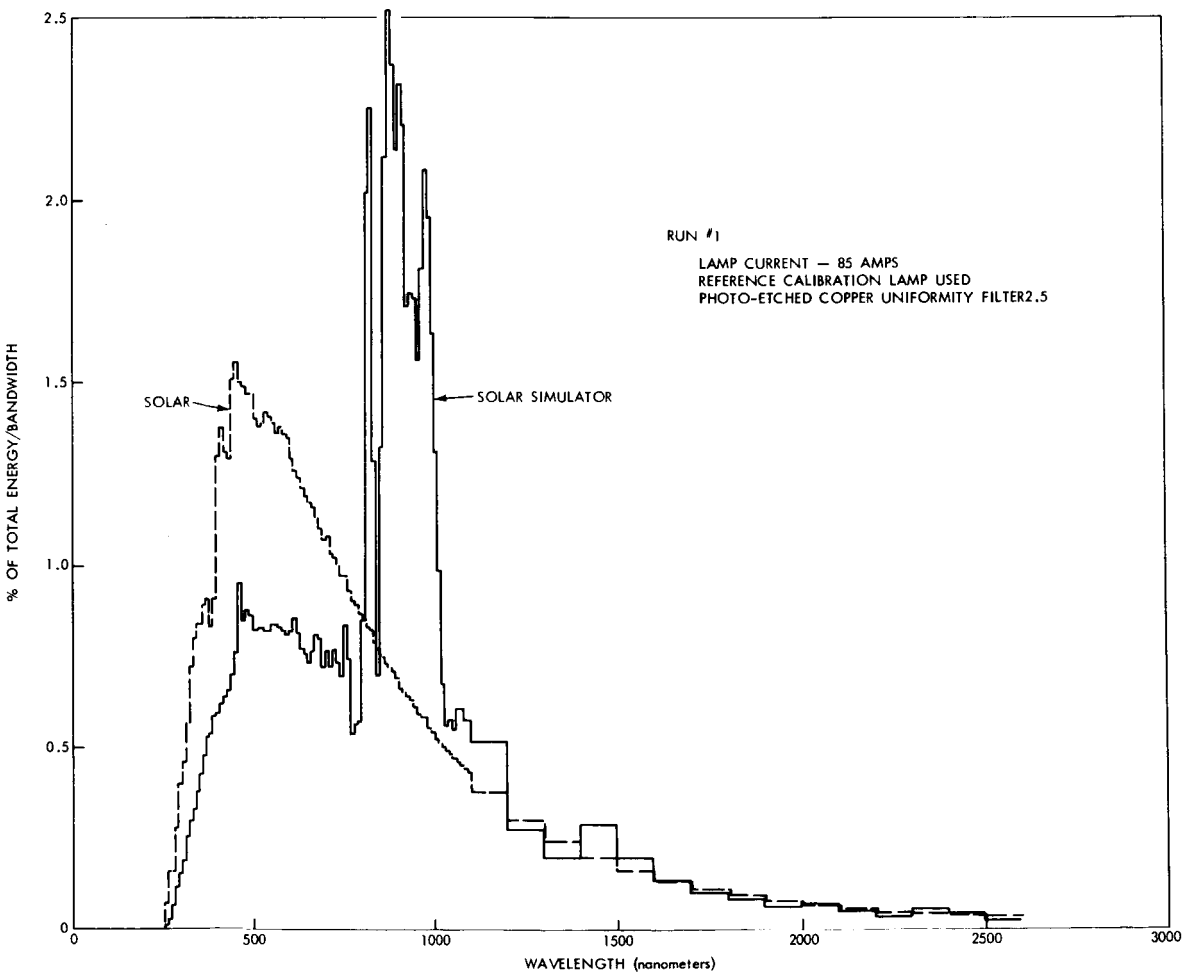

Figure 8—Spectral Irradiance of Simulator After 400 Hours

Comparing this curve with the curve of Figure 7, the effects of the degradation becomes obvious in the ultraviolet and visible regions. This degradation process is observed periodically by comparing total irradiance measurements and spectral irradiance measurements taken at different test time intervals. The effects of degradation probably are not linear with time but rather an effect that becomes more critical at a point near the end of the lifetimes indicated. In fact, degradation beyond these points is so rapid, irreparable damage to the components may be caused.

Modifications and Improvements

The uniformity filter used in this system has been the source of some problems. The diagram in Figure 2 shows that the filter is necessarily placed in an area where the simulated solar energy is converging. At this point, the irradiance is filtered so as to produce a uniform field. This uniform field is placed at the focal point of the projection lens assembly which in turn is placed at the focal point of the large collimator. This uniform field is accomplished with a filter whose transmission varies with the radial distance from its center (see Figure 9). The filter, is exposed to energy ranging from one hundred solar constants in addition to a concentration of ozone of eight (8) parts per million (PPM) when the GN_2 system is not used. These are severe conditions to withstand for periods of time in excess of 200 hrs.

Two methods of fabricating these filters have been used on eight types of metal films. The basic filter construction consists of vacuum deposited metal on an eight (8") inch diameter one eighth (1/8") inch thick ultraviolet transmitting quartz blank. The first method, used by Spectrolab, is the process of photoetching a dot pattern which is obtained by using a halftone screen and

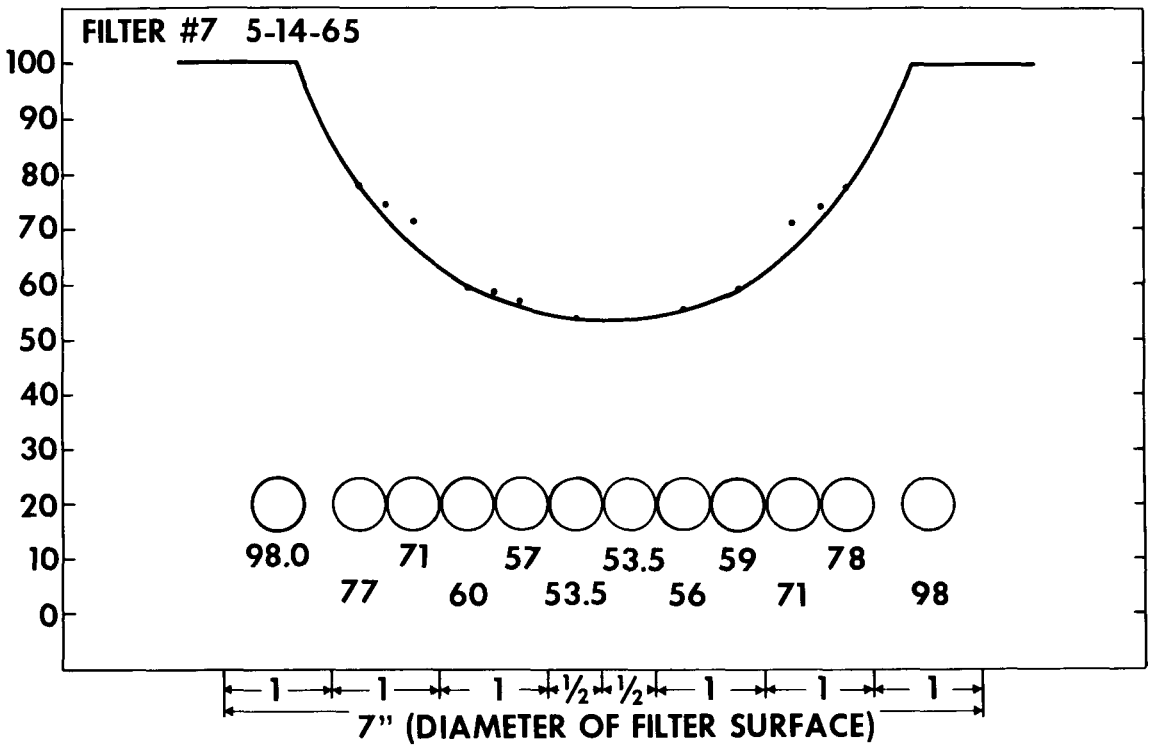

Figure 9 — Transmission of Uniformity Filter

photoetching process[2] on the quartz blank, previously coated with an opaque metal film. This gives the desired transmission as a function of radial distance (see Figure 2). Each dot in this case is completely opaque; no energy is transmitted where dots are and total energy is transmitted in the remaining area. This filter using aluminum is durable under these conditions but is sensitive to its position with respect to the field lens focal point in that these dots cause aberrations which are noticeable in the test volume. These dots have scaled off in the past causing hot spots at a corresponding position in the test volume when other types of metal were used i.e., copper.

A second and more successful method has been used to fabricate a more acceptable filter using a variable transmission neutral density filter. This

filter is fabricated in a vacuum chamber using a point source of deposition material and a rotating mask to achieve the transmission curve shown in Figure 9. Gold, Haynes Metal, Aluminum, Nickel, Platinum, Inconel and Titanium have been tried. The most satisfactory material was found to be platinum with a nine quarter wavelength (at 5460Å) silicon oxide coating (Si Ox). This silicon coating serves two purposes: 1. to protect the platinum from the ozone atmosphere and 2. to increase the emissivity of the filter enabling it to run at a cooler operating temperature. This filter has not shown any undesireable absorption band filtering characteristics that might be expected with this techniaue and is quite satisfactory.

It must be pointed out that this system will not require a uniformity filter of this type with an integrating (or lenticular) lens system; however, this type of filtering can be useful in other applications.

A problem existed in that the large sixty inch (60") collimating mirror contained in the vacuum chamber would reach temperatures in the range of -50°C (223°K) in the presence of a liquid nitrogen shroud during a test. When the test was terminated and the system returned to atmospheric pressure and ambient temperature, the collimating mirror remained cold and silicone diffusion pump oil condensed onto the mirror. This was prevented by installing a combination radiation shield and heater unit of 100 watts capacity on the back of the mirror. The temperature of the mirror is maintained at 30°C (300°K) which gives the approximate effective radiation of a 50°K black body.

Future plans

This system, while operating quite satisfactorily within its prescribed limits has the capability of maintaining much more desirable specifications

for thermal design of spacecraft if several changes in basic hardware components are made. These expected improvements are shown in Table IV.

The maximum continuous test time has been reduced to 250 hours because the increase in lamp wattage is expected to degrade the aluminum components at an increased rate. The uniformity of irradiance will be improved to ±5% deviation from the average with a lenticular lens system The spectral irradiance is expected to match that shown for the Radiometry Research Simulator[3] by using a Spectrolab spectral filter.

These two items have been contracted to Spectrolab for delivery in 1965. The specifications for the items are shown in Appendix I.

Summary

1. The Spectrolab A-1200 Solar Simulator delivered at GSFC met contract specifications and operates satisfactorily within these limits.

2. Several improvements were necessary to enable the solar simulator system to operate in a compatible fashion with the space simulator chamber.

3. The system possesses the potential to be modified to meet specifications comparable to present "state of the art" requirements by improving or changing hardware components.

REFERENCES

1. "Solar Simulation Research" C. Duncan - Proceedings of 3rd Solar Simulation Conference July 1965.

2. "Printed and Integrated Circuitry" T. D. Schlabach, D. D. Rider, McGraw Hill Book Co., N. Y., N. Y. 1963.

3. "Radiometry Research Simulator" D. Gallagher and R. McIntosh - Proc. of 3rd S. S. Conf. - July 1965

Table IV

PROJECTED PERFORMANCE SPECIFICATIONS FOR SOLAR SIMULATOR

MEASUREMENT	SPECIFICATION	METHOD	ACCURACY AND DATE ATTAINABLE
TARGET AREA SIZE	72"-96" DIA. 7' DEEP	ENLARGED COLLIMATING DEVICE	1/67
RADIANT FLUX DENSITY	2.5 SOLAR CONSTANT	(1) LARGER WATTAGE LAMPS (2) REVISED OPTICS	6/66
TEMPORAL VARIATIONS IN RADIANT DENSITY	SHORT TERM $\pm 2\%$ $\frac{\text{PEAK}}{\text{AVG.}}$		
	$< 1\%$ $\frac{\text{TOTAL RMS}}{\text{AVG.}}$		
	LONG TERM 250 HRS.	INCREASED COMPONENT DEGRADATION	
LAMP WARM-UP TIME	30 MIN.		
UNIFORMITY OF RADIANT FLUX DENSITY	$\pm 5\%$	REVISED OPTICS	10/65
	$\pm 2\%$ GOAL		10/66
COLLIMATION ANGLE	2° HALF ANGLE		$\frac{1}{2}$° MAX.-MIN. ARRAY SIZE
SPECTRAL DISTRIBUTION	BANDWIDTH MμMAXIMUM DEVIATION 250-400 $\pm 40\%$ 400-800 $\pm 10\%$ 800-1200 $\pm 15\%$ 1200-2600 $\pm 30\%$	REVISED FILTERING	10/65 $\pm 10\%$ RELATIVE $\pm 15\%$ ABSOLUTE
BLACK SPACE SIMULATION EFFECT	$\pm 2\%$ OF TOTAL	IMPROVED SHROUD DESIGN	
TEST TIME DURATION	250 HOURS	IMPROVED INSTRUMENTATION MONITORING	12/65

ACKNOWLEDGEMENT

The fabrication technique for the platinum uniformity filter was conceived by Albert Busch, Robert Sheehy and Eva Austin, and the Thermal Coating Group of Spacecraft Technology Division.

APPENDIX I

Specifications for A-1200 Solar Simulator

Specifications for Spectral Filter for A-1200

Specifications for Multiple Lens Integrating Optics for A-1200

Spec. No. 63-44
Rev. A
January, 1963

APPENDIX I

NASA/GSFC

SPECIFICATIONS FOR SOLAR SIMULATOR

SYSTEM FOR THERMAL SYSTEMS BRANCH

1.0 PURPOSE

The purpose of the system will be for the general environmental testing, including material studies, solar power systems evaluation, and thermal balance studies. A system of highest standards, yet one within the present state of the art is desired. Versatility, combined with a simplicity of operation and maintenance will be considered a system requirement.

2.0 PERFORMANCE REQUIREMENTS

As a minimum the initial installation shall meet the following requirements:

2.1 Illuminated Area

An approximately circular beam 110 cm in diameter shall illuminate the horizontally oriented test volume. This volume will be considered to be defined by a surface generated by three (3) coaxial, parallel, circles of diameter 100, 110, and 100 cm, respectively, and spaced 60 cm apart, left to right.

2.2 Intensity

2.2.1 Level

The intensity of illumination will be variable from 50 to 140 mw/cm^2.

2.2.2 Constancy

The intensity of illumination shall be automatically controlled to maintain an rms level within 1% for variations less .1 second, a constant level within ±1% for periods of 1 hour, and ±2% for long term variations over a 24-hour period.

2.2.3 Independence

Other performance parameters of the solar simulator system, including spectral distribution, uniformity, and size of beam, shall not vary, or be a function of, the simulator intensity level.

2.3 Collimation

The beam shall be collimated within ±2° at any point within the illuminated area.

2.4 Uniformity

The illumination shall be uniform within ±10% for any 15 cm diameter area in the specified test volume. It shall also be a design goal that the illumination shall be uniform within ±10% for any 10 cm diameter area in the specified test volume. The simulator system shall be so designed that up-grading in uniformity to within ±5% may be provided at a later time.

2.5 Cold Black Space Simulation

In compatibility with the chamber requirement for cold black space simulation, no uncooled optical element of the simulator shall be in direct line of sight from any point in the test volume.

2.6 Spurious Radiation and Re-reflection

The energy radiated or reflected from a test vehicle that is returned from the simulator optical system to the test vehicle must not exceed 3% of the

total energy originating from the solar simulator that is incident onto the test vehicle. This condition shall be satisfied with a test object equal in dimensions to the largest test zone and of reflectivity equal to .85 or better.

2.7 Spectral Distribution of Illumination

Simulation of the solar irradiance spectral distribution for zero-air-mass as defined by F. S. Johnson's paper "The Solar Constant," Journal of Meteorology, Volume II, No. 6, 431 (December, 1954), shall be considered a design goal. The spectral transmission of the optical elements of the simulator shall be 0.25 to 2.7μ. The simulator system shall be so designed and sized that filtering may be added at a later time to provide very close spectral match over the range of 0.25 to 2.7μ. The proposal shall describe the degree of match to be provided under this effort and the up-grading which can be achieved. The methods for modification shall be discussed.

2.8 Radiation Sources

The solar simulator radiant sources must be continuous in operation and have a minimum of 1,000 hours warranted life. No source shall contribute more than 10% to the intensity in the target volume.

2.9 Control and Instrumentation

All controls will be centralized on a master control console and will include at least the following:

2.9.1 Ganged intensity control for all radiation sources, with intensity control within sufficient resolution to set the level to within ±2% of any desired set point.

2.9.2 Resetable elapsed time indicators for each radiation source.

2.9.3 Volt and ammeter that can be switched to monitor any radiation source.

2.9.4 Master on-off switch.

2.9.5 Individual on-off switch and indicator light for each radiation source.

2.9.6 Cooling control switch and go-no-go indicator with interlock to prevent operation without covering.

2.9.7 All controls and indicator lights must be logically arranged so that the full operational state of the system is clearly indicated at all times.

3.0 DESIGN REQUIREMENTS

The simulator shall be designed to provide a trouble free, minimum, servicing operation. A "turn key" semiautomatic operation is desired. Equipment design shall conform to the following specific requirements:

3.1 Source Assembly

The source assembly shall provide for the simple replacement of lamps with no alignment and only intensity adjustment required.

3.1.1 Failure of one lamp should not result in more than a 10% loss of intensity.

3.1.2 The source assembly with lamp must be easily replaceable, providing a minimum of interference with the test in progress.

3.1.3 The source assembly and optical design should permit sources to be replaced by improved types when they become available, with minimum effect on the remainder of the optical system and space chamber.

3.2 Safety Requirements

3.2.1 Each power supply for ignition of a lamp must be provided with safety interlocks.

3.2.2 All wiring and switches must conform with good commercial practice.

3.2.3 All accessible external surfaces of the solar simulator system shall be sufficiently maintained at safe operating temperature to insure safety to operating personnel.

3.3 Cooling

3.3.1 Complete automatic cooling shall be provided for all components and systems of the simulator requiring such. Any cooling failure should automatically extinguish lamps.

3.3.2 All internal optics viewed at any point in the test volume must be cooled to a sufficiently low temperature so that they radiate less energy than the cold shroud at liquid nitrogen temperature.

3.4 Power Requirements

3.4.1 Unit must be designed for immediate connection into 480/277 3-phase power source.

3.5 Servo Controlled Power Supplies

3.5.1 The simulator system shall provide servo controlled power supplies for automatically maintaining constant intensity of each source.

3.5.2 The power supplies shall contain at least the following features:

(1) The power supplies shall be stable with minimum warm-up period.

(2) Be filtered to provide a current ripple of less than ±2%.

(3) Be compact for mounting in standard 19-inch wide rack and panel mountings no deeper than 24 inches.

(4) Operate with an efficiency exceeding .8 and a power factor exceeding .95.

3.6 Automatic Starters

3.6.1 Automatic starters shall be provided for igniting individual sources.

3.6.2 Each starter shall be automatically turned off after source ignition.

3.6.3 The starter array shall be programmed to start sources so as to minimize starting surge of power.

3.7 Uniformity Requirements

3.7.1 The simulator shall be designed to provide a control of the uniformity in the beam such that up-grading within a uniformity of ±5% may be provided at a later date. (Reference Paragraph 2.4 Specification for uniformity).

3.7.2 The loss of energy from any one source shall not degrade the uniformity in the test volume below the performance specification.

3.8 Area Control

The system shall be so designed that within the specified target region the illuminated area can be controlled and varied at a point external to the vacuum chamber so that smaller irregular test volumes may be illuminated and the heat load on cryogenics reduced when performing tests on small objects.

4.0 INSTALLATION

4.1 Accessibility

4.1.1 The complete external system is to be easily accessible.

4.1.2 The starter bank and power supply racks are to be readily accessible at all times.

4.1.3 The necessary blowers and filters must be accessible for service at all times.

4.1.4 Platforms shall be provided to service all elevated equipment requiring maintenance and service such as the source arrays, starters, power supplies, etc.

4.2 Schedule

4.2.1 The solar simulator unit will be acceptance tested at the Contractor's site in the presence of NASA/GSFC representatives. Such tests shall be performed using Contractor provided measurement equipments certified as to accuracy by the Government representative. The unit shall be ready for acceptance within ten (10) months from award of contract, and actual test dates must be coordinated with NASA/GSFC with sufficient advance notice for preparation.

4.2.2 The solar simulator will be crated and shipped to NASA/GSFC, then uncrated and installed, all under the supervision of the Contractor. Such installation shall be completed within twelve (12) months from award of contract.

4.2.3 Sufficient checks and tests will be performed by the Contractor following installation to verify performance previously obtained in acceptance testing. Such tests shall be completed within two (2) weeks following completion of installation.

4.3 System Compatibility

4.3.1 System must be such that it can be installed into and be compatible with an environmental space chamber with ten (10) feet diameter outside dimensions and containing a liquid nitrogen shield.

4.3.2 An interface specification describing all of the necessary penetrations, shrouds, mounting surfaces, and devices, with tolerances.

4.3.3 An equipment layout drawing showing location of simulator, power supply rack, control console, and their relation to the environmental chamber shall be provided.

5.0 MISCELLANEOUS REQUIREMENTS

5.1 Operation and Maintenance Instructions

The Contractor shall provide an operation and maintenance manual for the system upon final acceptance. The manual shall include:

5.1.1 Instructions for starting, operating, and extinguishing the solar simulator.

5.1.2 A manufacturer's parts list for all part numbers and drawings.

5.1.3 All electrical, pneumatic, cooling system, etc., schematic diagrams.

5.1.4 Maintenance instructions and schedules for the system and all components.

5.2 Training

The Contractor shall train NASA/GSFC personnel in the complete operation and maintenance of the solar radiation simulator. This training shall consist of instruction for a period not to exceed ten (10) man-working days.

Specification for Spectral Filter

1. Lifetime of filter - one year or longer.
2. Spectral match to Johnson's air mass zero solar irradiance to meet or exceed indicated values given in Table I. Spectral characteristics of present Goddard simulator with filter in optical train will be measured by GSFC personnel using 100A bandwidths to 1 micron and 1000A bandwidths from 1μ to 2.6μ. The area under the spectral curve between 2500A and 2.6μ will be set equal to 100%. The energy will be calculated for each of these intervals as a percent of the total energy under the curve and compared with Johnson's values for the same intervals. These values should be within the limits shown in Table I.

Table I

Wavelength Intervals Between	Maximum Deviations
250 mμ - 400 m	±40%
400 mμ - 800 m	±10%
800 mμ - 1200 m	±15%
1200 mμ - 2600 m	±30%

Specification for Multiple Lens Integrating Optics

1. General

The multiple lens integrating optics will replace present field and projection lens with the objective of providing improved uniformity distribution, increased test diameter and additional energy in the target volume.

2. Performance Requirements

Uniformity: ±5% throughout the volume as measured with a 1 x 1 cm detector (solar cell)

Intensity: Equal to or greater than the present with no increase in number of lamps (currently 140 w/ft^2 with 11 lamps)

Spectral Match: Integrating lens system to be capable of accepting components for spectral modification of beam

Diameter: Test diameter in a plane 8 feet from the collimating mirror will be increased to 4 feet.

3. Measurements

NASA/GSFC will provide uniformity mapping of present system prior to initiation of contract. Contractor will be responsible for system installation and initial alignment and measurement. GSFC will provide measurement equipment and technical assistance.

4. Other Requirements

a. The collimation angle may be increased to ±2 degrees.

b. A substitute vacuum sealing flange is desirable.

c. All optical elements to be manufactured from quartz or equal or better grade than presently installed in system.

d. All necessary auxiliary equipment such as cooling provisions, mounting hardware, focusing adjustments, etc., shall be provided.

APPENDIX II

Electronic System of A-1200 Solar Simulator

I. Function

A schematic of the electronic system of the A-1200 Solar Simulator is shown in Figure 10.

The intended functions of the electronic system of the A-1200 Solar Simulator are as follows:

1. Receive as input 460 ±20 volt line 3 phase 60 cps alternating electrical power and rectify this to direct power;

2. Provide on-off manual control of this power;

3. Provide continuous manual control of this power over a range of roughly 20 to 1. The top design value of regulated direct power is 54 KW;

4. Provide regulation to hold either the lamp electrical power or the lamp's total irradiance undisturbed at the level set in 3 above, despite line fluctuations, ambient temperature fluctuations, lamp resistance and efficiency variations. The effects of power supply to lamp wire resistance variations are also compensated when holding lamp's total irradiance;

5. Provide protective shutdown or prevent starting of entire system or critical components, determine by misplaced starters or current and temperature values.

6. Provide an easily interpreted display of the monitors of system operation;

7. Provide proper direct overvoltage and radio frequency burst for fast dependable starting of the lamps;

8. Provide circulation of a cooling gas around the lamps and a portion of the following optics through a heat exchanger where a liquid coolant loop may receive part of the heat produced by lamp and optic inefficiencies;

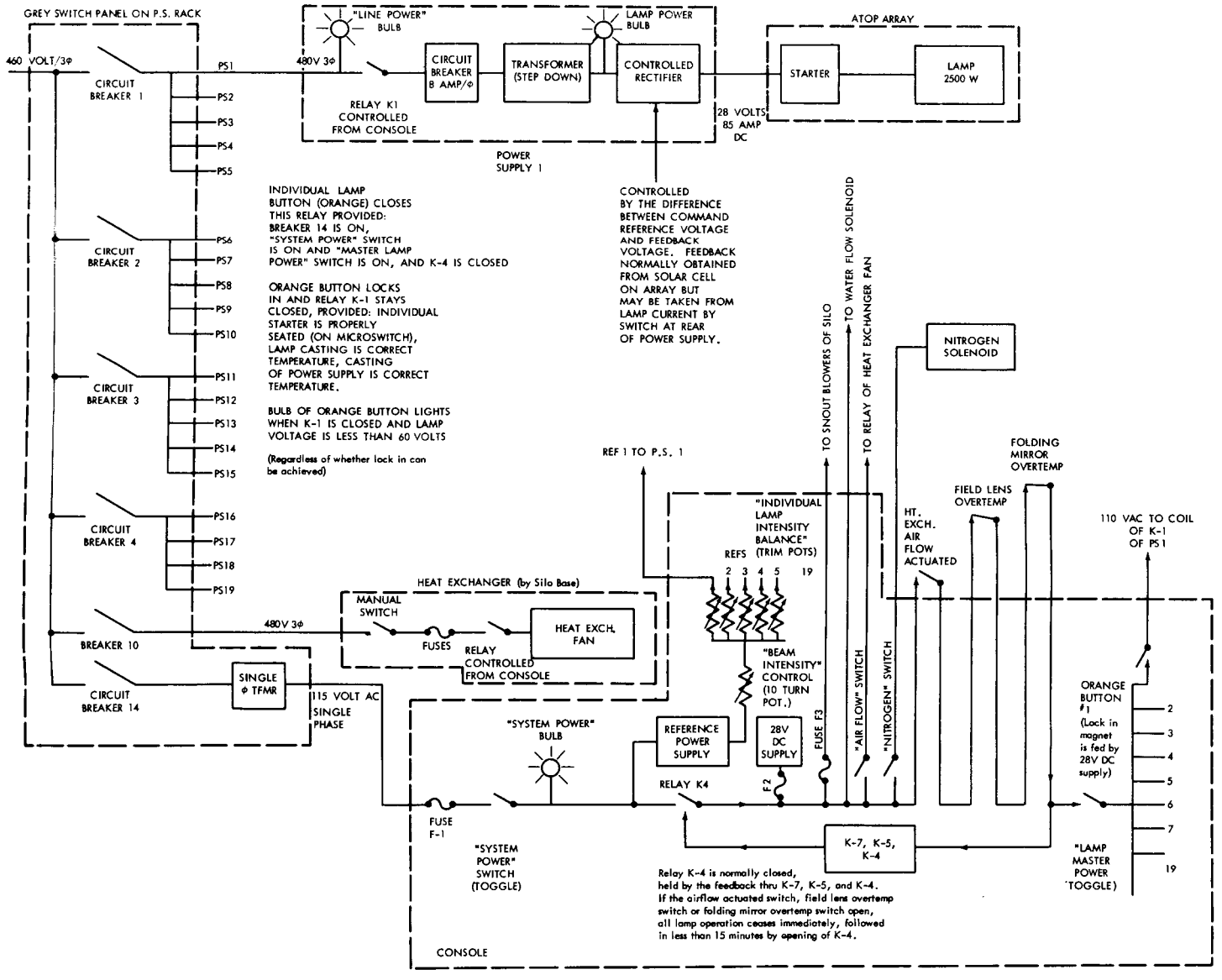

Figure 10 — Circuit Diagram of Simulator

9. To achieve the above functions with a minimum of electric shock hazards to personnel, with long times between failures, and ease of repairs when failures occur.

II. Design

The design of the electronic system of the simulator shows the intent to achieve the above functions by the following features:

1. The input transformers to the individual power supplies, (nineteen modular power supplies are used) are arranged in 460 volt ungrounded neutral to low voltage delta followed by a six diode 3 phase bridge of which 3 diodes are silicon control rectifiers. These are in turn followed by a choke and a pi filter, followed by the lamp.

2. On-Off control is exercised by manual circuit breakers which control several modular power supplies, a manual circuit breaker which provides power only to the control console and a manual circuit breaker which provides power to the I-8 function above. All these breakers are normally left on since they are all in series with more discriminating switches located at or controlled from the control console. These series switches for individual lamp operation are the relays K-1 of individual power supplies. To energize a K-1 relay of any individual supply, console switches "System Power", "Lamp Master Power" and a numbered push botton corresponding to the supply must be thrown.

The series switches for the I-8 function are a manual disconnect (normally left closed) and a relay controlled by the "Air Flow" push button at the console.

3. Total irradiance in the test volume can be controlled by the number of lamps operated at any one time. Nineteen lamps are in the array. A single 10 turn potentiometer on the control console which commands all power supplies

allows fine tuning of the total irradiance. This potentiometer controls smoothly any individual power supplies which are on, over a ±12% range about the 2.5 KW center. Center conditions for the reference as supplied to each supply is 57 mv from a 100 ohm source. This corresponds to 85 amps through and 30 volts across an operating lamp. A power gain of 500 for swings about this center when negative feedback from either the current shunt or the transducer is properly connected, insures a near linear relationship between reference voltage and lamp radiant output. Because of the gas regulator like I-V characteristic of the lamps, only the current through the lamp is varied linearly by the reference voltage with consequent linear radiant power change.

4. Susceptibility of lamp radiant output to disturbances is reduced by negative feedback from a solar cell which views the fireball of an individual lamp. The output of this cell is loaded for near linearity and compared to the reference voltage for this lamp. If the lamp output is high, solar cell voltage output is proportionally high relative to reference; an error signal is developed which after amplification lowers the duty cycle of the full wave rectifier bridge to correct the original condition. The same error reenergizing action occurs for low lamp conditions. A high open loop gain, stabilized by negative feedback taken from the radiant power of the lamp, is intended to reduce the influences listed in A-4 above.

5. Protective shutdowns of the entire system are intended to stop all lamp operation but to allow circulation of the water coolant and gas nitrogen coolant for a time adjustable to 15 minutes maximum after the fault. After this time both these are also stopped. These conditions which are intended to cause such a shutdown are over-temperature on the folding

mirror, over-temperature on the field lens housing or loss of actuation of the gas cooling flow switch.

Each individual supply is intended to be protected by series string of interlock switches which sense the placement of starter, temperature of lamp base casting, and rectifier heat sink temperature. Opening of any one of these stops the power supply concerned without affecting any other supply. In addition each supply contains a 3 phase thermal circuit breaker on its input leads for protection against those faults which manifest as over-current input.

Partial system shutdown is intended to take four supplies out of use together upon over-current sensed in the sum of the input currents feeding the four supplies. This feature is achieved by using one panel type circuit breaker for four supplies.

6. These events are shown on an array of indicator lights, visible toggle switches, lighted push buttons, panel meters, and elapsed time recorders arranged on a control console panel show this intent. At this single location it is possible to determine whether primary power is available to the whole system and any of its parts. It is possible to determine whether cooling water flow to the silo exists, and whether circulating gas flow exists in the silo. It is possible to determine the state of any lamp i.e., off, starting cycle, or running. It is possible to read lamp current, voltage, feedback transducer output and accumulated lamp hours of use for any lamp. It is possible to determine whether the protective interlock loop is intact for each lamp and whether the automatic system shutdown loop is intact. If automatic shutdown loop is not intact it is in some cases possible to isolate the location of the break. It is also possible to sense over-temperature in the SCR heat sinks of the power supplies.

7. The individual power supply consists of a heavy current low voltage controlled rectifier supply connected to one input of an OR gate with a 100 volt low current supply connected to the other input. The lamp is fed by the output which rises above 100 volts assuring part of the conditions for starting. Atop each lamp cage with short fixed post leads,an easily interchangeable R.F. starter is installed. This starter derives its energy from the lines feeding the lamp and releases this energy when the low voltage has reached a high enough point for starting. The energy is released as a burst of approximately 30KV at 4 Mc and coupled to appear across the lamp electrodes.

8. The main cooling gas circulation is accomplished by a 460 volt 3 ϕ fan installed adjacent to the heat exchanger. Direction of flow is consistent with natural convection in the silo. The heat exchanger is cooled by water at about 20°C inlet temperature. Secondary circulation of gas in the snout of the silo, where the main flow does not efficiently intrude and high light beam intensities occur, is intended to be achieved by two small squirrel cage fans drawing from and returning to the silo base.

9. The highest voltage location of the system which is the starter output during the brief starting burst is well covered by the starter top hat. To reach the high potential, approach would have to be made from an ajacent starter hole in the silo cover. Furthermore the post and stud connectors of the removable starters prevent energizing the starter out of its socket. The second highest voltage is input 460 and this is conducted in completely insulated plugs and receptacles. The voltage across an operating lamp poses no shock problem but a potential source of welding intensity heating to accidental short circuits. These same terminals pairs also rise above 100 volts during a starting cycle. Intent

to keep them harmless to personnel is shown in castellated insulation around the terminal posts as they emerge from the individual power supplies and their complete coverage by the starters at the lamp end.

The use of modular supplies mounted in racks with completely independent controls and cabling lengths long enough to permit an operating supply to be internally examined without complete removal from rack show the intent of easy maintenance. This approach also allows keeping supplies in reserve to replace any that might fail in service. Within supplies most of the small electrical components are mounted in a printed circuit card which is interchangeable to any other supply by a simple plug-in type connector.

III. Operational Experience

1. The line voltage as now supplied to the simulator system averages 480 V line-line at no load and 470 volts loaded by 16 lamps at 85 Amps D.C. output. With the ±16 volts swing expected, when one lamp only is in use, system may see 496 volts. During a run over several days and a quantity of lamps from one to twelve, a recording of line showed extremes of 460 and 490. The effects of an average high or low line are believed to be slightly degraded time stability specifications on the light output, decreased ability of power supply tracking of reference, and increased stress of components (high line) in the preregulator part of the individual power supplies. However the only component failure which can be definitely attributed to the high line condition was in the small power supply used to provide reference voltage to all supplies. It is fed by a step down transformer from the 480 line. Tantalum capacitors located in this supply were of marginal rating and are believed to have failed from over-voltage soon after December 1964, and the symptom, rapid ±2% variation of total target area light

intensity existed until they were replaced by higher rated components in May. (The trouble was such as to permit the reference supply to operate but with much greater output susceptability to input variations, hence the total light, commanded by the reference changed in synchronism with line variations.)

When the last 3 lamps are installed and a test has been made on the supply reference tracking ability versus line voltage, decisions will be made as to rewiring with lower impedance line and requesting a lower no load voltage.

The 600 volt rated "Twist Lock" plugs used to connect power supplies to the power supply rack for 460 feed failed by short circuit in three cases at random in the first 100 hours. In all cases the panel circuit breakers opened properly but one supply suffered welding of contacts on one phase of its K-1 relay. The Twist Lock plug secures the conductors out of sight of the man assembling, so misassembly is easy. All plugs have been replaced with nylon shell Bryant types which secure each conductor separately and in sight. No further such failures have occurred.

2. The on-off controls have operated well with the exception of contacts of relay K-1 in several supplies which have welded on one or more phases making shutdown from the console impossible and requiring that the supply be removed and contacts freed and dressed. Another exception has been the "system power" toggle switch which upon a short in the console failed open circuit before fuse F-1 could blow.

3. The resolution of the 10 turn "Beam Intensity" control has proven adequate in all tests, and the crosstalk between the light from the fireball of a particular lamp with straylight from other lamps falling on solar cell of the particular lamp has not been objectionable. Tight tracking of power supply amperages as

the beam intensity is increased from the design and alignment center value of 85 amps has not yet been achieved. At an average current of 95 amps over 12 lamps the extremes are 89 and 100 amps judged from individual current meters one point calibrated at 85 amp. The most useful alignment for tracking will be such that a single uniformity run made at the 85 amp level will be unchanged at any intensity level in the ±12% range. To get this it is necessary that the radiant wattages track, regardless of slight lamp current nontrack and consequent reduction in the range of variation. When the effect of line voltage on tracking is known; tests will be run to determine whether the radiant wattages track the reference.

4. The feedback solar cell tranducers required modification of their mounts to bring them to a position where the output of all could produce 57 mv at lamp 85 Amp with at least ±10% adjustment range. After 200 hours of running a realignment was made and the combination of degradations had resulted in only a 2% drop in cell output. Among the 16 error amplifier cards which have now accumulated about 400 hours each, there have been only two troubles. One card developed drift, the cause of which has not been determined. Another lost the common heat sink on the input transistors due to loose fit but has not given trouble since replacement. Ripple on the total simulator light output was determined for 60 cps and its harmonics by exposing a solar cell loaded for linearity and applying this to a wave analyzer tuned to the successive frequencies. The RMS values taken through 480 cps were added RMS wise and divided by the average. The stability over hours and days is measured by the excursions of the output of an Eppley normal incidence pyheliometer cross checked by the temperature of a black detector with a very stable receiving surface.

5. The protective system shutdown involves the risk that after a lamp stoppage by this system, the trouble may clear itself or be cleared by a technician and the whole hot array begin starting to the detriment of the lamp electrodes. Therefore the time delay has been set rather short at 3 minutes. The thermostat opening temperatures are high relative to the running temperatures measured with 16 lamps and these must be rechecked with 19 lamp operation. The components of this system have given no trouble.

The individual interlock thermostats are also high relative to temperatures measured in 16 lamp operation. The leaf type microswitches have been subjected to considerable bending and rebending. Contacts of one of these have become intermittent.

6. A few indicator lamps failed in the first 100 hours of operation, none have failed since. The remainder of the console indicators have been satisfactory. The console fuses are in nonindicating holders mounted in back of console which leads to delay in case of locating and replacing blown fuses.

7. The low voltage requirements for starting have been met at all times. The RF starters have opened in the high voltage coils in 3 cases over 16 starters over 100 starts each. The relays in all starters are of open construction and have developed sticking hinges, sticking contacts and/or high resistance contacts. Changing spring tension and armature travel for higher speed and dressing the contacts has given usable performance. The manufacturers have built a solid state version of the relay and will provide them at no cost in the near future to replace the originals. The interchangeability and small size of starter have proven very useful.

8. No electrical troubles have occurred in the gas cooling loop.

9. No R F shocks, no 460 volt shocks and no welding burn type injuries have occurred. Several light 110 VAC shocks have been received by men brushing the terminals of the thermal switches on the folding mirror and field lens housing without turning off "System Power Switch". The insulation on these has been improved subsequently. Several very slight shocks have been taken from undischarged capacitors after unsuccessful start attempts.

10. The low voltage feedthru of individual supplies are simple 1/4 inch studs without positive locking against rotation. These have loosened in several supplies causing high resistance joints which generated heat enough to melt solder and damage components.

Appendix III. Computer print out of spectral irradiance of simulator using Platinum with SiOx uniformity filter.

WAVELENGTH INTERVAL CONTAINING 1% OF THE TOTAL SOLAR ENERGY LYING BETWEEN 250NM AND 2500NM		PERCENTAGE OF THE TOTAL TEST LAMP ENERGY BETWEEN 250NM AND 2500NM WITHINTHE INTERVAL	PERCENT ERROR OF TEST LAMP DISTRIBUTION WITH REFERENCE TO THE SOLAR DISTRIBUTION
250.0	296.7	0.835	-16.495
296.7	316.3	0.870	-12.966
316.3	330.5	0.765	-23.505
330.5	342.4	0.770	-23.009
342.4	353.9	0.737	-26.338
353.9	365.1	0.982	-1.822
365.1	375.8	0.886	-11.380
375.8	387.1	1.097	9.716
387.1	397.9	0.950	-5.046
397.9	406.0	0.759	-24.088
406.0	413.2	0.741	-25.945
413.2	420.2	0.751	-24.950
420.2	427.6	0.556	-44.426
427.6	435.0	0.753	-24.705
435.0	442.2	0.785	-21.525
442.2	448.6	0.612	-38.785
448.6	454.8	0.683	-31.651
454.8	461.0	0.772	-22.770
461.0	467.2	0.828	-17.244
467.2	473.5	0.847	-15.301
473.5	479.7	0.744	-25.585
479.7	486.3	1.007	0.679
486.3	492.9	0.740	-25.984
492.9	499.4	0.721	-27.895
499.4	506.3	0.925	-7.457
506.3	513.2	0.669	-33.080
513.2	520.2	0.889	-11.070
520.2	527.2	0.670	-33.032
527.2	534.1	0.895	-10.463
534.1	540.9	0.665	-33.528
540.9	547.7	0.656	-34.416
547.7	554.6	0.861	-13.948
554.6	561.6	0.635	-36.540
561.6	568.7	0.832	-16.832
568.7	575.7	0.613	-38.708
575.7	582.8	0.802	-19.811
582.8	589.9	0.589	-41.067
589.9	597.0	0.770	-23.035
597.0	604.4	0.658	-34.168
604.4	611.9	0.923	-7.724
611.9	619.6	0.456	-54.407
619.6	627.3	0.901	-9.890
627.3	635.2	0.887	-11.258
635.2	643.3	0.441	-55.916
643.3	651.4	0.879	-12.121
651.4	659.7	0.431	-56.860
659.7	668.0	0.864	-13.621
668.0	676.5	0.880	-11.980
676.5	685.2	0.929	-7.132

685.2	694.1	0.445	-55.469
694.1	703.1	0.825	-17.478
703.1	712.1	0.842	-15.754
712.1	721.5	0.836	-16.446
721.5	731.0	0.851	-14.858
731.0	740.7	0.852	-14.817
740.7	750.6	0.813	-18.658
750.6	760.6	0.874	-12.627
760.6	771.0	0.915	-8.547
771.0	781.8	0.757	-24.297
781.8	792.7	0.700	-30.016
792.7	803.9	0.687	-31.312
803.9	815.3	1.402	40.224
815.3	827.1	2.029	102.933
827.1	839.2	2.035	103.500
839.2	851.7	1.724	72.429
851.7	864.7	0.679	-32.107
864.7	878.1	1.684	68.377
878.1	891.7	3.014	201.449
891.7	906.0	2.907	190.711
906.0	920.8	2.744	174.407
920.8	935.9	2.227	122.748
935.9	951.7	2.342	134.238
951.7	968.2	1.953	95.304
968.2	985.1	2.522	152.197
985.1	1003.0	1.804	80.380
1003.0	1021.9	4.125	312.468
1021.9	1041.4	1.242	24.217
1041.4	1061.8	0.901	-9.883
1061.8	1083.2	0.884	-11.567
1083.2	1106.2	1.101	10.066
1106.2	1131.7	0.889	-11.095
1131.7	1157.2	0.611	-38.899
1157.2	1182.7	0.811	-18.906
1182.7	1210.2	0.902	-9.817
1210.2	1242.1	0.551	-44.929
1242.1	1273.9	0.644	-35.566
1273.9	1307.2	0.675	-32.545
1307.2	1346.8	0.483	-51.677
1346.8	1386.4	0.542	-45.774
1386.4	1432.0	0.729	-27.083
1432.0	1480.7	1.198	19.796
1480.7	1536.1	0.734	-26.571
1536.1	1595.7	0.789	-21.077
1595.7	1666.9	0.736	-26.448
1666.9	1747.0	0.750	-24.985
1747.0	1840.6	0.626	-37.448
1840.6	1952.3	1.107	10.681
1952.3	2087.9	1.115	11.505
2087.9	2264.1	0.620	-37.971
2264.1	0.	0.073	-92.677

INTERVAL (IN NMS)	TEST LAMP ENERGY PERCENT TOTAL PER 10NM WAVELENGTH INTERVAL	SOLAR ENERGY PERCENT TOTAL	WAVELENGTH (IN NMS)	PERCENT ERROR
10.0	0.030	0.072	255.0	-59.05
10.0	0.084	0.166	265.0	-49.22
10.0	0.165	0.166	275.0	-0.55
10.0	0.276	0.290	285.0	-4.87
10.0	0.354	0.456	295.0	-22.26
10.0	0.422	0.476	305.0	-11.43
10.0	0.475	0.590	315.0	-19.47
10.0	0.547	0.746	325.0	-26.67
10.0	0.618	0.828	335.0	-25.37
10.0	0.701	0.870	345.0	-19.39
10.0	0.783	0.870	355.0	-10.00
10.0	0.853	0.922	365.0	-7.48
10.0	0.902	0.942	375.0	-4.32
10.0	0.918	0.859	385.0	6.85
10.0	0.958	0.942	395.0	1.71
10.0	0.935	1.346	405.0	-30.54
10.0	0.932	1.429	415.0	-34.80
10.0	0.930	1.357	425.0	-31.44
10.0	0.962	1.336	435.0	-28.02
10.0	1.003	1.564	445.0	-35.85
10.0	1.174	1.615	455.0	-27.33
10.0	1.408	1.605	465.0	-12.30
10.0	1.293	1.595	475.0	-18.92
10.0	1.249	1.522	485.0	-17.95
10.0	1.219	1.522	495.0	-19.92
10.0	1.150	1.450	505.0	-20.65
10.0	1.111	1.429	515.0	-22.26
10.0	1.116	1.439	525.0	-22.46
10.0	1.116	1.470	535.0	-24.12
10.0	1.093	1.460	545.0	-25.14
10.0	1.068	1.439	555.0	-25.80
10.0	1.042	1.408	565.0	-26.00
10.0	1.016	1.429	575.0	-28.89
10.0	0.988	1.408	585.0	-29.85
10.0	0.959	1.398	595.0	-31.39
10.0	0.932	1.336	605.0	-30.23
10.0	0.915	1.305	615.0	-29.84
10.0	0.901	1.284	625.0	-29.82
10.0	0.887	1.253	635.0	-29.17
10.0	0.882	1.232	645.0	-28.41
10.0	0.869	1.212	655.0	-28.29
10.0	0.864	1.201	665.0	-28.09
10.0	0.880	1.170	675.0	-24.78
10.0	0.929	1.139	685.0	-18.47
10.0	0.864	1.108	695.0	-22.01
10.0	0.823	1.118	705.0	-26.45
10.0	0.847	1.067	715.0	-20.56

10.0	0.834	1.056	725.0	-21.00
10.0	0.863	1.036	735.0	-16.65
10.0	0.831	1.004	745.0	-17.28
10.0	0.818	1.004	755.0	-18.55
10.0	0.933	0.963	765.0	-3.12
10.0	0.834	0.932	775.0	-10.56
10.0	0.716	0.922	785.0	-22.31
10.0	0.692	0.901	795.0	-23.24
10.0	0.695	0.880	805.0	-21.05
10.0	1.050	0.859	815.0	22.15
10.0	2.029	0.849	825.0	138.99
10.0	2.035	0.818	835.0	148.76
10.0	1.331	0.797	845.0	66.98
10.0	0.706	0.777	855.0	-9.13
10.0	0.817	0.756	865.0	8.05
10.0	1.233	0.746	875.0	65.39
10.0	1.980	0.735	885.0	169.36
10.0	2.045	0.715	895.0	186.27
10.0	1.896	0.683	905.0	177.39
10.0	1.910	0.673	915.0	183.83
10.0	1.573	0.663	925.0	137.30
10.0	1.488	0.652	935.0	128.16
10.0	1.614	0.632	945.0	155.51
10.0	1.383	0.611	955.0	126.41
10.0	1.298	0.601	965.0	116.14
10.0	1.481	0.601	975.0	146.51
10.0	1.041	0.570	985.0	82.86
10.0	0.835	0.559	995.0	49.36
10.0	2.253	0.538	1005.0	318.45
10.0	2.180	0.528	1015.0	312.77
10.0	1.073	0.518	1025.0	107.20
10.0	0.574	0.507	1035.0	13.19
10.0	0.489	0.497	1045.0	-1.54
10.0	0.450	0.487	1055.0	-7.52
10.0	0.431	0.476	1065.0	-9.55
10.0	0.442	0.466	1075.0	-5.11
10.0	0.459	0.456	1085.0	0.65
10.0	0.447	0.445	1095.0	0.30
100.0	0.328	0.392	1150.0	-16.37
100.0	0.207	0.314	1250.0	-33.89
100.0	0.132	0.253	1350.0	-47.92
100.0	0.210	0.205	1450.0	2.32
100.0	0.121	0.168	1550.0	-27.75
100.0	0.108	0.139	1650.0	-22.30
100.0	0.075	0.115	1750.0	-34.93
100.0	0.063	0.096	1850.0	-34.97
100.0	0.122	0.082	1950.0	49.61
100.0	0.066	0.069	2050.0	-5.32
100.0	0.040	0.059	2150.0	-31.95
100.0	0.029	0.051	2250.0	-42.48
100.0	0.042	0.043	2350.0	-3.55
100.0	0.037	0.038	2450.0	-3.88

THE RADIOMETRY RESEARCH SIMULATOR

Daniel Gallagher

Roy McIntosh

Radiometry Group, Thermal Systems Branch

Spacecraft Technology Division

THE RADIOMETRY RESEARCH SIMULATOR

Daniel Gallagher

Roy McIntosh*

Radiometry Group, Thermal Systems Branch

Spacecraft Technology Division

ABSTRACT

The Radiometry Research Simulator consists of: A Spectrolab X-25L solar simulator and a General Electric thermal vacuum system. The X-25L solar simulator, has excellent uniformity, one solar constant intensity, 2° half-angle collimation of a 12" dia. beam, and close spectral correspondence to air mass zero solar irradiance. The General Electric ultra clean, high vacuum system has a 10^{-12} Torr vacuum capability and a thermal system which has a range from LN_2 temperatures to 250°C. These two systems combine into a versatile tool for the testing and calibration of detectors, solar cells, coatings, and instrumentations.

*Taag Designs, Inc., employee at GSFC under contract NAS5-2382.

THE RADIOMETRY RESEARCH SIMULATOR

INTRODUCTION

Solar simulators which accurately reproduce the conditions found in space are necessary because of the stringent requirements on accuracy and reliability that are placed on measurements and calibrations for satellite application. A radiometry research simulator has been developed to satisfy these requirements.

This radiometry research simulator consists of a General Electric ultra-high vacuum chamber with thermal control shroud and a X-25L solar simulator developed and manufactured by Spectrolab Inc. - Sylmar Calif. Both units operating simultaneously can produce close solar simulation, ultra-high vacuum, a variety of chamber temperatures and other parameters associated with outer space conditions

X-25L Solar Simulator

The Spectrolab model X-25L solar simulator is a mobile rack-mounted instrument which simulates very closely the intensity, spectral distribution, and uniformity of the sun's rays. The specifications for this system are included as Appendix I.

The X-25L optical system in conjunction with the specially designed lenticular lens array, collects and distributes the radiation from an Osram 2500 watt Xenon short arc lamp onto a plane 12 inches in diameter and 96 inches from the unit. A spectral filter is incorporated within the system to correct the xenon spectrum to the sun's spectrum.

In the lenticular lens system, the lamp energy in the field lens plane is broken up into nineteen parts which are superimposed at the target plane.

The primary part of the optical system is the specially developed source collecting mirror mounted with its focus coincident with the arc of the lamp. The optical contour of this collector is an aconic section that optimizes the energy from the lamp to the optical elements of the system. The light is then directed onto the field lens system where a uniform image is formed. The field lens system then directs the image through the lenticular lens system to the target plane. Figure 1 is an optical schematic of the system.

The X-25L is powered by a regulated D-C power supply. The lamp output is controlled by a closed feedback loop that maintains the intensity selected on the front panel. This feedback is accomplished by a high level solar cell positioned in the collecting mirror where it can see the arc lamp and detect any change in the output. The solar cell signal is then made proportional to the signal set at the control panel and the difference in level is called the error signal which maintains the regulated lamp output.

Also incorporated in the X-25L, is the ability to re-align all of the optical elements after lamp replacement or whenever necessary, plus the added feature of push button control of the beam height over a 24-inch distance.

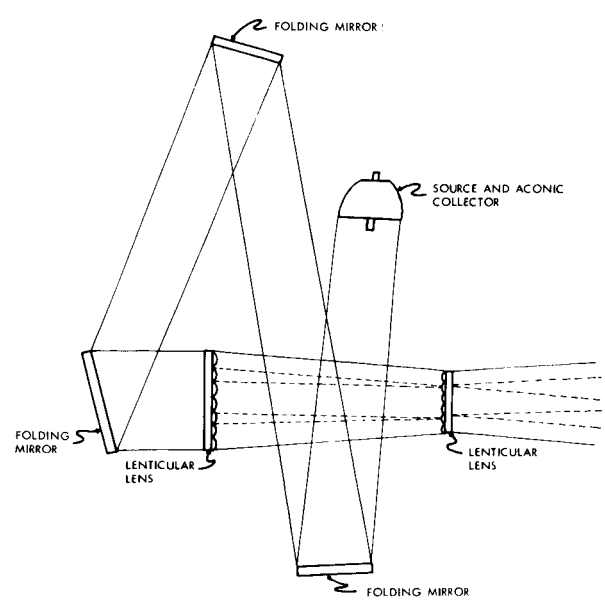

Figure 1—X-25L Optical Schematic

Figure 2 shows the uniformity obtainable with this unit. Note that a uniformity of ±1.1% is obtainable for a 10 inch diameter beam. This measurement was made with a 1cm x 1cm N/P silicon solar cell. The linearity of this detector is shown in Figure 3. The intensity was varied by the use of neutral density filters.

Figures 4 and 5 represent the spectral distribution of the simulator averaged over different bandwidths. Figure 4 is averaged over 100A bandwidths from 2500A to 11,000A and 1000A bandwidths from 11,000A to 26,000A. Figure 5 is averaged over 1000A bandwidths for the entire wavelength interval. Table I is a tabulation of the spectral data based on the bandwidths specified in the procurement for the X-25L, both the spectrolab and GSFC measurements are

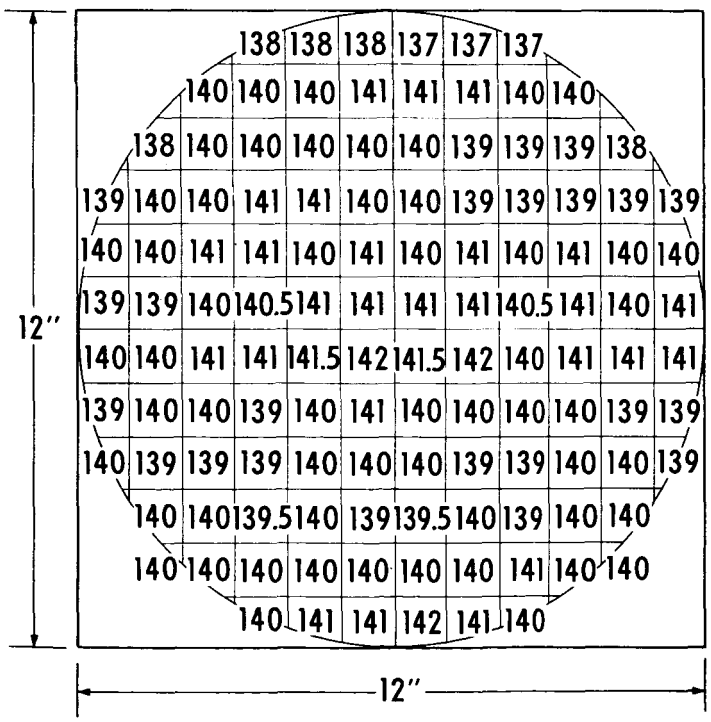

Power Input= 30v, 92 amps

Intensity: Pryl.=136mw/cm²

Epp. Thermo.=146mw/cm²

Uniformity:

13 in. beam = ±2.1%

12 in. beam = ±1.7%

10 in. beam = ±1.1%

Detector:

1cm. × 1 cm. solar cell

Figure 2—Uniformity of the X-25L

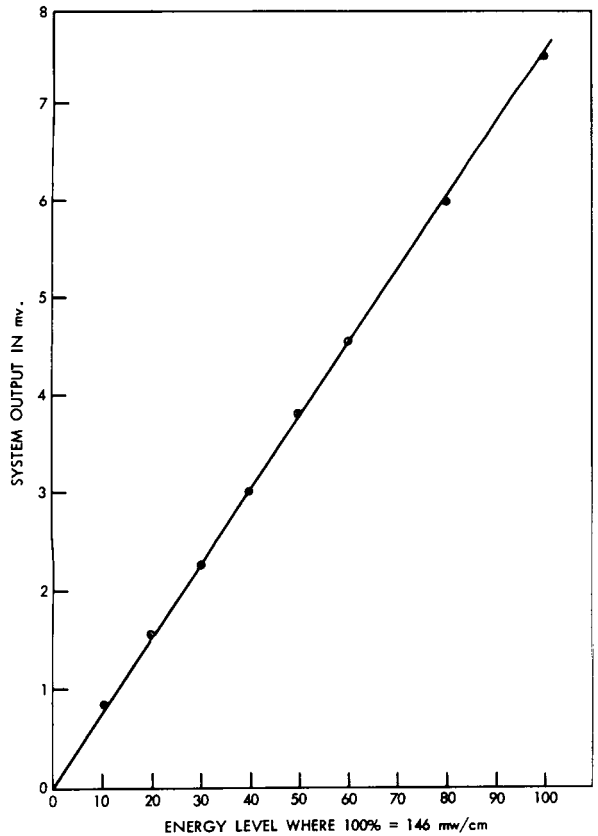

Figure 3—System Output vs Energy for Uniformity Scanner System Linearity

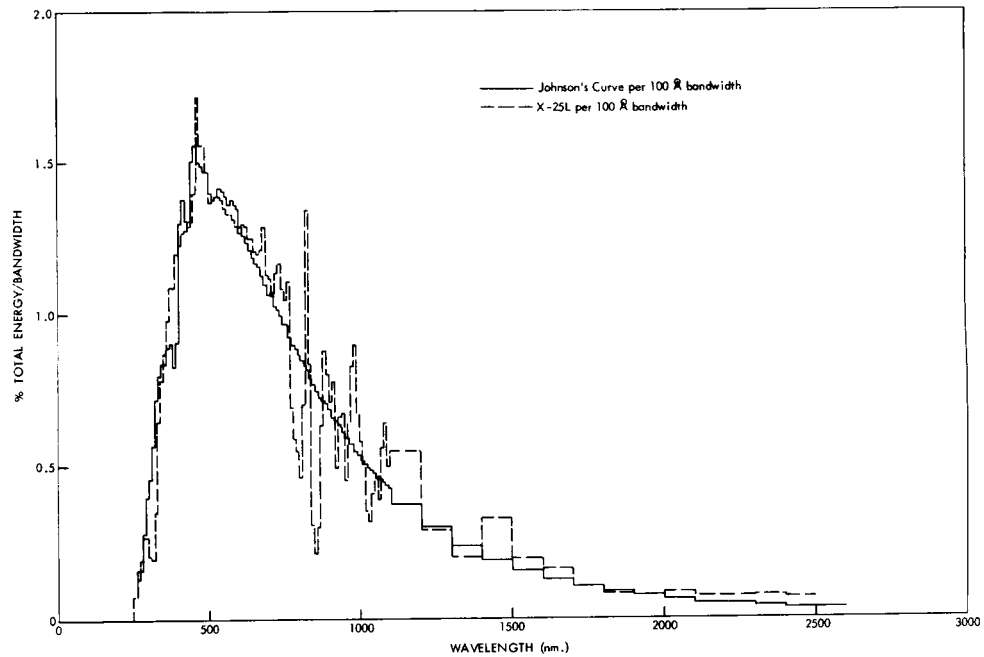

Figure 4—Spectral Distribution Comparison Curves per 10 nm. Bandwidths

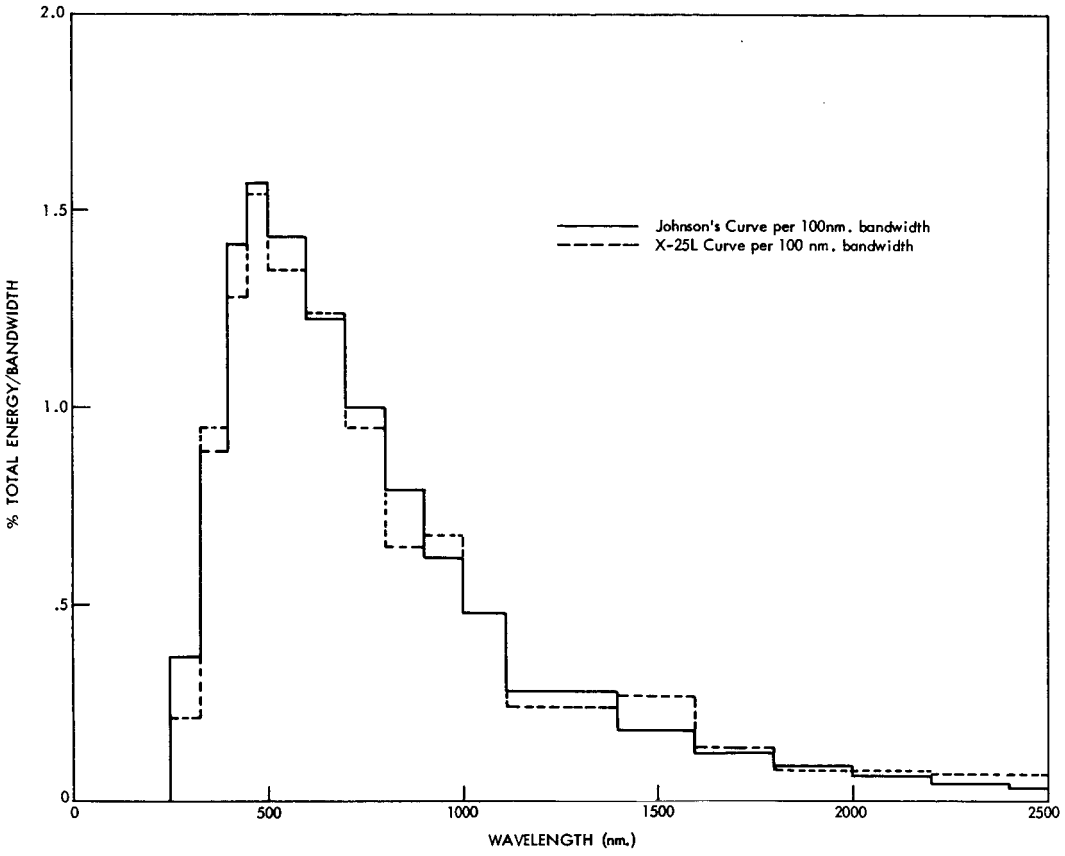

Figure 5—Spectral Distribution Comparison Curves per 100 nm. Bandwidths

Table I

Spectral Distribution of X-25L

Wavelength (in Microns)	% Deviation From Johnson's Curve	
	Spectrolab Computation	NASA Computation
.25 - .33	-30	-43
.33 - .40	+8.5	+6.7
.40 - .45	-9.9	-8.6
.45 - .50	-5.1	-2.0
.50 - .60	-6.8	-5.6
.60 - .70	-.3	+1.6
.70 - .80	-.4	-4.5
.80 - .90	-12.8	-17.7
.90 - 1.0	+9.4	+8.9
1.0 - 1.2	+8.8	+15.0
1.2 - 1.4	-7.1	-12.0
1.4 - 1.6	+37	+44.6
1.6 - 1.8	+2.1	+10.2
1.8 - 2.0	-8.4	-9.0
2.0 - 2.2	+15.1	+28.0
2.2 - 2.4	+35.4	+51.0

Table II

Computer printout of the spectral distribution of the X-25L per 100A bandwidths to 11,000A and 1000A bandwidths from 11,000A to 25,000A. The percent mismatch for each of these bands compared to air mass zero solar irradiance is also shown.

INTERVAL (IN NMS)	TEST LAMP ENERGY PERCENT TOTAL PER 10NM WAVELENGTH INTERVAL	SOLAR ENERGY PERCENT TOTAL	WAVELENGTH (IN NMS)	PERCENT ERROR
10.0	0.073	0.072	255.0	0.10
10.0	0.130	0.166	265.0	-21.81
10.0	0.193	0.166	275.0	16.20
10.0	0.271	0.290	285.0	-6.50
10.0	0.269	0.456	295.0	-40.94
10.0	0.208	0.476	305.0	-56.27
10.0	0.198	0.590	315.0	-66.38
10.0	0.351	0.746	325.0	-52.86
10.0	0.645	0.828	335.0	-22.08
10.0	0.786	0.870	345.0	-9.65
10.0	0.869	0.870	355.0	-0.10
10.0	0.987	0.922	365.0	7.12
10.0	1.088	0.942	375.0	15.45
10.0	1.086	0.859	385.0	26.35
10.0	1.202	0.942	395.0	27.57
10.0	1.230	1.346	405.0	-8.63
10.0	1.273	1.429	415.0	-10.93
10.0	1.278	1.357	425.0	-5.76
10.0	1.313	1.336	435.0	-1.73
10.0	1.316	1.564	445.0	-15.86
10.0	1.403	1.615	455.0	-13.12
10.0	1.723	1.605	465.0	7.36
10.0	1.552	1.595	475.0	-2.69
10.0	1.535	1.522	485.0	0.82
10.0	1.471	1.522	495.0	-3.39
10.0	1.374	1.450	505.0	-5.22
10.0	1.382	1.429	515.0	-3.30
10.0	1.393	1.439	525.0	-3.20
10.0	1.387	1.470	535.0	-5.69
10.0	1.378	1.460	545.0	-5.61
10.0	1.349	1.439	555.0	-6.27
10.0	1.333	1.408	565.0	-5.35
10.0	1.334	1.429	575.0	-6.67
10.0	1.314	1.408	585.0	-6.70
10.0	1.289	1.398	595.0	-7.82
10.0	1.271	1.336	605.0	-4.84
10.0	1.302	1.305	615.0	-0.19
10.0	1.291	1.284	625.0	0.57
10.0	1.252	1.253	635.0	-0.05
10.0	1.252	1.232	645.0	1.58
10.0	1.212	1.212	655.0	0.07
10.0	1.204	1.201	665.0	0.20
10.0	1.224	1.170	675.0	4.58

Table II (Continued)

10.0	1.289	1.139	685.0	13.15
10.0	1.133	1.108	695.0	2.25
10.0	1.119	1.118	705.0	0.07
10.0	1.066	1.067	715.0	-0.02
10.0	1.142	1.056	725.0	8.11
10.0	1.167	1.036	735.0	12.73
10.0	1.081	1.004	745.0	7.62
10.0	1.048	1.004	755.0	4.38
10.0	1.109	0.963	765.0	15.11
10.0	0.683	0.932	775.0	-26.75
10.0	0.590	0.922	785.0	-36.01
10.0	0.548	0.901	795.0	-39.19
10.0	0.462	0.880	805.0	-47.46
10.0	0.705	0.859	815.0	-18.00
10.0	1.346	0.849	825.0	58.47
10.0	0.835	0.818	835.0	2.04
10.0	0.304	0.797	845.0	-61.89
10.0	0.213	0.777	855.0	-72.55
10.0	0.297	0.756	865.0	-60.65
10.0	0.632	0.746	875.0	-15.22
10.0	0.881	0.735	885.0	19.85
10.0	0.796	0.715	895.0	11.42
10.0	0.712	0.683	905.0	4.24
10.0	0.779	0.673	915.0	15.70
10.0	0.494	0.663	925.0	-25.41
10.0	0.659	0.652	935.0	1.06
10.0	0.675	0.632	945.0	6.84
10.0	0.446	0.611	955.0	-26.95
10.0	0.645	0.601	965.0	7.37
10.0	0.827	0.601	975.0	37.76
10.0	0.904	0.570	985.0	58.79
10.0	0.670	0.559	995.0	19.87
10.0	0.581	0.538	1005.0	7.87
10.0	0.497	0.528	1015.0	-5.86
10.0	0.347	0.518	1025.0	-33.03
10.0	0.318	0.507	1035.0	-37.31
10.0	0.411	0.497	1045.0	-17.31
10.0	0.458	0.487	1055.0	-5.86
10.0	0.389	0.476	1065.0	-18.38
10.0	0.563	0.466	1075.0	20.84
10.0	0.644	0.456	1085.0	41.25
10.0	0.494	0.445	1095.0	11.05
100.0	0.551	0.392	1150.0	40.48
100.0	0.287	0.314	1250.0	-8.41
100.0	0.205	0.253	1350.0	-18.71
100.0	0.332	0.205	1450.0	62.16
100.0	0.207	0.168	1550.0	23.48
100.0	0.166	0.139	1650.0	19.71
100.0	0.114	0.115	1750.0	-1.11
100.0	0.082	0.096	1850.0	-14.56
100.0	0.080	0.082	1950.0	-2.22
100.0	0.091	0.069	2050.0	31.23
100.0	0.073	0.059	2150.0	23.87
100.0	0.068	0.051	2250.0	34.30
100.0	0.075	0.043	2350.0	73.48
100.0	0.071	0.038	2450.0	86.11

Table III

Computer printout of the energy contained within one percent bandwidths of the solar irradiance between 2500A and 25,000A. The deviations from solar irradiance for each interval are shown also.

WAVELENGTH INTERVAL CONTAINING 1% OF THE TOTAL SOLAR ENERGY LYING BETWEEN 250NM AND 2500NM		PERCENTAGE OF THE TOTAL TEST LAMP ENERGY BETWEEN 250NM AND 2500NM WITHINTHE INTERVAL	PERCENT ERROR OF TEST LAMP DISTRIBUTION WITH REFERENCE TO THE SOLAR DISTRIBUTION.
250.0	296.7	0.894	-10.616
296.7	316.3	0.405	-59.498
316.3	330.5	0.503	-49.708
330.5	342.4	0.840	-15.961
342.4	353.9	0.820	-18.023
353.9	365.1	1.106	10.577
365.1	375.8	1.061	6.056
375.8	387.1	1.309	30.906
387.1	397.9	1.174	17.434
397.9	406.0	0.977	-2.263
406.0	413.2	1.002	0.153
413.2	420.2	1.026	2.590
420.2	427.6	0.765	-23.530
427.6	435.0	1.038	3.814
435.0	442.2	1.047	4.667
442.2	448.6	0.800	-19.996
448.6	454.8	0.831	-16.883
454.8	461.0	0.886	-11.419
461.0	467.2	1.041	4.130
467.2	473.5	1.042	4.154
473.5	479.7	0.879	-12.142
479.7	486.3	1.235	23.506
486.3	492.9	0.925	-7.532
492.9	499.4	0.846	-15.438
499.4	506.3	1.102	10.155
506.3	513.2	0.823	-17.662
513.2	520.2	1.109	10.869
520.2	527.2	0.836	-16.401
527.2	534.1	1.116	11.579
534.1	540.9	0.827	-17.333
540.9	547.7	0.828	-17.195
547.7	554.6	1.088	8.809
554.6	561.6	0.801	-19.860
561.6	568.7	1.067	6.656
568.7	575.7	0.801	-19.891
575.7	582.8	1.061	6.125
582.8	589.9	0.785	-21.467
589.9	597.0	1.033	3.289
597.0	604.4	0.890	-10.956
604.4	611.9	1.283	28.326
611.9	619.6	0.655	-34.459
619.6	627.3	1.291	29.131
627.3	635.2	1.252	25.237
635.2	643.3	0.623	-37.733
643.3	651.4	1.245	24.466
651.4	659.7	0.597	-40.318
659.7	668.0	1.204	20.364

Table III (Continued)

668.0	676.5	1.224	22.378
676.5	685.2	1.289	28.888
685.2	694.1	0.590	-40.986
694.1	703.1	1.096	9.630
703.1	712.1	1.105	10.490
712.1	721.5	1.079	7.882
721.5	731.0	1.185	18.474
731.0	740.7	1.124	12.418
740.7	750.6	1.038	3.777
750.6	760.6	1.134	13.368
760.6	771.0	0.891	-10.878
771.0	781.8	0.601	-39.341
781.8	792.7	0.580	-41.974
792.7	803.9	0.501	-49.860
803.9	815.3	0.929	-7.062
815.3	827.1	1.346	34.560
827.1	839.2	0.835	-16.523
839.2	851.7	0.403	-59.657
851.7	864.7	0.250	-75.042
864.7	878.1	0.794	-20.642
878.1	891.7	1.283	28.279
891.7	906.0	1.107	10.692
906.0	920.8	1.037	3.696
920.8	935.9	0.895	-10.456
935.9	951.7	0.909	-9.125
951.7	968.2	0.857	-14.266
968.2	985.1	1.732	73.178
985.1	1003.0	0.952	-4.779
1003.0	1021.9	0.980	-1.987
1021.9	1041.4	0.664	-33.596
1041.4	1061.8	0.877	-12.261
1061.8	1083.2	1.104	10.373
1083.2	1106.2	1.525	52.544
1106.2	1131.7	1.209	20.933
1131.7	1157.2	0.904	-9.591
1157.2	1182.7	1.974	97.359
1182.7	1210.2	1.109	10.921
1210.2	1242.1	0.760	-23.984
1242.1	1273.9	1.194	19.410
1273.9	1307.2	0.693	-30.735
1307.2	1346.8	0.758	-24.159
1346.6	1386.4	0.915	-8.517
1386.4	1432.0	1.119	11.871
1432.0	1480.7	1.993	99.340
1480.7	1536.1	1.332	33.160
1536.1	1595.7	1.146	14.603
1595.7	1666.9	1.134	13.448
1666.9	1747.0	1.156	15.551
1747.0	1840.6	0.925	-7.470
1840.6	1952.3	0.877	-12.281
1952.3	2087.9	1.238	23.835
2087.9	2264.1	1.266	26.582
2264.1	-0.0	0.147	-85.323

shown. The differences in the values result from different measurement techniques, instrumentation, and methods of data reduction. Table II is a computer printout of the data for Figures 4 and 5. Table III is a computer printout of the same data averaged over 1% energy bandwidths.

Thermal Vacuum System

The thermal vacuum system used in the Radiometry Research Simulator was manufactured by the Vacuum Products Division of the General Electric Company specifically for this application. It was designed to meet the most rigid requirements of vacuum and temperature necessary to the simulation of space environments which a solar cell or other satellite components might encounter within 500 kilometers of the earth. The specifications for this system are included as Appendix II.

The chamber consists of a bell jar and sump with a shroud lining the interior of both. The useable diameter of the bell jar is 18 inches and the total useable height of the bell jar and sump is 50 inches. A flat circular plate partially separates the bell jar from the sump on which test objects can be mounted. The plate is part of the shroud so as to maintain thermal integrity within the chamber. The shroud is separated from the walls of the chamber by about 3/4 of an inch and is painted with cat-a-lac black paint to minimize internal reflections. The reflectance of the walls is below one percent.

There are two 6 inch diameter ports made of optical quality quartz. These ports are 90° apart so that the earth's albedo can be simulated, if necessary, as well as the normal illumination of the X-25L.

The system was designed to entirely eliminate contamination of the test samples by the vacuum system. No oils or fluids of any type are ever allowed

to enter the chamber. In order to accomplish this, the latest types of vacuum pumps were used.

The roughing system is composed of three molecular sorption pumps which are pre-chilled with liquid nitrogen. The sorption medium in each pump is three pounds of 1/8 inch diameter pellets of zeolite. By using the pumps one at a time it is possible to evacuate the chamber from atmospheric pressure to 20 microns (2.10^{-2} Torr) in an hour.

The system has two types of high vacuum pumps, one General Electric model 22TP300, 500 liter/sec ion pump and four 4000 liter/sec titanium sublimation pumps. It is possible to start both high vacuum pumps at 20 microns. Ion pumps maintain pumping speeds over a wide range of pressures as shown in Figure 6. The power consumed by the pump decreases with pressure as shown in Figure 7. This is in contrast to the pumping speeds and power consumptions of diffusion pumps. With the combination of ion pump and titanium sublimation pump, the system can attain an ultimate pressure of 5.10^{-11} Torr within 18 hours at ambient temperatures and 5.10^{-12} Torr with LN_2 cooling the shroud.

The system is somewhat unique in that the ion pump and titanium pumps are an integral part of the system. The ion pump modules encircles the bottom of the sump and the titanium pumps are in the center of the ion pumps. This means that the pumps are operating directly on and within the system without having to pump through a valve or any constriction which would lower the efficiency of the pumps.

The pressure measuring gauges used in the system are a thermocouple gauge, a nude ionization gauge and a trigger discharge gauge.

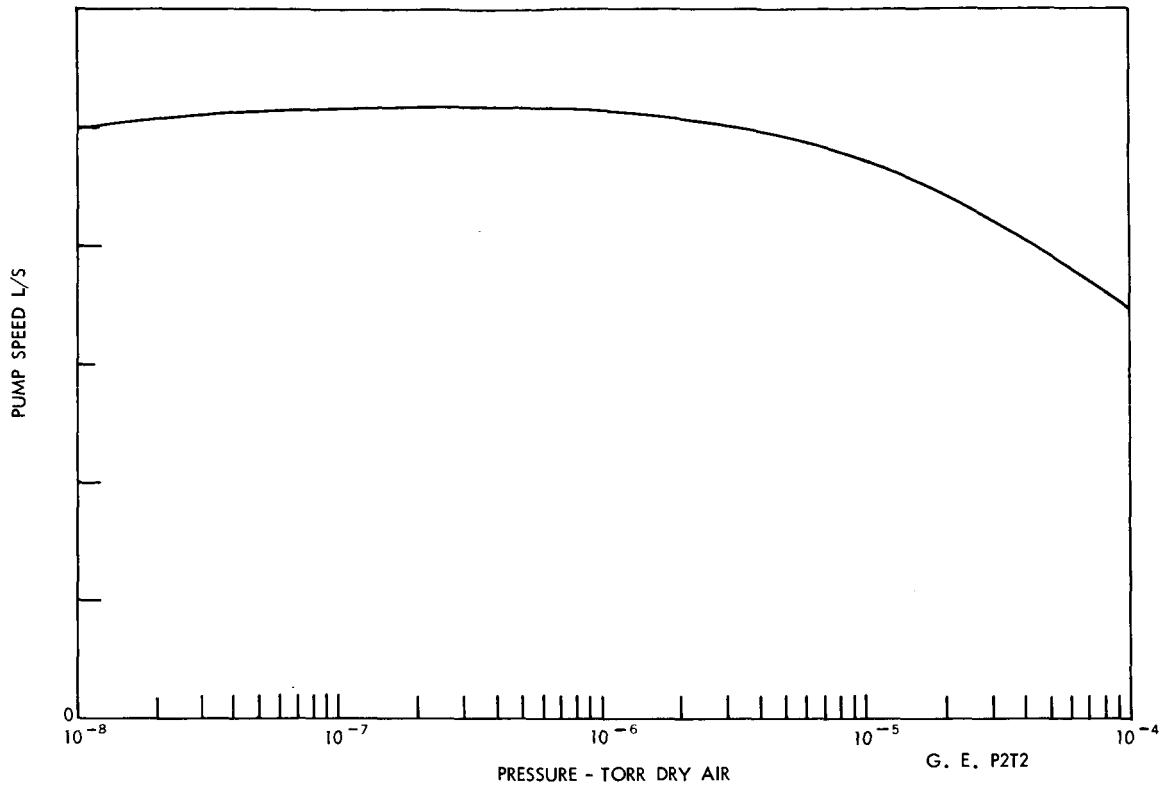

Figure 6—General Electric Ion Pump Characteristic

In order to properly simulate the outer space environment, it is necessary to provide not only a very hard vacuum, but also a wide temperature variation. In this system, the shroud temperature is controlled to within ±5°C over the range of -50°C to +250°C, plus the shroud can also be flooded with LN_2 to reach -180°C. These temperatures and control are obtained by using a heat exchanger manufactured by the Thermotron Corporation. It uses a single silicone fluid (G.E. SF-96-5) to cover the before mentioned ranges. This one fluid system simplifies many problems. Most systems which cover this large range use two or more heat exchange fluids.

When the shroud is to be heated, the silicone fluid is passed through a 35 kw heater which is controlled by a General Electric Type 521 recorder controller

which is in turn controlled by a thermocouple affixed to either the shroud or a test sample. A very high power heater was purposely used in order to provide the very fast response time needed to hold the temperature to ±5°C. The heating process can be further aided by baking the bell jar and ion pump with heaters which have been provided to raise the temperature to 250°C in a very short time. Of course, these bakeout heaters on the bell jar and ion pump are always used during a run (in the range 20 microns) to remove any gas which may have been adsorbed onto or absorbed into the stainless steel walls.

This heating of the shroud, although necessary, nonetheless produces some problems in maintaining a very hard vacuum. For instance if the shroud is run at +250°C the best vacuum which can be maintained is in the range 5.10^{-7} Torr. Of course, this would be a problem in any system and the difficulties decrease as the required temperature decreases.

The cooling of the shroud is accomplished with the same fluid as mentioned above. Here a Freon 13-Freon 502 cascade refrigeration system is used; and, as in the heating cycle, any temperature can be maintained between room temperature and -50°C to within ±5°C. The control here is obtained by monitoring a copper-constantan thermocouple affixed to the shroud or test sample. The thermocouple voltage is fed into a General Electric Type 524 position and modulation controller which actuates a Honeywell modulating valve to provide more or less liquid to the shroud providing the necessary cooling. In the case of both heating and cooling the fluid flow through the shroud is maintained at about 20 gal/min by a specially designed pump which will operate over the wide temperature range herein encountered.

SUMMARY

The capabilities of the Radiometry Research Simulator are as follows:

1. Ultra-high vacuum ranging from atmospheric pressure to 5 x 10^{-12} Torr;

2. extremely clean system through the use of sorption, ion and titanium sublimation pumps;

3. Temperature control in the chamber of ±5°C from -50°C to +250°C with a single fluid system plus the capability of reaching LN_2 temperatures;

4. Intensities of 155 mw/cm^2 variable to 80 mw cm^{-2};

5. Beam uniformity of ±1.7% over a twelve inch diameter target - 30 inches deep;

6. Excellent spectral distribution where the percent deviation from Johnson's curve is as low as 1 to 2% at some points; and,

7. Collimation half angle of 2°.

The capabilities of these two units incorporated into the Radiometry Research Simulator are extensive. The system can be used to calibrate solar cells or any other photoelectric conversion device under outer space conditions. It is also useful in the calibration of thermopiles and other detectors; or, as a research tool in coating degradation and thermal balance. Future plans include the following: increase the size of the illumination port from 6 inches to 12 inches; use of recently available, faster sorption fore pumps to minimize pump down time; and, the addition of a residual gas analyzer to permit accurate quantitative and qualitative analyses of gases to which the test samples will be exposed.

Spec. No. 63-133

March 1964

APPENDIX I

SOLAR SIMULATOR

Specifications

I. Spectrum

1. Coverage to be from 250 nm to 2500 nm
2. Spectral match to Johnson's air mass zero solar irradiance is to meet or exceed indicated values given in Table I.
3. Bidders are requested to submit evidence that they can meet or exceed the values given in Table I.

II. Intensity and Uniformity

1. Maximum intensity shall be at least 150 watts/ft^2
2. Intensity shall be adjustable to 50 watts/ft^2 either continuously or in discrete steps of 50 watts/ft^2 or less.
3. Uniformity of the intensity at any point within test volume shall be ±2% or better of the operational intensity level (i.e., 150 watts/ft^2 to 50 watts/ft^2). Uniformity of intensity shall be measured with a 1 inch detector.
4. Uniformity of intensity in time shall not vary more than ±1% of the operational intensity level for any point in the test volume. This also to be measured with a detector not exceeding 1 inch in area.

III. Collimation

1. Collimation half angle to be no greater than 1° 30'.

IV. Test Volume (Minimum Requirement)

1. Test volume to be a cylinder one foot in diameter and 12 inches deep, or similar geometrical figure compatible with volume and linear dimensions given.

V. Miscellaneous

1. Simulator to be equipped with wheels and leveling jacks for ease of movement within laboratory.
2. Unit to operate without operator attention for a minimum of 24 hours.
3. If horizontal beam is supplied, height adjustment of ±16 inches from normal position will be required.

Table I

Wavelength Interval	Deviation from Johnson's Values
250 mu - 330 mu	±40%
330 - 400	20
400 - 450	10
450 - 500	10
500 - 600	10
600 - 700	10
700 - 800	10
800 - 900	15
900 - 1000	15
1000 - 1200	15
1200 - 1400	20
1400 - 1600	20
1600 - 1800	20
1800 - 2000	30
2000 - 2200	30
2200 - 2400	30
2400 - 2600	30

APPENDIX II

SPECIFICATION FOR ULTRA HIGH VACUUM SYSTEM, GSFC SPEC. NO. 63-132

I Vacuum System Requirements

1.1 General Specifications - This ultra-high, extremely clean, vacuum system will be used by the Solar Simulation Section of the Thermal Systems Branch. The system will be capable of simulating thermal vacuum conditions of outer space necessary for the exact testing of solar cells, experimental photovoltaic devices and future satellite experiments. The capabilities of the system will enable the cells to be tested at vacuum pressures approaching 10^{-10} Torr and at pre-selected temperatures in the range of -180°C to 250°C. Two quartz viewing ports will enable the specimens to be continuously irradiated by a carbon arc solar simulator or a xenon compact arc lamp. Included in the system will be all instrumentation necessary for measuring pressure levels within the chamber, temperatures of selected points in the test area and temperatures of the test chamber itself. All controls, gauges, etc., will be centralized on a control panel which is easily accessible and conveniently located.

1.2 System Description - The complete system shall be composed of a test chamber, bakeout system, temperature control system, pressure control system and measuring and recording instrumentation. The vacuum chamber is composed of a stainless-steel bell jar, a stainless-steel sump mated to the bell jar, and a hoist to facilitate installation and removal of the bell jar and bakeout system. The bakeout system consists of heating elements and controls for raising the temperature to 250°C. The temperature control

system consists of fluid lines within the bell jar together with cooling system, heaters, and heat exchangers to achieve chamber temperatures of -180°C to 250°C. The pressure control system is composed of a sorption roughing system, an ion pump, titanium sublimation pumps and all necessary controls. The instrumentation system measures and records test chamber pressure and temperature, test item temperature and heat transfer fluid temperature. Instrumentation for measurement of test item performance will be government furnished equipment with exception of the penetration ports and feed-through facilities.

II Mechanical Requirements of Test Chamber

2.1 Configurations and Dimensions of Test Chamber - The test chamber consists of two sections: bell jar and sump. The bell jar shall be a vertical right-circular steel cylinder with a useable inner diameter of 18 inches and a useable internal height of 30 inches. The top of the bell jar shall be closed. The bottom of the bell jar shall be open and terminate in a rotatable flange. The sump shall be a vertical right-circular steel cylinder with a useable diameter of 18 inches and a useable internal height of 20 inches. The bottom shall be closed. The top shall be open and terminate in a flange that mates with the bell jar flange.

2.2 Chamber Penetrations - In addition to the penetrations required for the sorption roughting system, ion pump, thermal shroud and internal sensors used for facility control, the chamber shall have the penetrations as described below. All penetrations, with the possible exception of those described in 2.4 a, b, c, and d, will accommodate con flat flanges or their equivalent as follows:

Type of Penetration	Flange Nominal O.D.	Flange Nominal I.D.
I	2-3/4"	1-1/2"
II	4-1/2"	2-1/2"
III	6"	4"
IV	8"	6"

2.3 Bell Jar Penetrations - In the lateral surface of the bell jar there shall be two (2) Type IV penetrations located 90° apart and approximately 15 inches above the bottom of the bell jar.

2.4 Sump Penetrations - The lateral surface of the sump shall have the penetrations as follows:

(a) Two (2) for titanium sublimation pumps as described in 4.1.3

(b) Two (2) for liquid nitrogen feed-throughs

(c) One (1) for a nude ionization gauge described in 4.2.2

(d) One (1) for a redhead gauge described in 4.2.3

(e) The following additional penetrations for instrumentation:

(1) Five (5) Type I

(2) Two (2) Type II

(3) One (1) Type III

(4) One (1) Type IV

2.5 Penetration Plates - The following penetration plates with con flat flanges or equivalent, bakeable to 250°C shall be supplied:

Quantity	Size to Fit Type	Description
5	I	Low Voltage electrical feed-through, 8 pins or more designed to mate with Cannon or Amphenol connector.
3	I	Octal thermocouple feed-through with copper-constantan leads
1	I	Sealed rotary motion feed-through capable of transmitting 4.5 in-lbs. at 500 rpm.
2	I	Liquid nitrogen feed-through with 3/8" I.D., 1/2" O.D. tubing.
4	I	Blank flanges
1	II	Blank flanges
1	III	Blank flanges
1	IV	Blank Flanges
2	IV	Blank flanges
2	IV	Viewing port shall meet the following specifications: a) Shall be made from Corning Optical grade fused Silica #7940 or Material with equivalent or better transmission properties. b) Effective I.D. of 6 inches. c) Surface shall be polished flat to 1/8 of 5461A wavelength.

d) Capable of operating at pressures to 1×10^{-10}

e) Capable of withstanding 250° bakeout temperatures.

2.6 Materials - The bell jar and sump shall be made of Electro Polished 304L stainless steel.

2.7 Opening and Closure System - The ultra-high vacuum system shall include an electrical hoist capable of lifting the bell jar with the thermal shroud at least 30 inches above the sump and pivoting it completely to one side. The hoist shall be capable of operating in a room with an 108-inch ceiling.

2.8 Junctions and Connections - Flanges on the bell jar and sump will be of the Wheeler type or equal. All junctions shall be inert gas welds or con flat flanges.

2.9 Seals - All seals between con flat and Wheeler flanges shall be OFHC copper gaskets bakeable to at least 250°C.

2.10 Safety Factors - The test chamber and hoist structure shall have a safety factor equal to or greater than the standards listed by the American Society of Mechanical Engineers Boiler and Pressure Vessel Code and National Electrical Code.

III Thermal Requirements

3.0 Temperature - Temperature control of test articles within the test volume shall be effected by a heated or cooled shroud which lines the interior of the bell jar. Selected shroud temperatures from -50°C to 250°C shall be maintained by circulating a single heated or cooled fluid through a closed-

loop heat transfer system. A final temperature of -180° shall be effected by a compatible liquid nitrogen system.

3.1 Shroud Configuration - One portion of the thermal shroud shall line the interior walls and top of the bell jar and shall be rigidly attached to the bell jar. Provisions will be allowed for an un-obstructed path in line with the viewing ports. Another portion of the shroud capable of carrying a 50 lb. concentrated load shall be placed across the open bottom of the bell jar and shall be rigidly attached to the sump.

3.2 Temperature Range - The shroud surfaces that face the test area shall be controlled to within ±5°C in the range of -50°C to 250°C. The extreme low temperature range shall be -180°C or lower.

3.3 Heat Load - The cooling system shall be capable of maintaining -50°C shroud temperature under a chamber heat load of 2 KW and a temperature of -180° or less with a chamber heat load of .5 KW.

3.4 Heat Transfer Rate - The closed loop-heat transfer system shall be capable of varying the temperature of the shroud 40°C per hour in the range -50°C to 250°C in the presence of test articles that emit or absorb 0.2 KW.

3.5 Heat Transfer Medium - The heat transfer medium of the closed loop system shall be a single fluid capable of operating in the range -50°C to 250°C.

3.6 Shroud Insulation - Heat exchange between shroud and bell jar or sump shall be minimized by insulation, spatial separation or both.

3.7 Shroud Feed-Through - A dual feed-through bakeable to 250°C shall be provided for the entrance and exit of heat-transfer fluid through the bell jar. The feed-through tubes shall be sized to meet maximum heat transfer requirements.

3.8 Fluid Purge - It shall be made possible to purge the heat-transfer fluid of the closed loop system by means of compressed air. Cut off the vent valves shall be provided to allow complete isolation of the shroud from the remainder of the closed loop system during purging.

3.9 Reflectivity - The reflectivity of all surfaces exposed to test articles in the chamber shall be as low as possible compatible with the 10^{-10} Torr Vacuum requirement. A design goal will be surfaces whose reflectivities are 0.05 or less over the spectral interval 0.25 to 2.6 microns. The surfaces of the shroud and chamber walls which face each other shall have a reflectivity of 0.90 or more over the same specified interval.

3.10 Shroud Cooling System - The ultra-high vacuum system shall include a mechanical refrigeration system with necessary heat exchangers in addition to the liquid nitrogen system.

3.11 Shroud Heating System - The ultra-high vacuum system shall include a heating system with necessary heat exchangers.

3.12 Bakeout System - The ultra-high vacuum system shall include systems for baking the interior of the chamber, shroud, sorption fore pumps, ion pump, and the titanium sublimation pumps to 250°C. Temperatures shall be automatically controlled to ±5°C. Bakeout heat shall be provided by external, non-corroding, electrical heaters in thermal contact with the parts to be baked in addition to hot fluid in the shroud.

3.13 Bakeout Heating Rate - The bakeout system shall be capable of heating the parts to be baked out from 20°C to 250°C within one hour.

3.14 Bakeout Control System - Bakeout shall be effected by energizing the bakeout electrical heaters in addition to those heating the shroud. Bakeout

temperature for the electrical heaters shall be sensed on the exterior surface of the chamber adjacent to the strip heaters. This temperature shall be controllable to ±5° over the range of +20°C to +250°C. No spot on the chamber surface shall differ from the control point by more than 30°C. The bakeout system shall be controlled by chamber pressure. The turn-on point shall be adjustable in the range of 1×10^{-4} Torr to 1×10^{-6} Torr and the turn-off point shall be adjustable in the range of 5×10^{-5} Torr. Chamber pressure shall operate both the electrical heaters and the shroud heating during bakeout.

3.15 Interlocks - Interlocks on the electrical and fluid systems shall be provided to prevent overheating. The interlock shall deactivate the bakeout system and turn on an alarm light when the temperature exceeds the preset control point in the range of +20°C to 250°C.

3.16 Recorder - A temperature recorder shall be provided to record the bakeout system control point temperature over a minimum period of 72 hours.

3.17 Shroud Temperature Control System - The ultra-high vacuum system shall include a system for automatically controlling and recording the shroud temperature within +5°C of selected values in the range -50°C to +250°C. The control system shall permit manual temperature settings at any temperature in the range -50°C to +250°C within the specified tolerances.

3.18 Sensors - The control system shall be governed by any one of three sensors. These sensors shall be mounted as follows:

a) On the fluid efflux tube not more than 4 inches outside the test chamber

b) On the inner surface of the shroud in the bell jar not more than 6 inches from the efflux feed through

c) At some point within the test chamber volume at least 2 inches from the shroud

A selector switch shall be provided to permit alternative selection of the sensors as the control element in the temperature control system.

3.19 Temperature Stabilization - The sensor located within the test chamber at least two inches away from the shroud shall achieve temperature stabilization within ±5°C with 10 minutes after reaching any set temperature in the range of -50°C to +250°C.

3.20 Recorder - The control system recorder shall record the temperature of an additional sensor placed at least 2 inches away from the shroud. A minimum record of 72 continuous hours shall be provided. This recorder can be combined with the bakeout system temperature recorder.

3.21 External Insulation - The test chamber shall be enclosed in an outer metal shell that shall have provisions for all penetrations and viewing ports. Thermal insulation shall be provided between the outer shell and test chamber. The insulation shall be non-organic, non-hydroscopic, non-settling and fire-proof. The type and thickness of the insulation, and the material and surface properties of the outer shell shall be such that their combined thermal influence prevents outer shell temperatures from exceeding 32°C when the chamber is at 250°C and room temperature is 22°C.

3.22 Moisture Seal - The outer shell and insulation shall be integrally attached to the test chamber and provisions shall be made for the removal of condensation between the two metal walls. A moisture-collection pan

with a drain tube shall be installed to collect any condensate from exposed cold surfaces.

IV Pressure Requirements

4.0 Pressure - The pressure system is composed of pumps, instrumentation and controls. A pressure of 1×10^{-10} Torr is to be attained. Pumping speed requirements are listed in the final systems test.

4.1 Pumping System - The vacuum pumping will be accomplished by three types of pumps:

a) Sorption Forepumps - Initial rough pumping to 1×10^{-2} Torr shall be provided by three VacSorb forepumps or their equivalent. Each pump shall be provided with valve separation from the pumping system. Bakeout units and liquid nitrogen containers will be provided for each pump in addition to the standard pump accessories.

b) Ion pump - A 500 L/S (liter per second) ion pump will be provided as a second stage in the pumping process. The pump will be fitted with a stainless steel screen between the ion pump and the test volume. The ion pump shall be provided with internal bakeout capabilities.

c) Titanium Sublimation Pumps - two (2) tri-filament titanium sublimation pump cartridges of 2000 L/S capacity will be provided as an additional stage in the pumping process. The pump baffles shall be cooled by liquid nitrogen.

4.2 Pressure Measurement Devices - The ultra-high vacuum system pressure shall be measured by the following types of gages:

a) Thermocouple gage shall be provided with the capability of measuring pressures from 1.0 Torr to 1×10^{-3} Torr.

b) Ionization gage - A Bayard-Alpert nude ionization gage shall be provided with the capability of measuring Pressures from 1×10^{-3} Torr to 1×10^{-10} Torr. This gage control can be combined with the thermocouple gage.

c) A Redhead gage shall be provided with the capability of measuring pressures from 10^{-4} to 10^{-11} Torr.

4.3 Control System - Controls shall be provided for the following:

a) Ionization pump

b) Two (2) titanium sublimation pumps

c) Thermocouple gage

d) Ionization gage

e) Redhead gage

V Systems Integration Requirements - The ultra-high vacuum system shall be divided into three units:

5.1 Test Unit - The following shall be provided and integrated into the test unit:

a) Vacuum chamber including bell jar, sump and penetrations

b) Opening and closure system

c) Ion pump

d) Three (3) sorption pumps

e) Two (2) titanium sublimation pumps

5.2 Systems Console - The following controls and recorders shall be provided and mounted in a systems console:

a) Electrical bakeout control unit and temperature recorder

b) Thermal shroud control unit and temperature control unit

c) Ion pump control unit

d) Titanium sublimation pumps control unit

e) Thermocouple gage control unit with meter

f) Ionization gage control unit with meter

g) Redhead gage control unit with meter

h) 24 point temperature recorder compatible with copper-constantan thermocouples

5.3 Thermal Unit - This unit shall contain the system for heating, cooling and circulating the thermal shroud fluid.

VI System Fabrication, Compatibility, and Reliability Standards

6.1 Materials and Workmanship - Materials shall conform to standard trade requirements for comparable equipment. Design and construction of all components, assemblies and electrical wiring shall reflect the most modern practice and skilled workmanship. The work shall conform to the highest standards with regard to ease of operation, maintenance, structural integrity and physical appearance.

6.2 Reliability - The contractor shall assure system reliability by providing adequate component derating, inter-locks, and overload devices.

6.2.1 Lifetime - The equipment shall have a service life not less than 40,000 hours under normal laboratory conditions of continual operation at 10^{-6} Torr.

6.2.2 Simplicity - Sufficient simplicity shall be designed into the system to insure prescribed reliability and accuracy.

6.2.3 Maintainability - The system shall be designed for easy, infrequent maintenance. Modular construction shall be used where appropriate, and

similar modules shall be interchangeable. Each module shall have accessible test points.

6.2.4 Conformance with Code and Standards - Electrical materials, components, and assembly procedures shall conform with the requirements given in the National Electrical Safety Code and the American Society of Mechanical Engineers Boiler and Pressure Vessel Code, Section VIII.

6.3 Compatibility

6.3.1 Environment - All components located inside the vacuum chamber shall survive exposure to any possible combination of the following conditions:

a) Temperature: -180°C to +250°C

b) Relative humidity: 0 to 100 percent

c) Pressure: Atmospheric to 1×10^{-10} Torr

d) Radiation: 0 to 250 watts per square foot distributed between .23 to 2.5 microns.

6.3.2 Thermal Expansion - Operation of the test chamber or its components shall not be compromised and test articles shall not be damaged by differential thermal expansion of materials in physical contact under any changes of temperature.

6.3.3 Corrosive Materials - The chamber and its components shall contain no materials that might release substances corrosive to the test items or test fixtures during normal testing and bakeout operations.

6.4 Spare Parts Requirements - Equipment furnished by the contractor shall include the following parts in addition to any previously specified:

Quantity	Description	Reference
2	Titanium sublimation pumps, 2000 L/S bakeable to 250°C	4.1.3
1	Nude ionization gage, flanged, pressure range 1×10^{-3} to 1×10^{-10} Torr	4.2.2
1	Thermocouple (low-vacuum) gage bakeable to 250°C, pressure range from 1.0 to 1×10^{-3} Torr	4.2.1
1	Feed-through connector for thermocouple gage bakeable to 250°C	
1	Redhead gage, bakeable to 250°C, pressure range from 10^{-4} to 10^{-11} Torr	4.2.3
1	Standard Carton of chart paper for all recorders	

VII Tests and Checkout - The following tests shall be conducted within the time schedule given in 2.3. The contractor shall submit detailed test procedures for Goddard's approval at least twenty (20) days prior to scheduled initiation of testing. Both the pressure and the thermal systems shall be tested.

7.1 Pressure System - The test sequence shall be as follows: Bakeout the system, maintaining 250°C for not more than six (6) hours. During bakeout, the required temperature uniformity and pressure control of bakeout shall be demonstrated. Following bakeout the system shall attain a pressure of 1×10^{-9} Torr or lower in six (6) hours or less with a thermal shroud temperature of +20°C. The chamber shall then be evacuated to 1×10^{-10} Torr or lower in eighteen (18) additional hours or less, with shroud temperature maintained at +20°C.

7.2 Thermal System - The test sequence shall be as follows: The chamber shall be maintained at ultimate vacuum 1 x 10^{-10} Torr or less. With the chamber initially at +20°C, a temperature step function shall be programmed from +20°C to +250°C. The shroud sensor shall be the control element. The temperature shall be maintained at +250°C for twenty-four (24) hours. A second temperature step function shall then be initiated from +250°C to -50°C and then maintained at -50°C for 24 hours. The final temperature step cycle utilizing the liquid nitrogen system shall maintain the shroud temperature at -180°C for a period of 12 hours. During this sequence, the requirements for thermal stability, temperature uniformity and control, temperature recording and adequacy of insulation shall be fully demonstrated.

7.2.1 Instrumentation - At least 12 temperature sensors shall be installed for these tests. Half of these sensors shall be mounted on the exterior surface of the chamber wall and outer shell to demonstrate temperature uniformity and insulation effectiveness. The remainder will be mounted on the shroud to permit evaluation of the thermal shroud system. The 24 point temperature recorder shall measure these temperatures. The accuracy of these measurements shall be within ±5°C.

PRESSURE CHAMBER ARC STUDIES

John Flemming

Dan Lester*

Radiometry Group

Thermal Systems Branch

Spacecraft Technology Division

*Taag Designs, Inc. employee at GSFC - Contract No. NAS 5-2382

PRESSURE CHAMBER ARC STUDIES

John Flemming

Dan Lester

Radiometry Group

Thermal Systems Branch

Spacecraft Technology Division

ABSTRACT

Research oriented towards the development of improved light sources for solar simulators using a pressure arc chamber which has the capability of operating at pressures up to 5000 psig has been undertaken. Gas composition, electrode configuration, electrode separation and arc power are also variable with this facility.

The data obtained for argon indicate no significant advantage from the use of high pressures. However, the use of argon in short arc lamps at normal pressures appears to have definite value.

PRESSURE CHAMBER ARC STUDIES

INTRODUCTION

Many improvements have been made in solar simulation in the last few years; however, several areas remain in which significant progress is lacking. One of these areas is the spectral irradiance correspondence to air mass zero solar spectral irradiance inside the test volume of the simulator.

Filters are available which correct the xenon spectrum to more nearly simulate the solar spectrum; but the stability and lifetimes of these filters are not accurately known. The replacement costs of these filters could become excessive if lifetimes of several years cannot be obtained. Systems without much reserve energy may be unable to use such filters and maintain a solar constant of irradiance in the test volume. The resulting spectrum which gives considerable improvement does not result in a perfect correspondence to the solar spectrum.

The basic problem is the spectral distribution of the sources used in the simulator. A research program to improve the spectral radiances of sources suitable for solar simulators has been undertaken. Success in this endeavor would mean greatly improved solar simulator efficiency over that now obtainable with filtered xenon systems. The filter manufacturers could then concentrate on fine-tuning the spectral distribution inside the test volume of solar simulators.

It is unnecessary to develop a light source radiating as a 5800 degree Kelvin blackbody to be successful in this program. Methods which would suppress the energy contained in the strong emission lines of xenon would be useful. Any combination of two, three, or more different arc sources, when used in a system

in which each lamp illuminates the entire test volume, could result in a significant improvement to the spectral irradiance of a solar simulator. The object of the program is to obtain a combination of gases and impurities which will yield a spectral radiance similar to the solar irradiance.

PRESSURE ARC CHAMBER

The Pressure Arc Chamber is well suited to this research in that several of the more important arc parameters may be varied. These parameters are gas composition, gas pressure, electrode configuration, electrode separation, and input power.

This system has the capability to investigate the effects of pressure on arc efficiency and spectral radiance. The arc chamber has a maximum rated working pressure of 5000 psig, or about 330 atmospheres as compared to 15 or 20 atmospheres common to the short arc lamps now in general use.

Increasing the gas pressure is known to produce several interesting spectral effects. In addition to line broadening and strengthening of the continuum, violet shifts and red shifts are observed. New bands appear in both the ultraviolet and infrared regions.[1, 2, 3, 4]

An increase in the gas pressure results in a decrease in the arc diameter resulting in an increased arc radiance. This decreases the rate of electrode evaporation permitting longer useful lamp life. This also increases the voltage gradient across the arc, permitting the use of smaller currents and electrodes for a given power level.[5]

The system consists of an arc chamber, power supply, igniter, vacuum pumping system, gas compressor, and gas manifold unit.

The arc chamber is shown in figure 1. It is essentially a cylinder made of air-hardened tool steel. It has two diametrically opposed windows, two primary electrodes for the arc discharge, and two auxiliary electrodes which were intended for use with an outgassing furnace. The interior dimensions are 6 inches in diameter by 6 inches high. The end plates are 2-1/2 inches thick, while the side walls are 1-11/16 inches thick. The steel pressure chamber is surrounded by a hard copper water-jacket. As seen here fully assembled, the chamber weighs about 400 pounds.

At the top of the chamber may be seen a thermocouple which senses the temperature of the inside surface of the upper end-plate, a gas line through which the chamber is evacuated, an electrical connection to the anode, and a cooling water inlet to the water-jacket. Another water inlet, the electrical connection to the cathode, and the gas line through which gas enters the chamber are located at the bottom of the chamber. The cooling water outlets, the outgassing electrodes and the windows are located on the sides of the chamber.

Figure 2 is a general view of the equipment. The arc igniter is located in the open space beneath the chamber. Next to the chamber are the vacuum pumping system and most of the valves controlling the gas flow.

Figure 3 shows the gas compressor, which is an Andreas Hofer two-stage diaphragm compressor with a maximum discharge pressure of 5000 psig.

Figure 4 shows a homemade gas dryer. The line from the gas cylinder is coiled and submerged in liquid nitrogen. The intent is that all water or carbon dioxide which may be present in the commercial grade argon being used will be condensed on the cold walls of the tubing. This technique is not very satisfactory for two reasons: first, unless enough gas flow is maintained in the line the argon

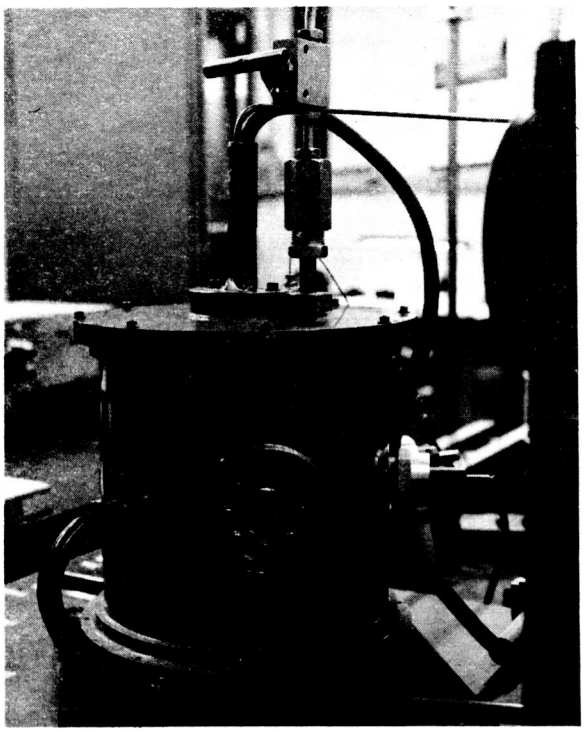

Figure 1—Pressure Arc Chamber

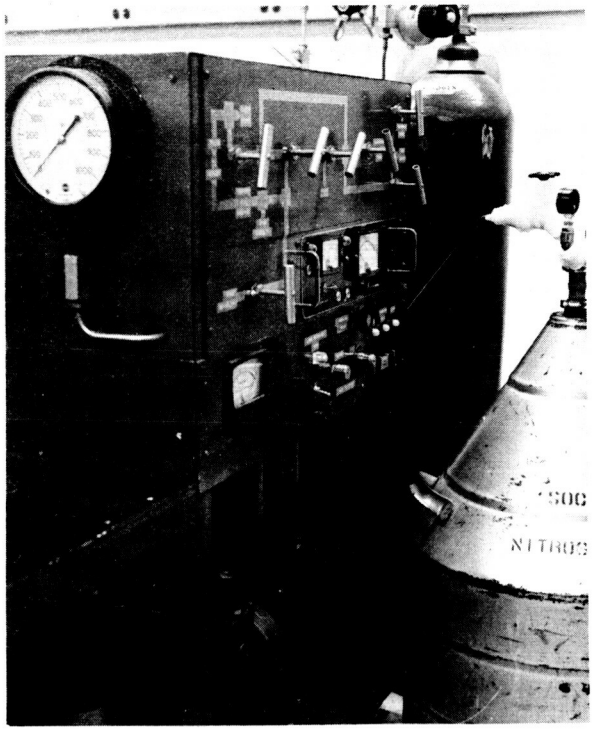

Figure 2—General View of Equipment

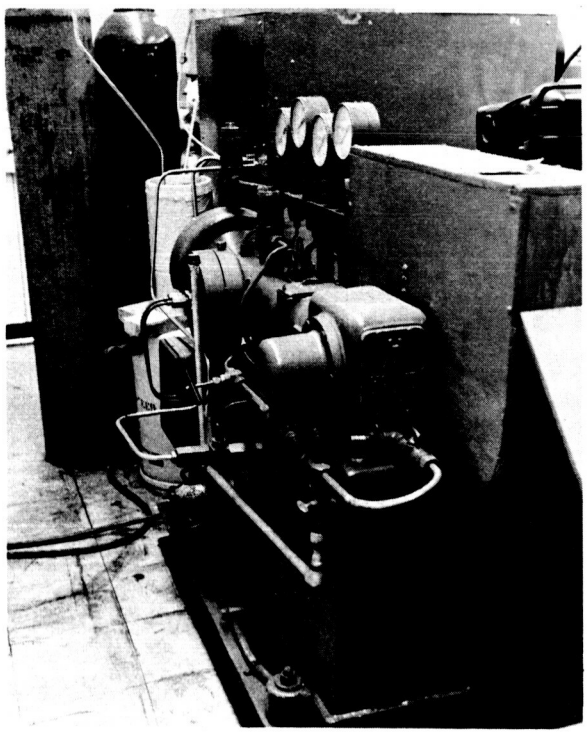

Figure 3—Gas Compressor

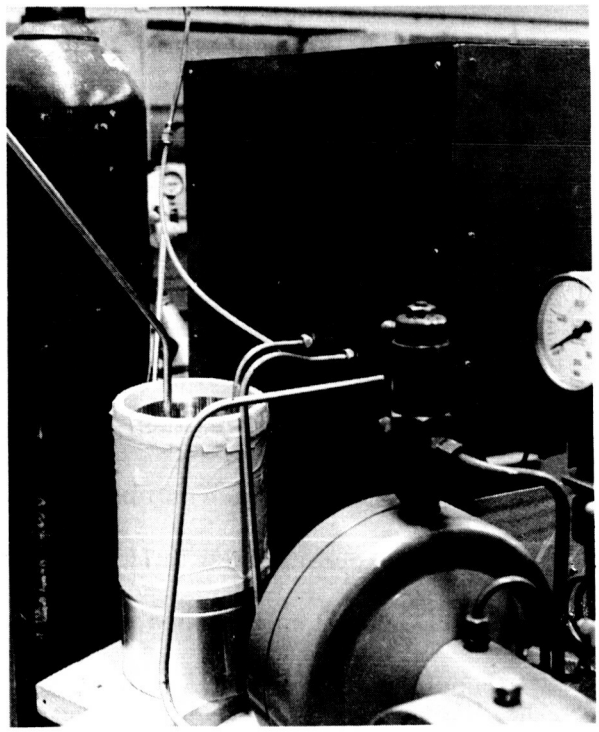

Figure 4—Gas Dryer

itself will freeze and completely close the line. Second, at the high pressures sometimes used the mean free path becomes so short that a large proportion of the gas molecules probably never impact on a cold surface. Unfortunately no commercially available dryer has yet been found which will handle the pressure.

Figure 5 is a schematic drawing of the system showing all of the gas lines and valves. This is a revision of the original system. It was found that by re-arranging the components and valves, it was possible to increase the vacuum pumping speed in the chamber by more than a factor of three.

Electrical power is supplied to the arc by a Christie "X" series D.C. power supply capable of supplying up to 6500 watts. The igniter is made by Bauch and is rated at 150 amps.

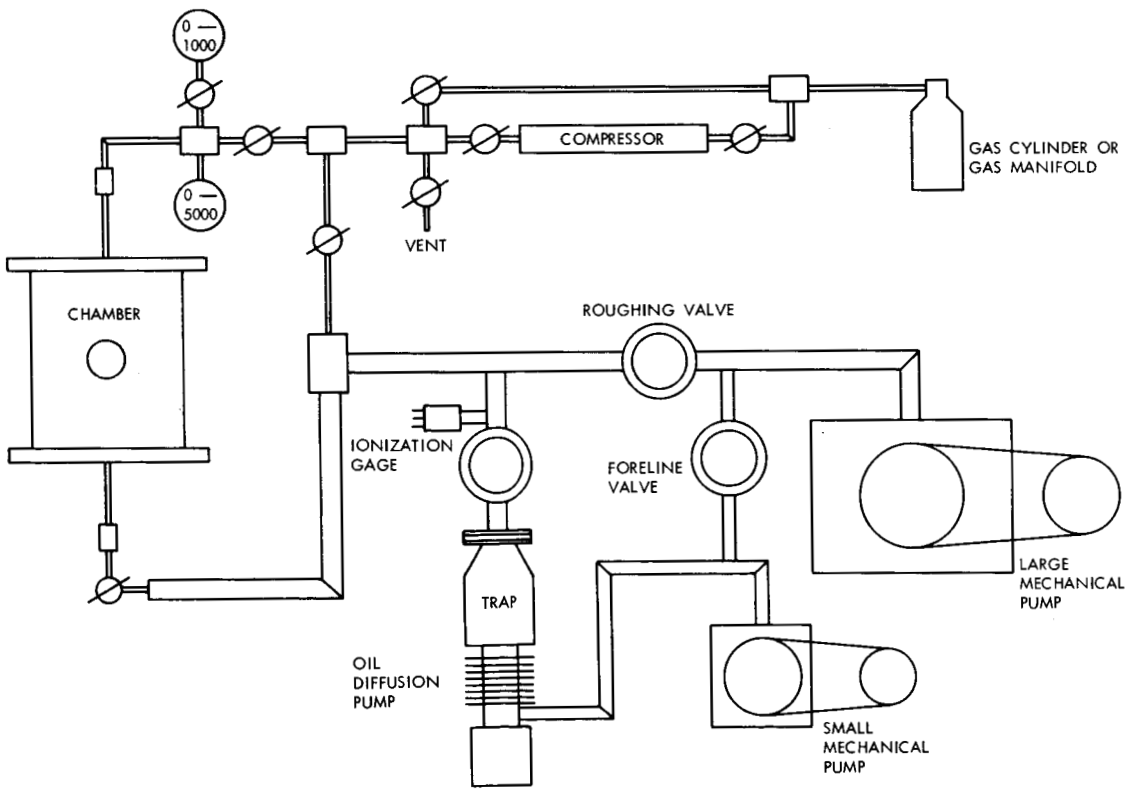

Figure 5—Experimental Arc Facility

A number of problems in using this system became apparent almost immediately. The first problem was how to outgas the system effectively. The need for a thorough outgassing is apparent from figures 6 and 7. These pictures were taken after operating an arc in argon for about 30 minutes at 1500 watts. Figure 6 was taken looking down into the chamber with the top end-plate removed. The interior of the chamber was originally gold-plated to prevent formation of oxides. As is apparent from the finger marks on the left side, the sides of the chamber were covered with a heavy coating of blue-black powder. The bottom of the chamber had only a light coating. The heater electrodes, one with a melted tip, can be seen extending from the chamber wall.

Figure 7 shows the top end-plate and the anode. The coating of the blue powder was most severe here. It also may be seen that the anode is held only by a set-screw.

On subsequent runs, a yellow powder was sometimes produced in place of the blue, and the anode was never again so colorful. Analysis by wet chemistry and x-ray diffraction methods showed the presence of tungsten trioxide and tungstic acid. The coloration of the anode was due to oxides of tungsten being formed over a range of temperatures from the very hot tip back to the cooler shank.

It is believed that tungsten trioxide predominates only when oxygen is present in relatively copious quantities, either from a leak or from grossly inadequate evacuation. Vacuum pumping is greatly hampered by the tiny orifice of the high pressure valve between the arc chamber and the vacuum pumps. The estimated conductance of this valve alone is under 1 liter per second.

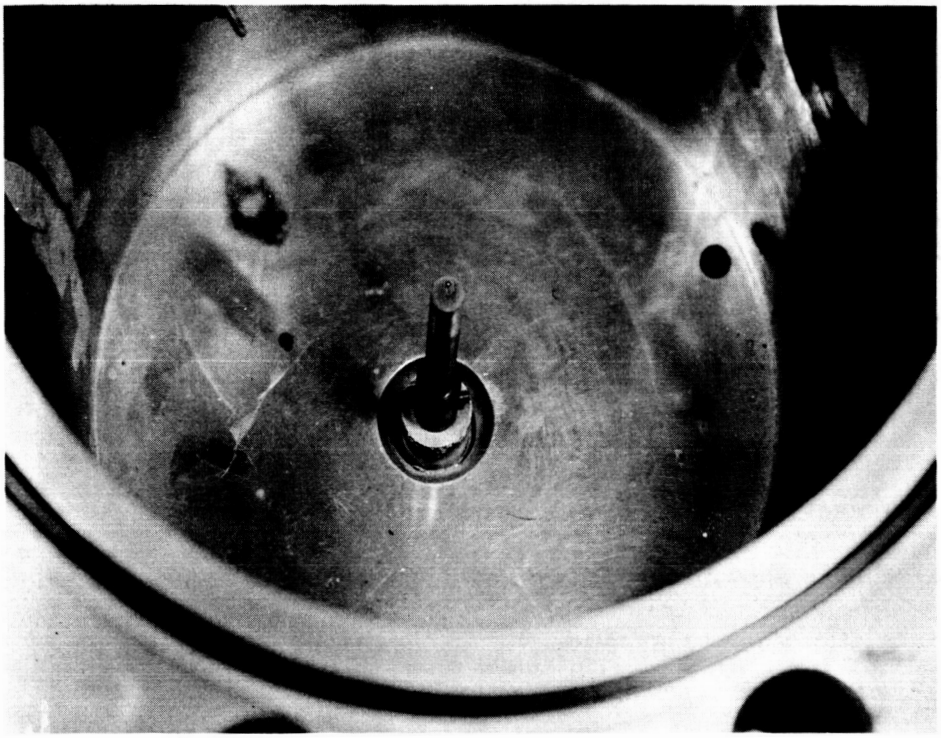

Figure 6—Cathode

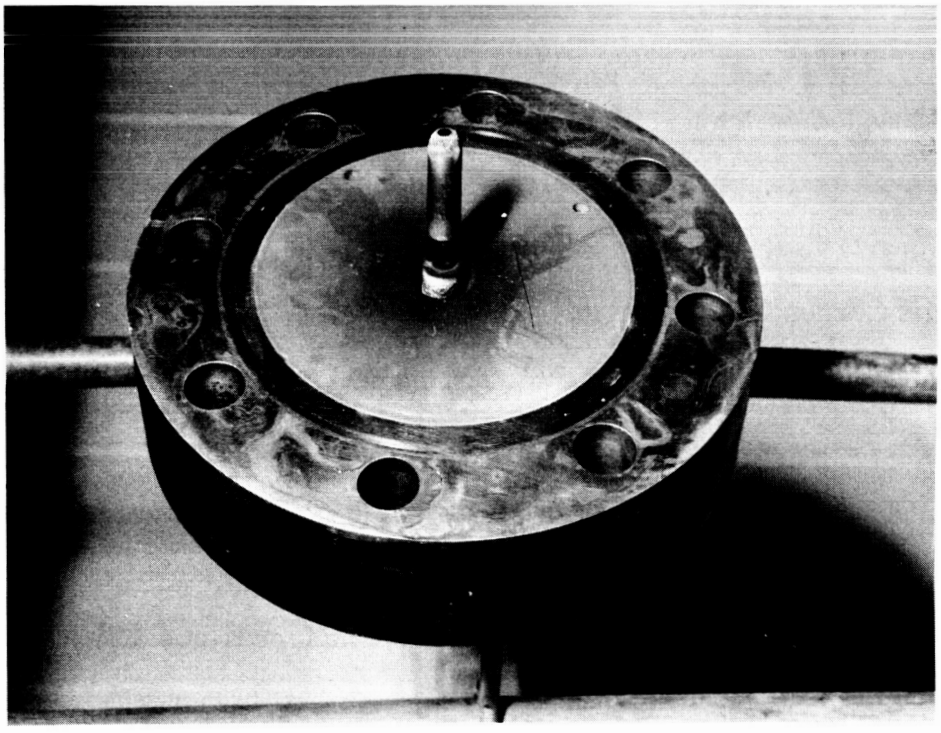

Figure 7—Anode

The formation of tungstic acid may be the result of absorbed water-vapor coming off the chamber walls as they are heated by the arc.

The problem was finally solved by operating the arc at 20 to 30 psi and reduced power while continually flushing argon through the chamber for several hours. When opened, the chamber was very clean. As part of our normal procedure, we now flush the chamber for several minutes following arc ignition.

Another chronic problem has been deterioration of the anode. After operating the arc for several hours at higher pressures, the anode is invariably deeply pitted. This is shown in figures 8 and 9. This type of damage is said to be characteristic of power supplies with excessive ripple. In this case, ripple was measured and found to be less than 1%. It is believed that the decrease in arc diameter due to the higher pressures increased current density to the point where localized melting of the anode took place. If this is proven to be the case, the implication would be that water-cooling of the anode is necessary for high pressure arcs. This problem should not seriously hamper the research program.

A problem which has been more troublesome is window breakage. Figure 10 shows a collection of broken quartz windows. These windows, which are optical grade quartz, measure approximately 1-1/3 inches long by 1-1/4 inches in diameter. When installed in the chamber, the clear aperture is about 1 inch in diameter. Figure 11 shows some details of the window assembly. The high pressure seal is made of nylon and has a triangular cross-section. The base of the triangle is compressed against the middle of the window by squeezing the sides of the triangle between the chamber and the retaining ring.

The break was a shearing fracture on the high pressure side of the seal in general. In some cases, the window was sheared off in two or three places.

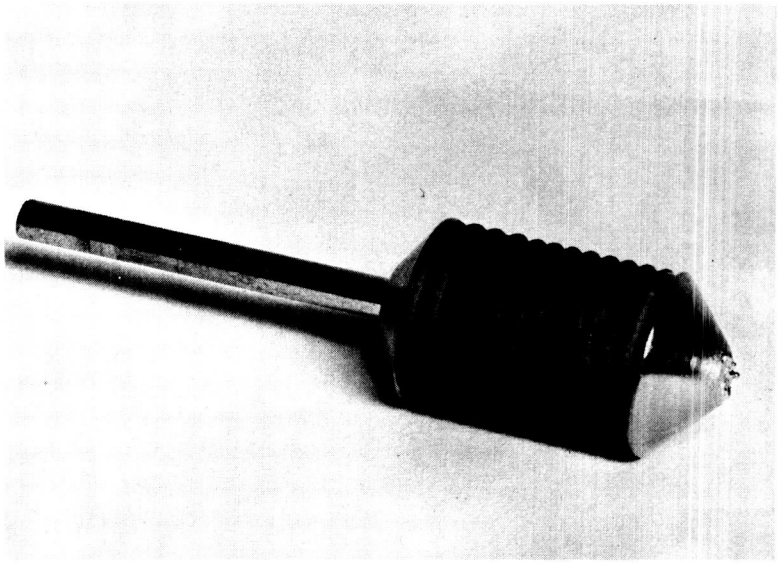

Figure 8—Anode

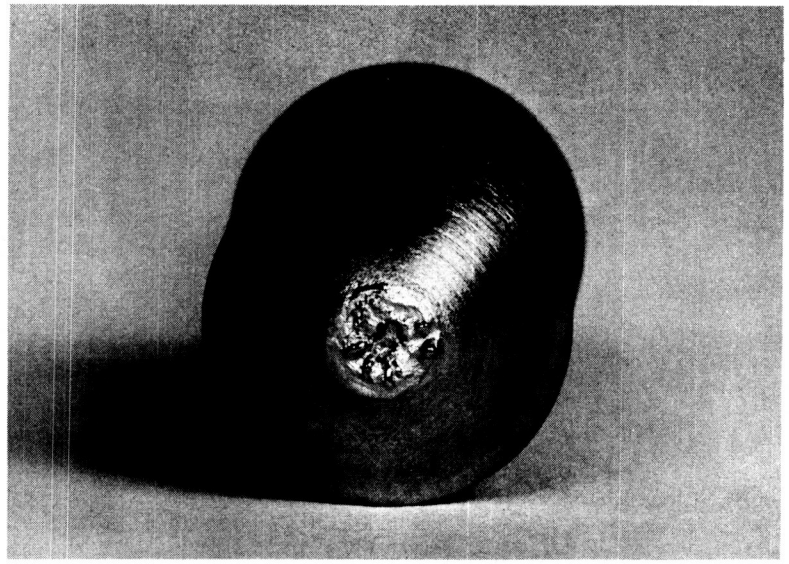

Figure 9—Anode

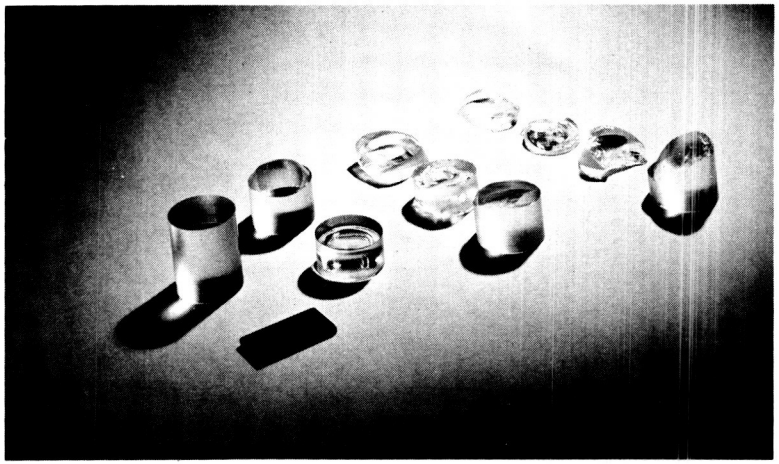

Figure 10—Quartz Windows

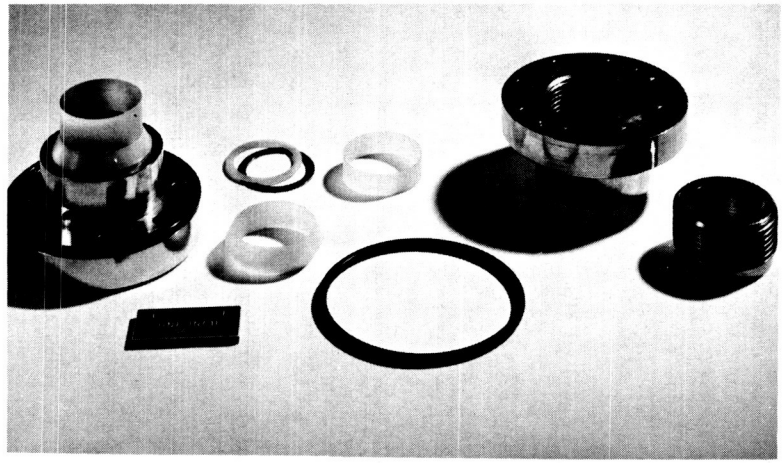

Figure 11—Window Assembly

These broken windows have caused nothing more than slow leaks. Recent changes in window installation techniques have corrected the situation.

RESULTS AND ANALYSIS OF DATA

All of the results presented here are for argon. Figure 12 shows that arc voltage is insensitive to changes in arc current. The upward trend of the voltage for the curve labeled 1500 psig was caused by increasing pressure due to increasing temperature.

Figure 13 shows the effect of pressure on the arc voltage. This data was taken for constant input power.

Figure 14 shows the effect of pressure on the radiance of the arc near the anode and near the cathode. Note that the radiance of the arc near the anode increases more rapidly with increase in pressure than does the arc near the cathode. This data was taken by imaging the arc upon an opaque surface and

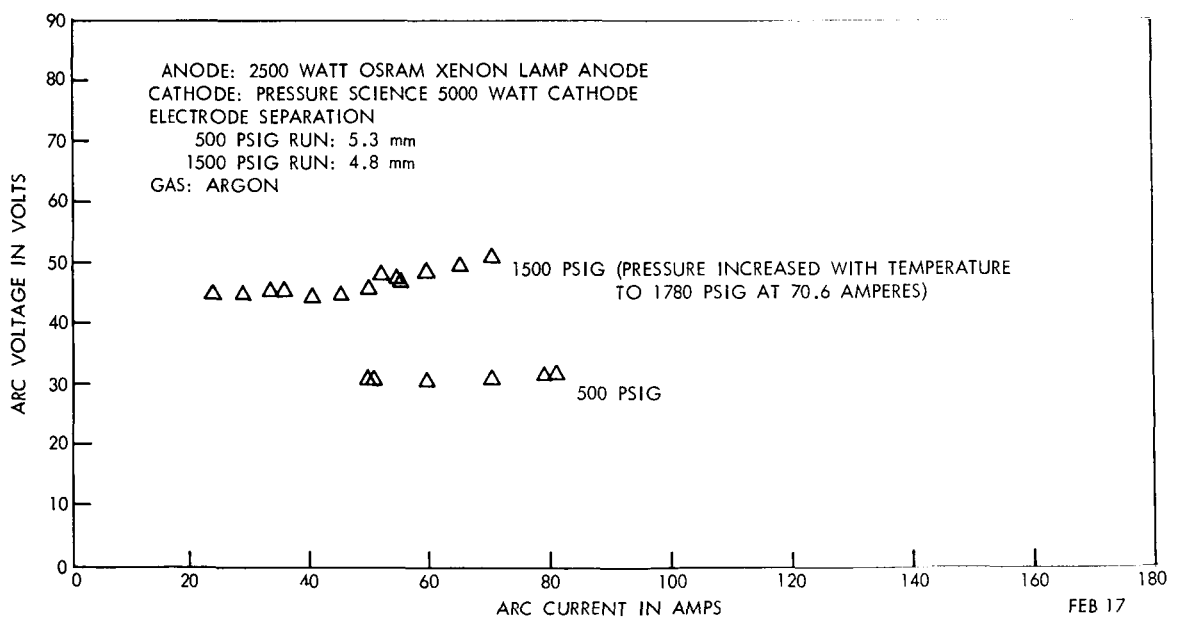

Figure 12—Voltage Current Characteristic

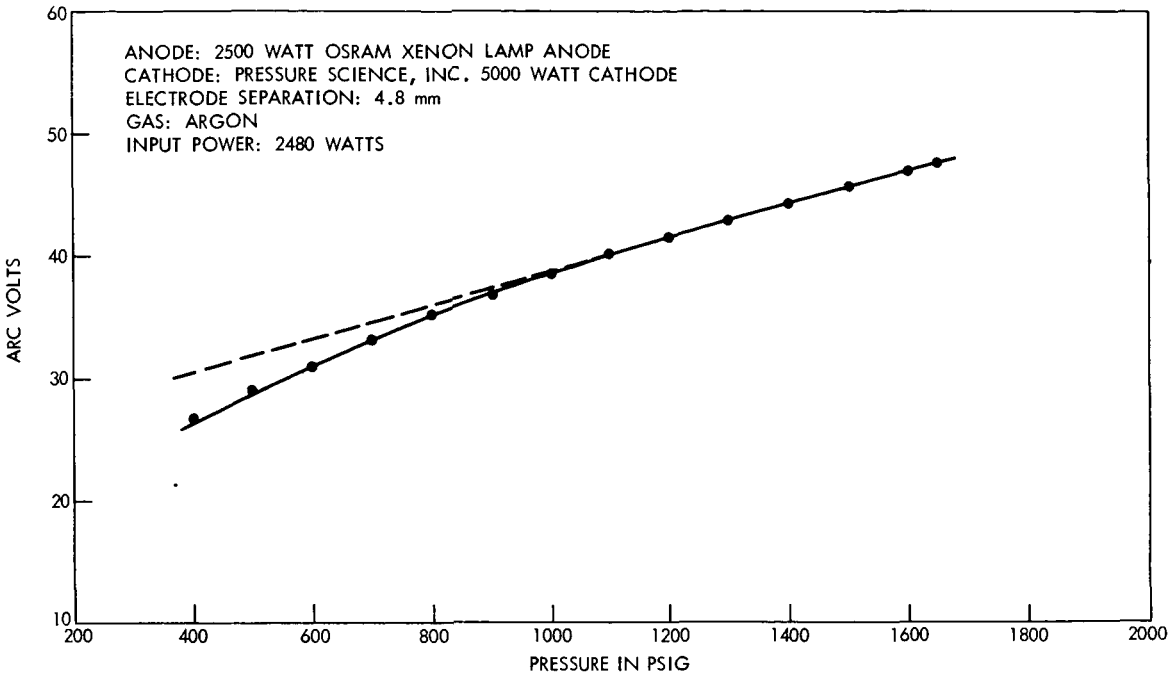

Figure 13—Voltage Pressure Characteristic

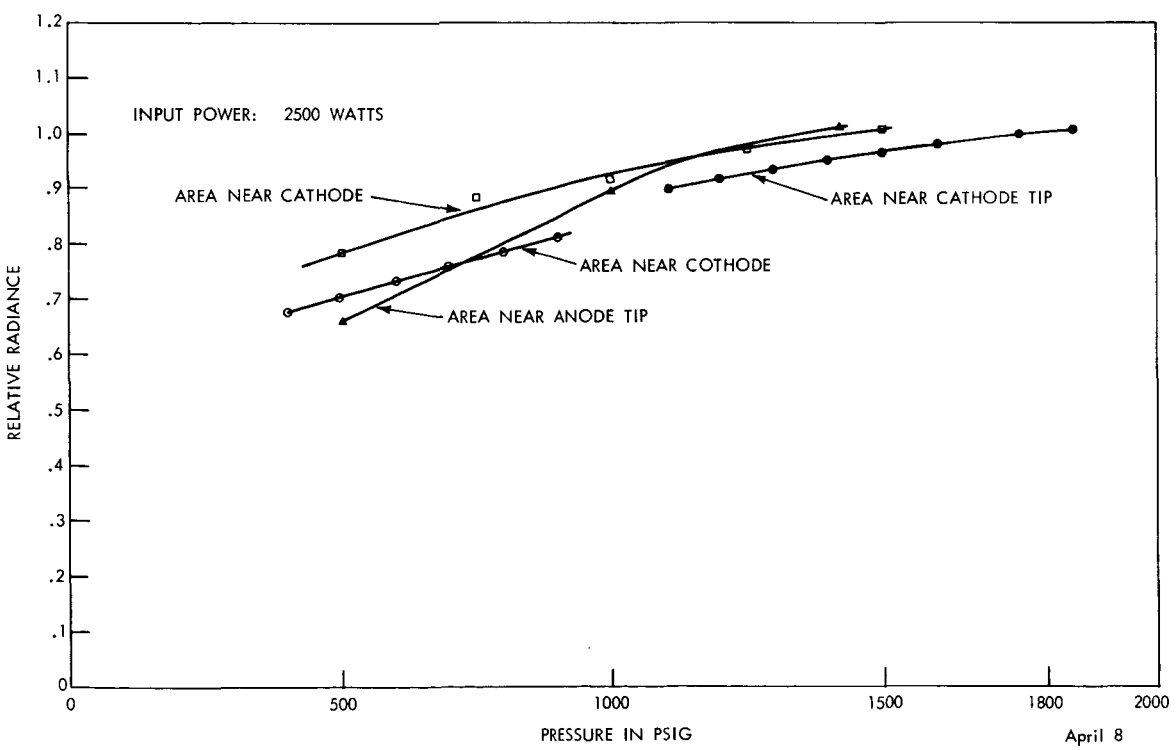

Figure 14—Pressure Radiance Characteristic.

allowing a small portion of the image to pass through a hole and to fall onto a thermopile. Again the data was taken for constant input power.

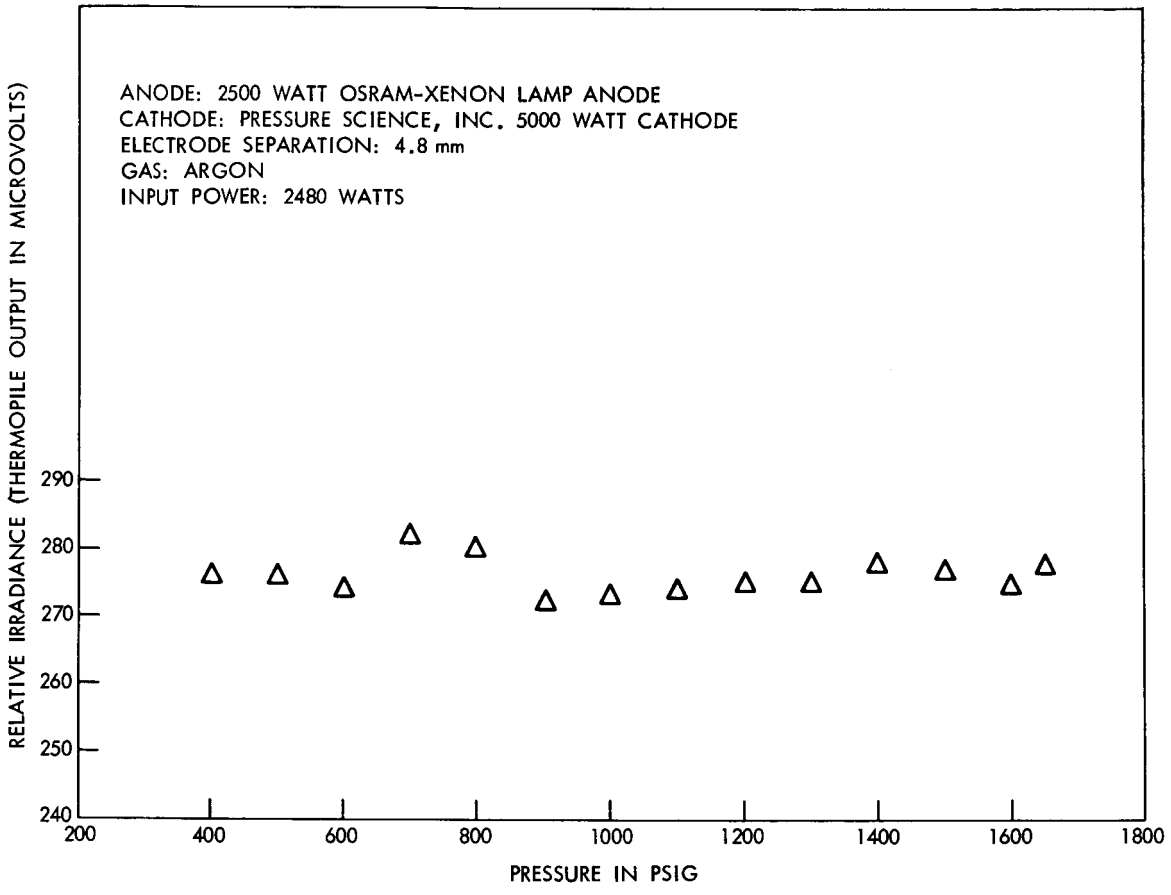

Figure 15—Pressure Irradiance Characteristic

Figure 15 shows the effect of pressure on the total amount of power radiated by the arc. This data was taken by placing a thermopile where it could view the entire arc and then observing thermopile output as the pressure was varied. Input power was again constant. In terms of total radiated power, this data shows no advantage to be derived from the use of high pressure.

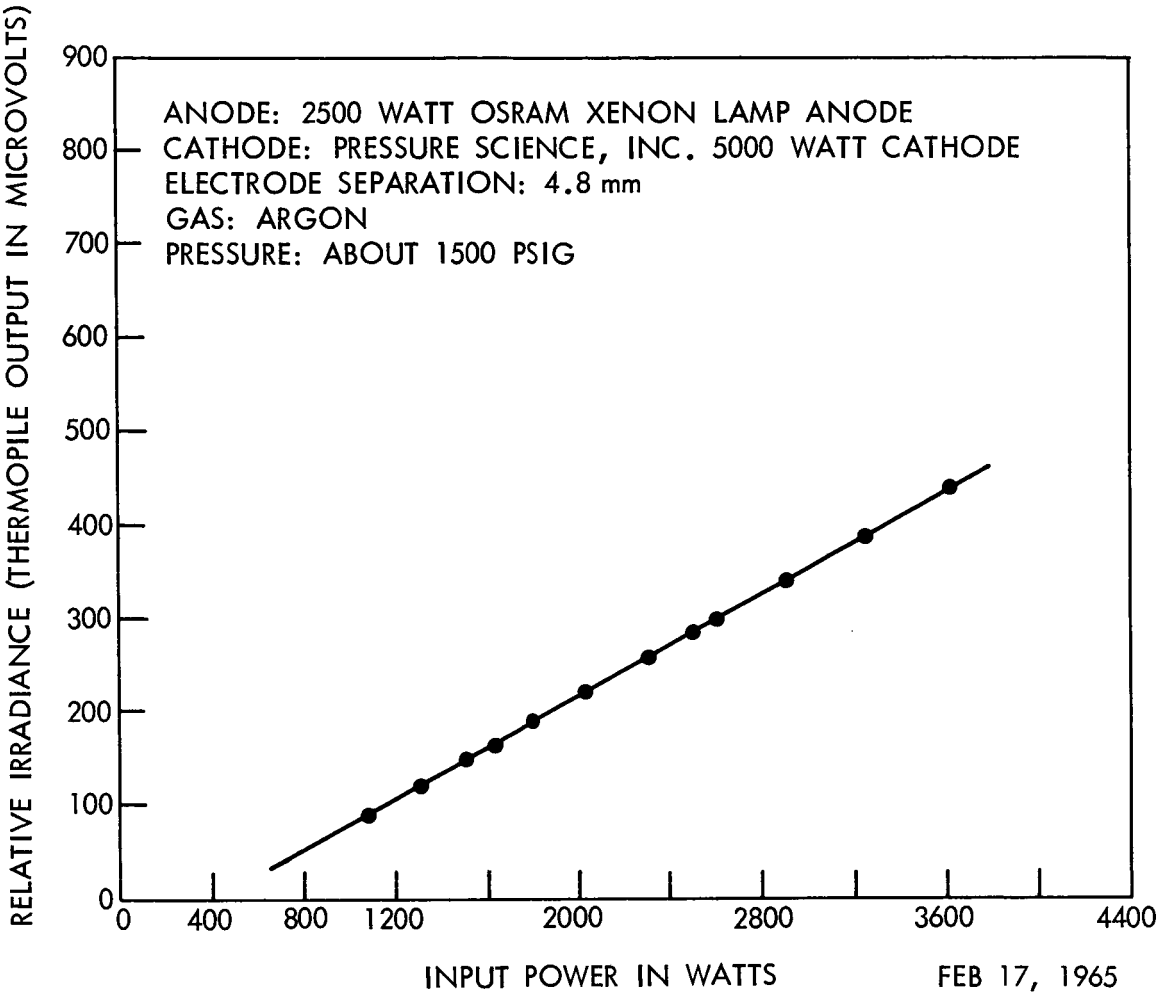

Figure 16—Power Irradiance Characteristic

For the data shown on figure 16, the pressure was held at about 1500 psig while the input power was varied. The output of a thermopile viewing the entire arc was observed as a function of input power. The relationship is linear for the region where data was recorded, but one might wonder why the x-axis is intercepted at an input power of 400 watts. If the curve were extended, the

y-axis would be intercepted at -60 microvolts. This cannot be attributed to heating of the thermopile because the thermopile was shielded from the radiation between measurements.

The spectral effects of pressure are illustrated by figures 17 and 18.

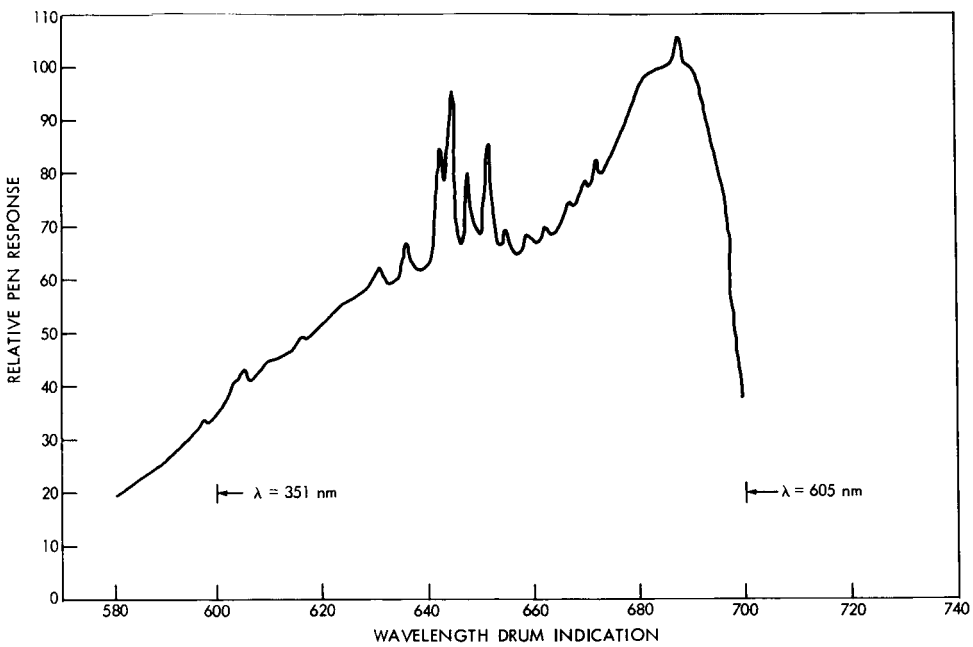

Figure 17—Argon at 100 psig

Figure 17 is the spectrometer output plotted as a function of the wavelength drum indication for an argon arc operating at a pressure of 100 psig. Note that even at this relatively low pressure the spectrum is mostly continuum. Figure 18 shows the same spectrum except that the pressure was 1700 psig. Note that many of the weaker lines have disappeared and that those lines which remain have been broadened. There have been no major energy shifts, though this may be hard to see in such a restricted wavelength interval. Future data will cover the entire range of interest.

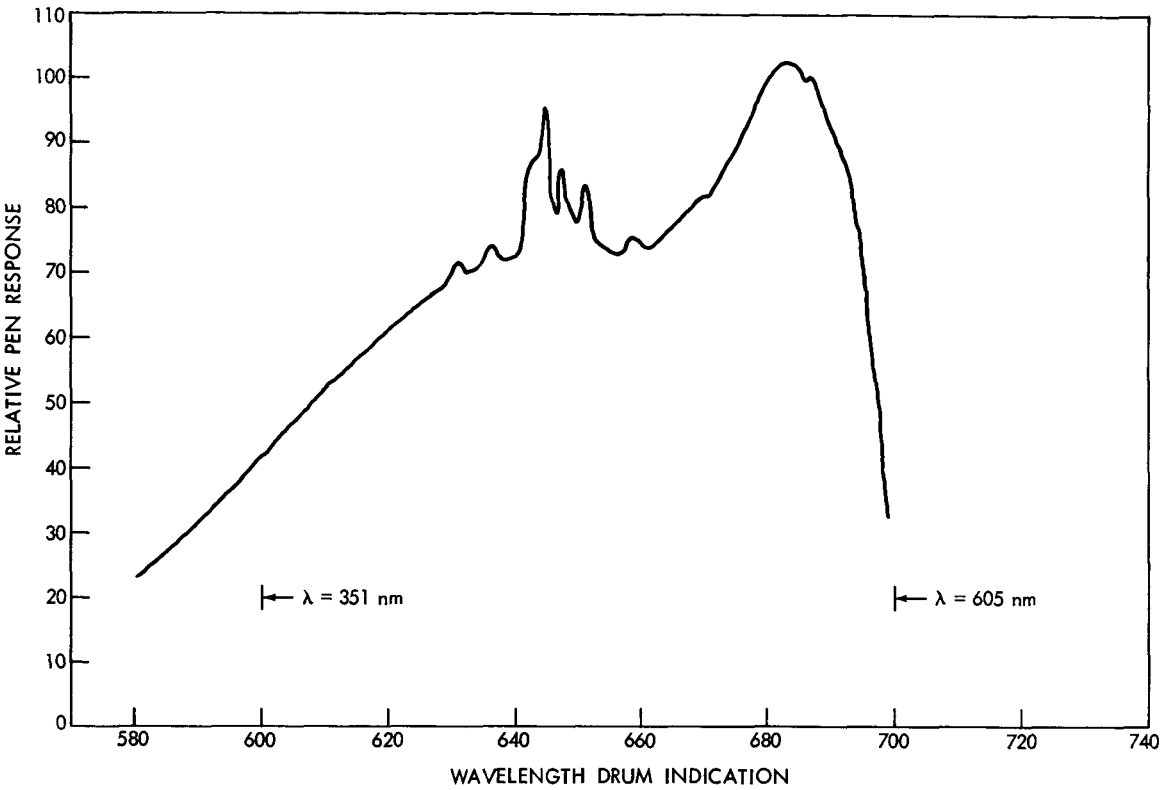

Figure 18—Argon at 1700 psig

Figure 19 shows the spectral energy distribution of an argon arc operated at 2500 watts and a pressure of about 40 atmosphere (uncorrected for transmission through 1 1/3 inches of quartz). At first glance the distribution appears to be very similar to that for a xenon lamp. There are differences, however, which may be of value to solar simulation technology.

First of all, the data show that this argon arc was radiating about three times as much energy between 250 nm and 300 nm as would a xenon lamp. If terms of total energy between 250 nm and 350 nm, the data show that an argon lamp is about equivalent to a HgXe lamp. This energy is all continuum. Argon has no line structure below 400 nm.

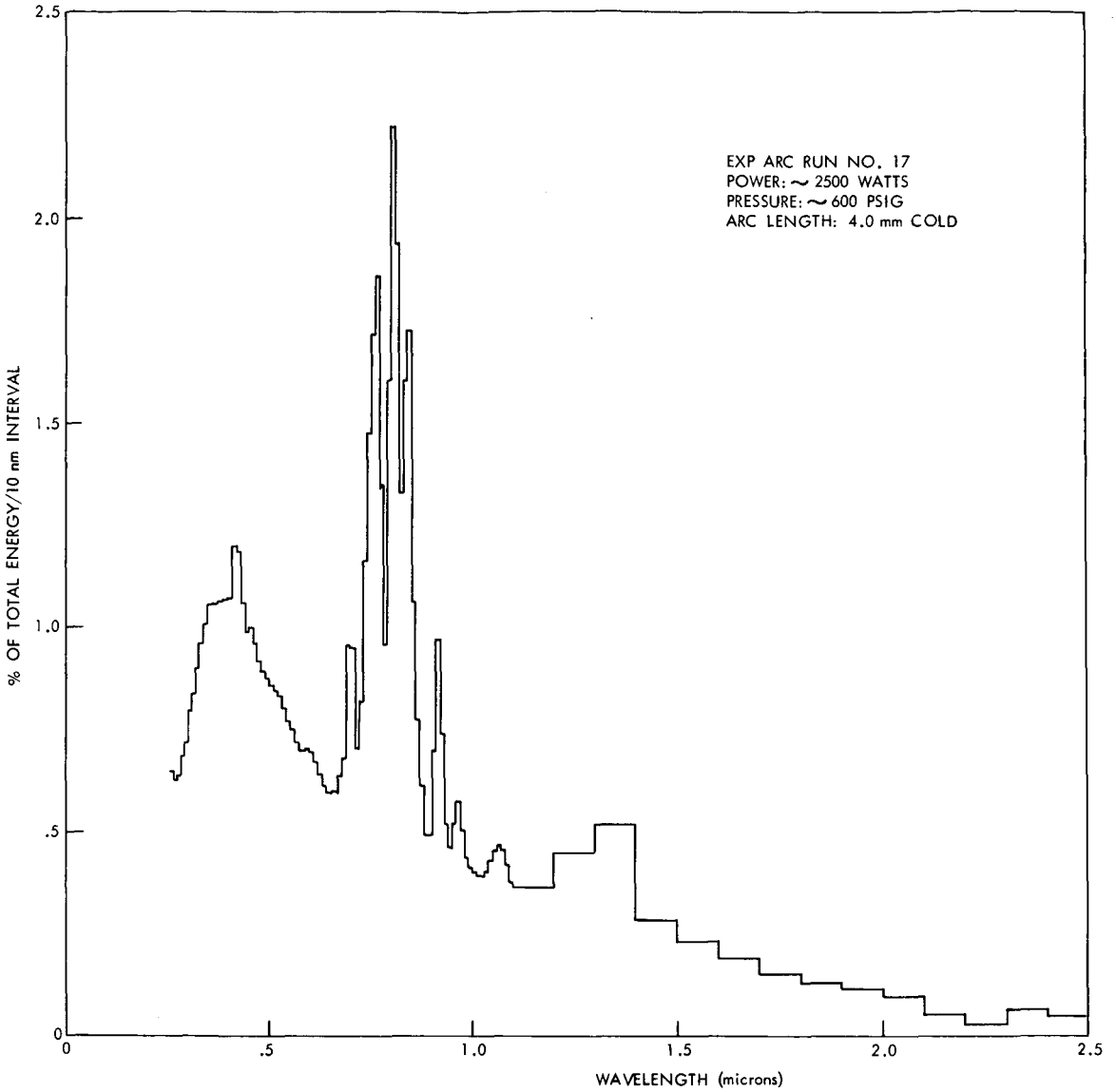

Figure 19—Spectral Irradiance of Argon

This has some interesting implications. Argon lamps would apparently make fine sources for UV degradation studies. It is a relatively efficient source of UV, and there is a complete absence of sharp emission lines which is a highly desirable property for coatings and materials research.

Another possible application for the argon lamp would be in solar simulators.

Due to the degradation of reflective coatings and the normal selective attenuation of ultraviolet, solar simulators seem to have a chronic deficiency of UV energy. It appears that argon lamps could well be used in place of xenon. This should help considerably to correct this deficiency. For those simulators having suitable optical systems, a mixture of argon and xenon lamps might be attractive. The calculated result of mixing argon and xenon lamps in a 1 to 1 ratio is shown in Figure 20. Dashed spectrum is the calculated result of mixing argon and xenon lamps. The solid line is the spectrum of xenon alone.

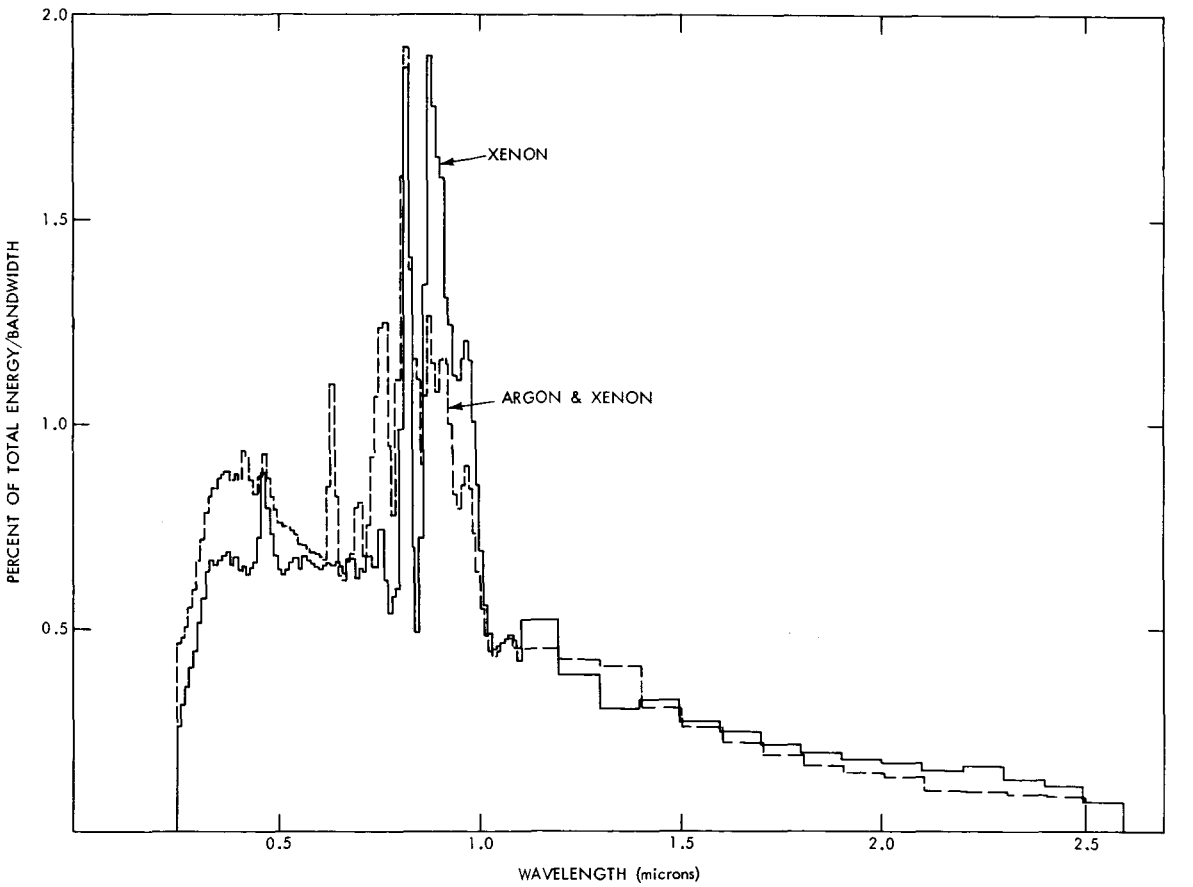

Figure 20—Computed Spectral Irradiance of Argon and Xenon 1/1 Mixture

There is a wavelength difference between the center of the argon infrared emission band and the center of the xenon infrared emission band of about 100 nm. When the lamps are mixed this difference results in a broader and somewhat more regular band which could perhaps ease the filtering problem. There is also the expected strengthening of the UV and the blue end of the visible.

The use of a mixture of argon and xenon lamps would not complicate matters by requiring new power supplies with different characteristics. The pressure and electrode separation could be specified so as to operate at the same voltage as xenon lamps. This information can be obtained from the pressure arc chamber.

It is not being suggested that everyone rush out and replace their HgXe and Xe lamps with lamps filled with argon. The suggestion is that there may be lamps readily obtainable and quite compatible with existing electrical systems which would be superior for some purposes to the lamps habitually used. An argon lamp may be one of these. It is hoped that others will be identified.

REFERENCES

1. Michels, H. Tjin, A. Djie, DeKluiver, and Seldum - Physica XXIII, p. 115.
2. Michels, DeKluiver, and Castle - Physica XXIII, p. 1131.
3. Michels, DeKluiver, and Middlekoop - Physica XXV, p. 163.
4. Bradley, "High Pressure Physics and Chemistry", Vol. 1, Academic Press, 1963.
5. Thouret and Strauss - "High Wattage Xenon and Mercury Vapor Compact Arc Lamps as Radiation Sources for Imaging Furnaces" - Duro-Test Corp., North Bergen, New Jersey.

PRELIMINARY INVESTIGATIONS OF THE PLASMADYNE VORTEX STABILIZED RADIATION SOURCE

Stan Neuder

Roy McIntosh

Radiometry Section

Thermal Systems Branch

Spacecraft Technology Division

PRELIMINARY INVESTIGATIONS OF THE PLASMADYNE VORTEX STABILIZED RADIATION SOURCE

Stan Neuder

Roy McIntosh*

Radiometry Section

Thermal Systems Branch

Spacecraft Technology Division

ABSTRACT

In order to achieve an improved solar spectral match, studies have been undertaken to better understand the basic characteristics of arc plasmas. One of the experimental systems used for this purpose is the Plasmadyne Vortex Stabilized Radiation Source (VSRS). The VSRS is a highly versatile system, permitting a wide variance of important arc parameters. As such it is a potentially promising tool for achieving improved solar simulation. This paper will describe briefly the VSRS system, the experimental apparatus, and preliminary results.

*Employee of Taag Designs Inc. on NASA-GSFC Contract No. NAS5-2382

PRELIMINARY INVESTIGATIONS OF THE PLASMADYNE VORTEX STABILIZED RADIATION SOURCE

I. VSRS Description.

Figure 1 is a sketch of the vortex stabilized source. The arc electrodes are tungsten and copper, axially positioned within two concentric, accurately spaced, quartz cylinders. The inner cylinder is approximately 5 1/2 cm long by 3 cm in diameter. A desired gas is fed in under pressure at the anode section, passes between the quartz cylinders, and into the cathode. The gas is spirally injected into the inner chamber by means of nearly-tangential nozzles in the cathode wall and is exhausted through the central bore of the anode. The gas vortex restricts the plasma to a well-defined cylindrical symmetry. Typical plasma dimensions

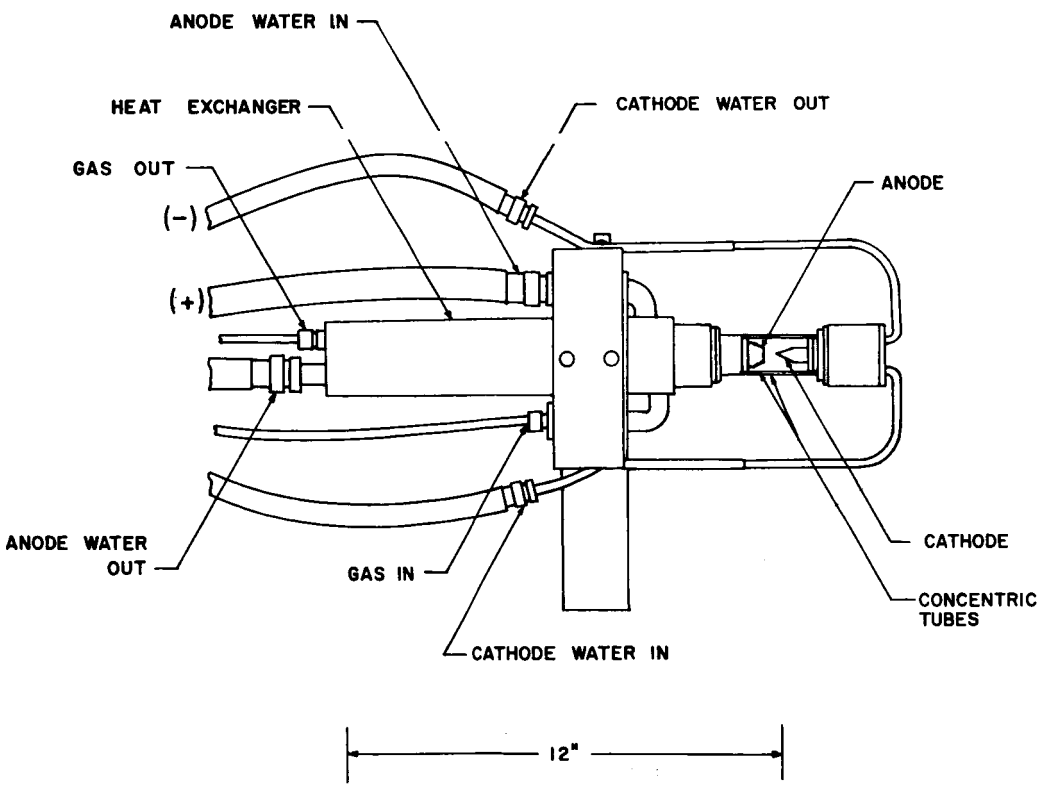

Figure 1—VSRS Configuration

are: 2mm diameter by 10mm long. The working gas is cooled by the heat exchanger and continuously recirculated by means of a diaphragm pump so that there is no gas loss during operation. The gas pressure in the system may be increased to over 18 atmospheres.

The power input ranges from about 3,000 to 25,000 watts with currents up to 250 amps readily obtainable. The electrodes and small cylindrical housing (not shown) are water cooled. The central block is an insulating support post for the VSRS and housing.

II. Instrumentation.

Figure 2 is a block diagram of the VSRS system and the experimental apparatus for obtaining the spectral radiation data. The Leiss double prism monochromator is calibrated in the spectral range 0.25 to 2.4 microns. The radiation

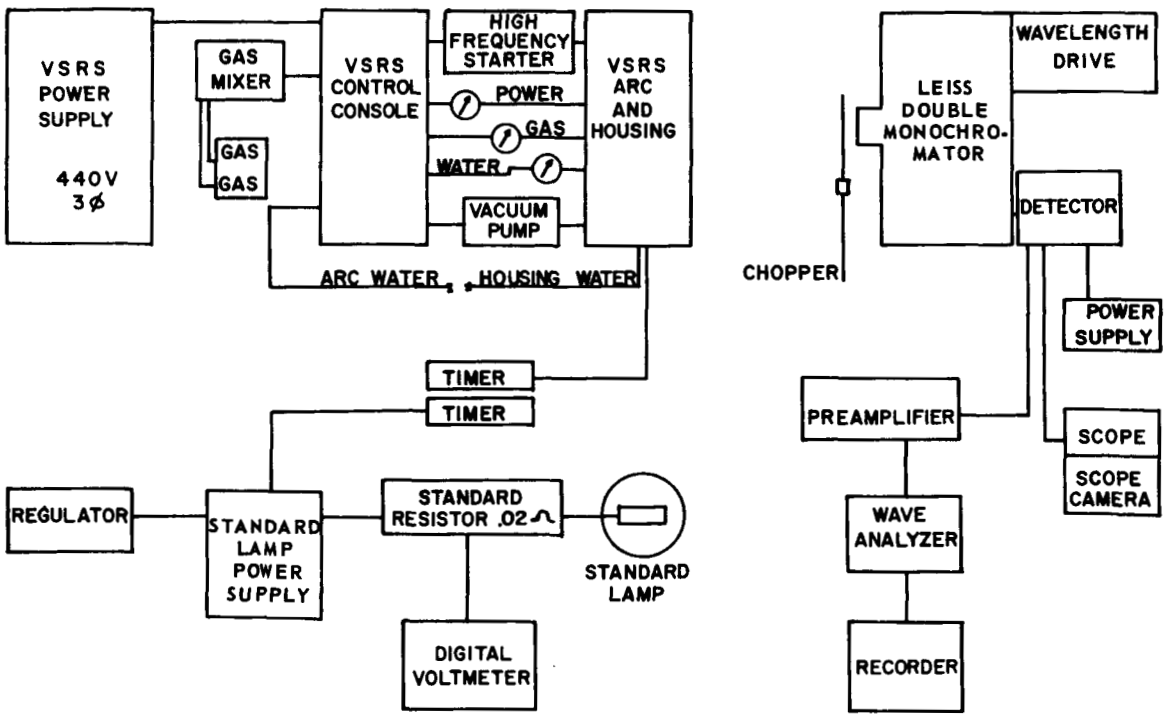

Figure 2—Instrumentation

is chopped at the entrance slit and detected by means of a photomultiplier or photoconductive cell. The signal is either displayed on a scope or is accurately amplified, frequency discriminated, and displayed on a strip chart recorder. The measured response is calibrated by means of the spectral radiance standard. The optically activated timers record the VSRS and standard operation time. The gas mixer is capable of pre-mixing to several parts per million. The pump is utilized for desorption purposes as well as pressure control.

Figure 3 is a simplified sketch of the monochromator optics and the external focussing system. The neutral density filter is used only in the arc beam.

Because of the large discrepancy between the radiance of the standard and that of the VSRS at higher input powers, the calibration procedure is now being modified to use the standard of spectral irradiance, integrating sphere, and no auxiliary optics.

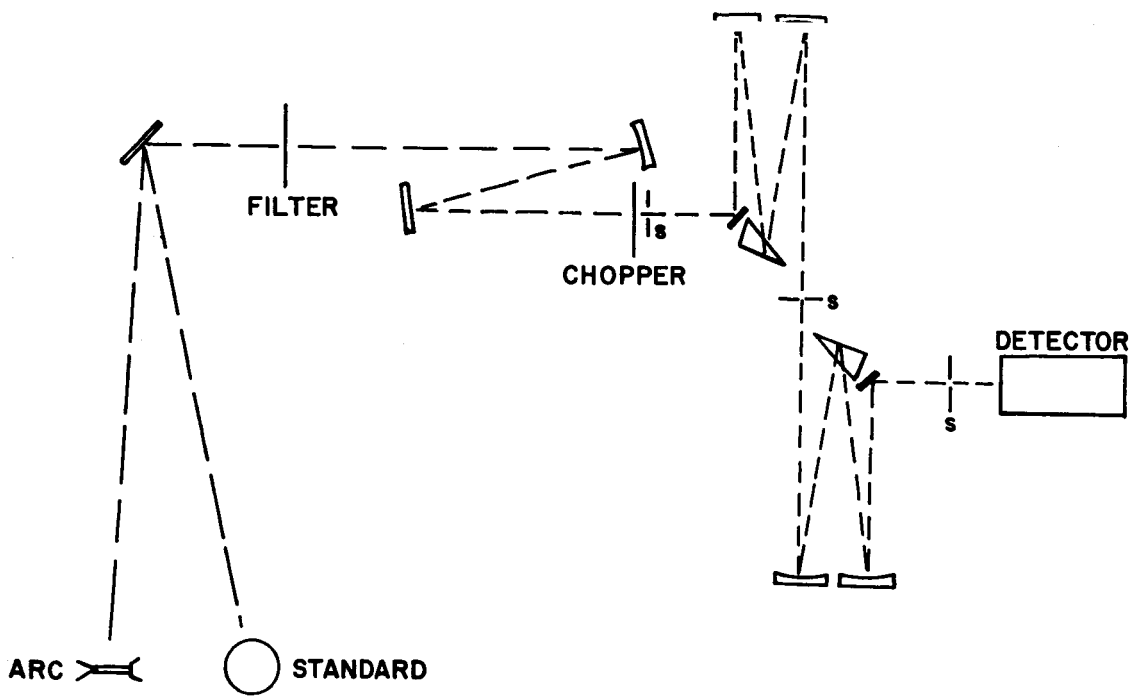

Figure 3—Optical System

III. Physical Characteristics of Electrode and Plasma

Figure 4 is a close-up photograph of the cathode and anode while the arc is in operation. The bright streaks are due to light scattering from striations in the quartz envelope.

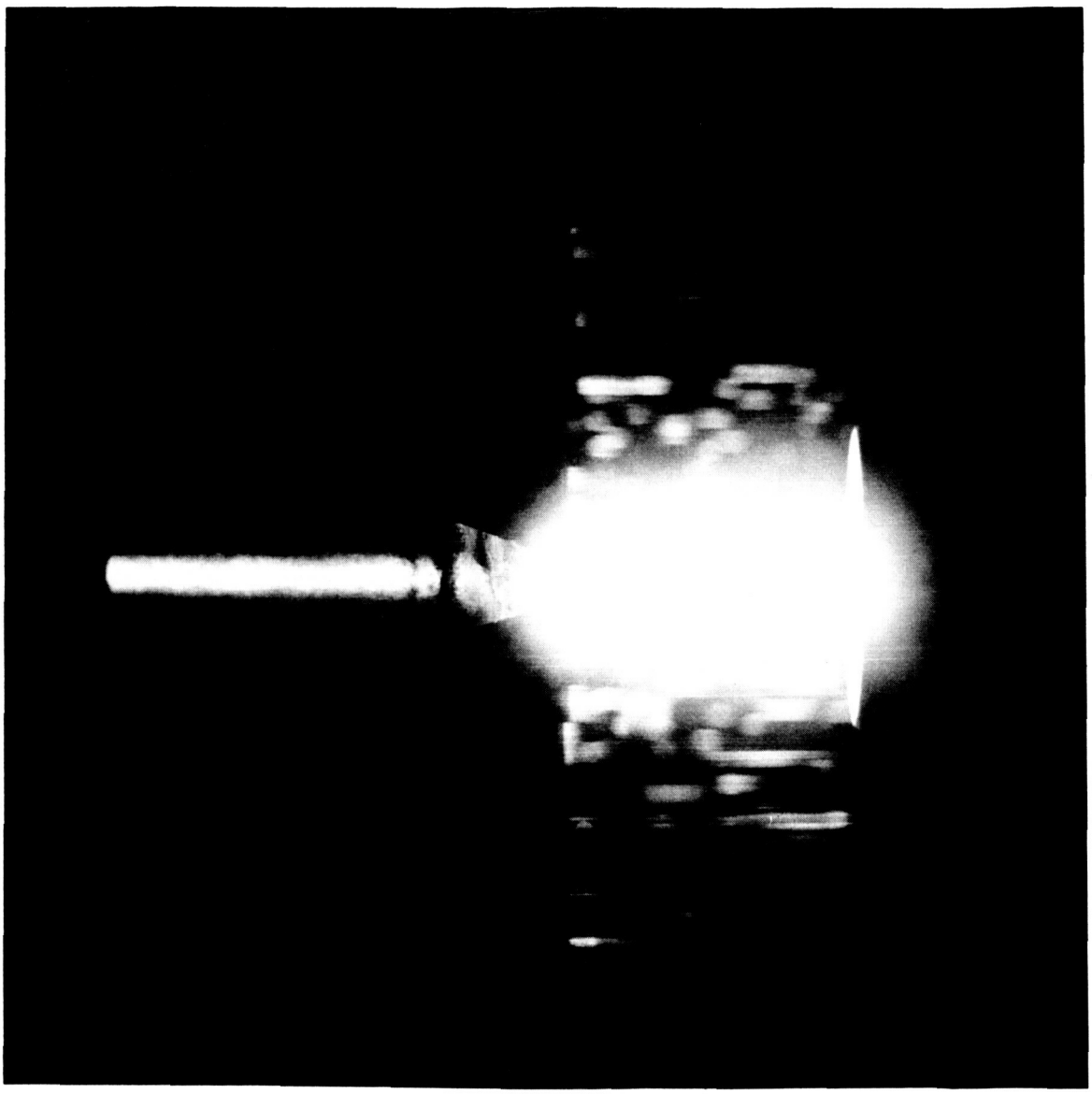

Figure 4—Electrode Operation

A more detailed photograph of the electrodes following 100 hours of operation is shown in Figure 5. Note the configuration of the gas nozzles surrounding the tungsten tip of the cathode and the central exhaust bore of the anode.

Figure 6 is a photograph of the plasma column with the arc operating at 40 amps and 4,000 watts at 8.4 atmospheres of argon. The dimensions of this plasma are 10 mm long by 1.5 mm in diameter. The cathode section is on the left. Figure 7 shows the plasma with the arc operating at 115 amps and 12,000

Figure 5—Electrodes After 100 Hours

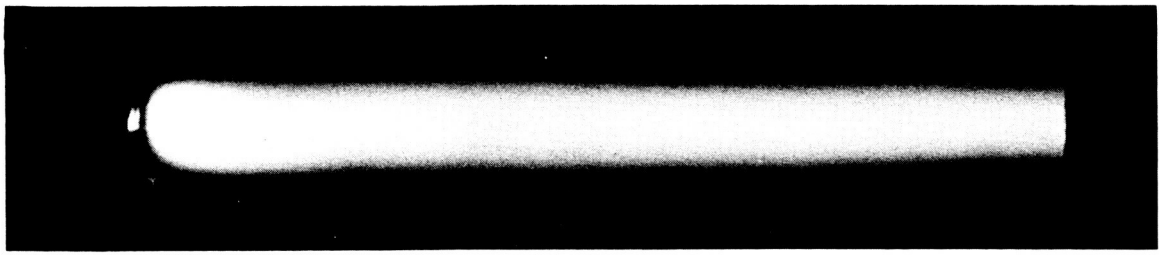

Figure 6—VSRS Plasma at 4 KW and 8.4 Atm.

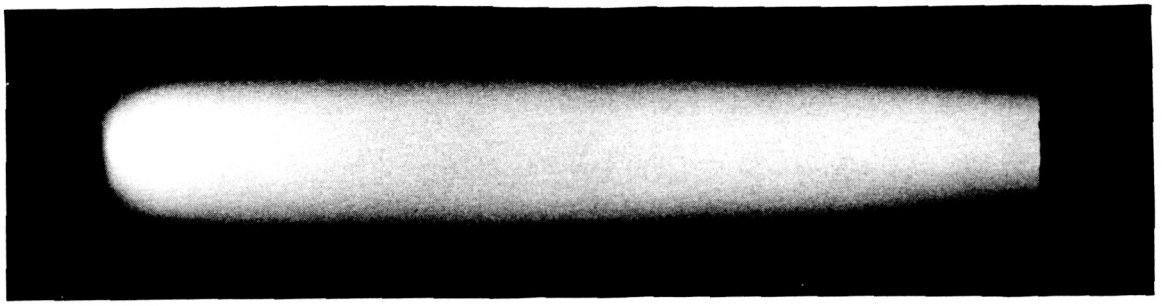

Figure 7—VSRS Plasma at 12 KW and 8.4 Atm.

watts at 8.4 atmospheres. Figure 8 is a 200 amp, 18,000 watt plasma column at 8.4 atmospheres. The diameter of the latter column is 2.5 mm, and the current density is over 4000 amps/mm^2.

The total visible radiance distribution was measured with a Jarrell-Ash recording microphotometer. The upper curve in Figure 9 is a plot of the microradiance along the center line of the plasma operating in argon at 4000 watts. The lower curve is an average microradiance along two lines halfway between the edge and the central portion of the plasma. This microradiance distribution corresponds to Figure 6. The two shaded regions in the plasma of Figure 6

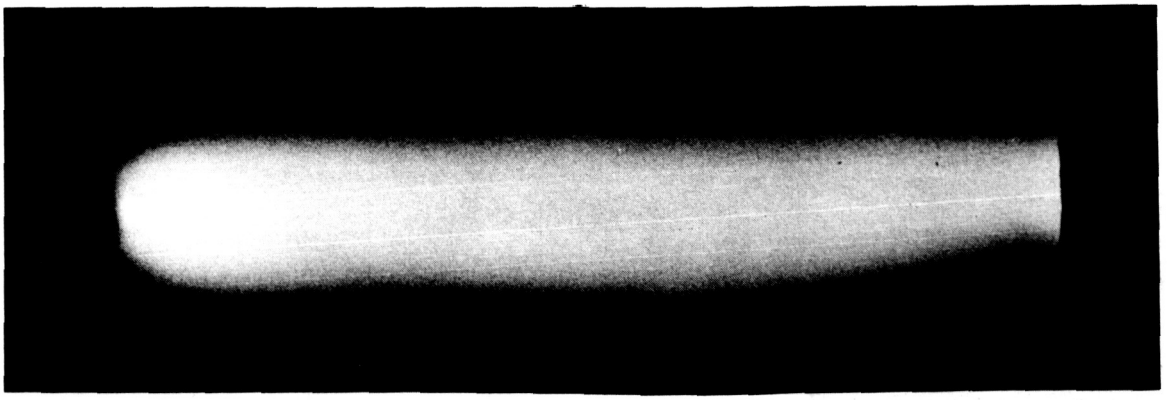

Figure 8—VSRS Plasma at 18 KW and 8.4 Atm.

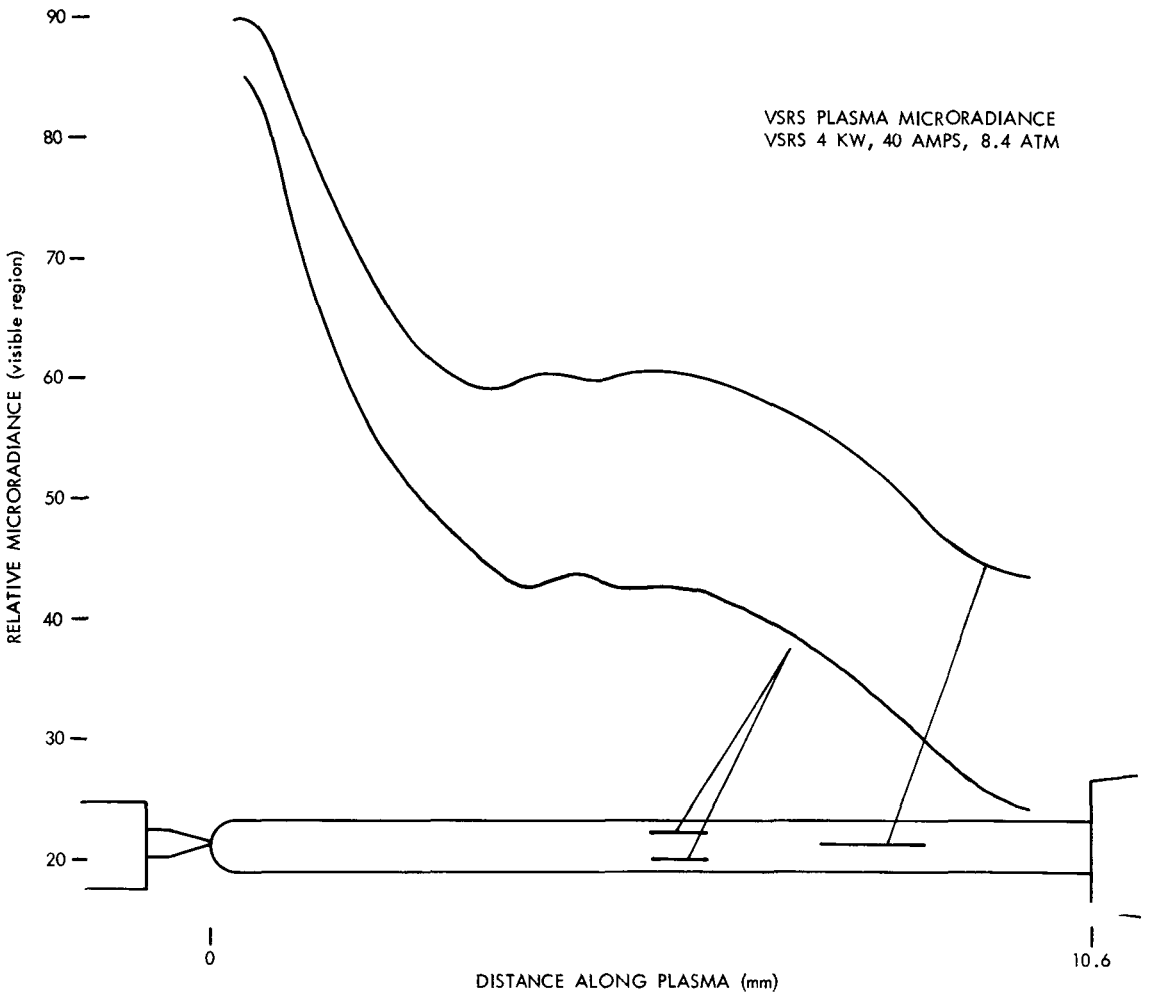

Figure 9—Relative Microradiance

corresponds to the two dips in the curves of Figure 9. The microradiance changes by a factor of two or three going from cathode to anode.

The isoradiance contour of the entire plasma in argon at 4000 watts is shown in Figure 10. The contour asymmetry may be due to gas turbulence or non-uniform cathode heating.

IV. VSRS Performance Characteristics

Using a calibrated Eppley thermopile and fixed arc chamber pressures, the dependence of the total irradiance on current and on power input was investigated.

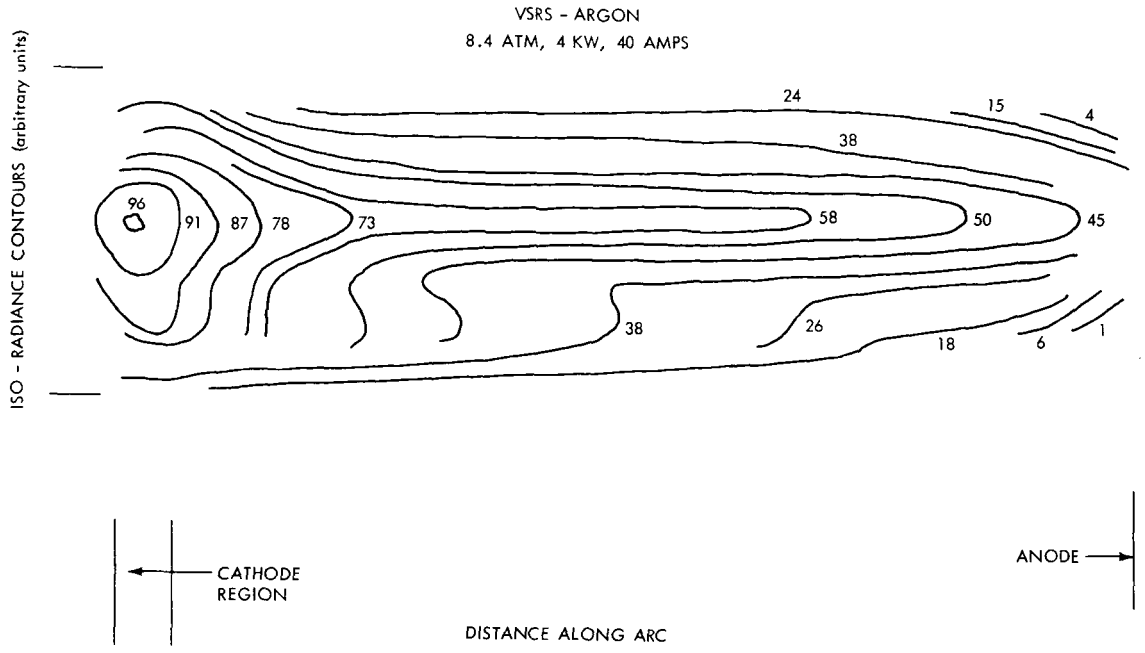

Figure 10—Isoradiance Contours

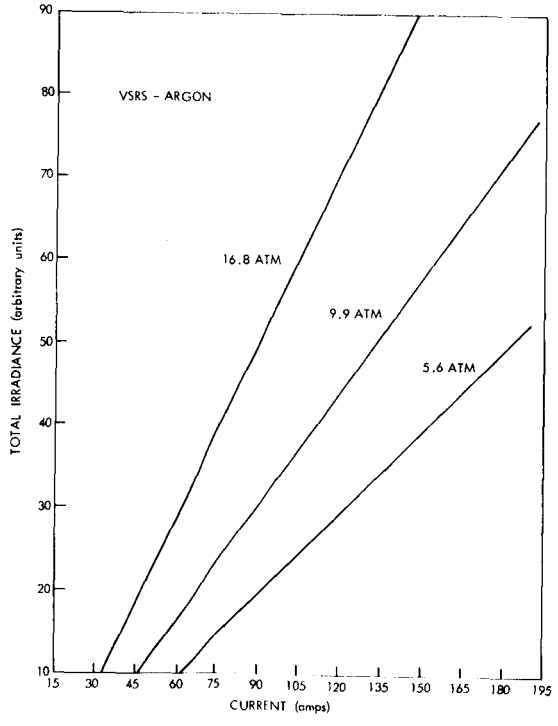

Figure 11—Total Irradiance Against Current

Throughout most of the current range, the total irradiance is a linear function of current, (Figure 11), with the proportionality constant being slightly pressure dependent. The slope of the curve of total irradiance against input power increases with increasing power input, (Figure 12), but is not appreciably pressure dependent. Thus the efficiency of the VSRS with argon ambient is only slightly pressure dependent in the measured range, but is quite sensitive to power input.

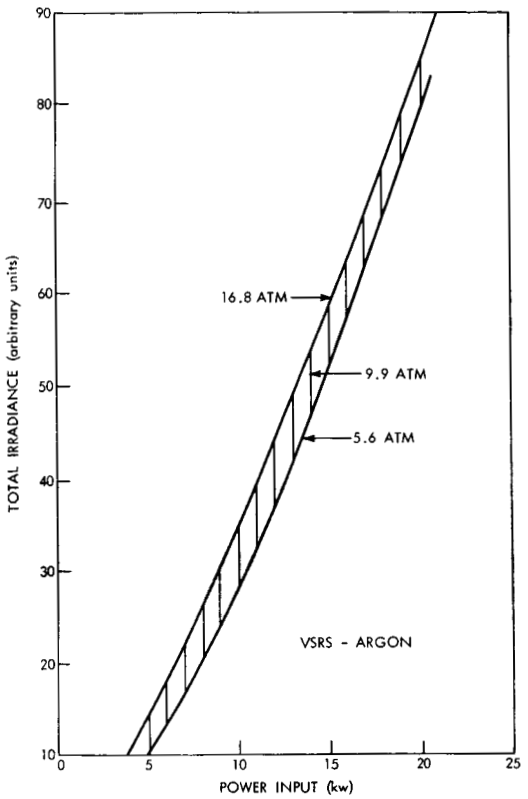

Figure 12—Total Irradiance Against Power

More meaningful relationships of the VSRS performance parameters are plotted in Figure 13. The solid curves are plots of voltage against current at three different pressures. The dashed curves are the power input hyperbolas. The numbers in parenthesis along the isobars are relative irradiance figures. The curves of positive slope are the physical plasma diameters.

V. Preliminary Spectral Measurements.

Figure 14 is a plot of the relative spectral energy distribution in the wavelength range 0.3 to 2.2 microns for argon at 5.5 atmospheres, 4500 watts, and 50 amps. The ratio of line to continuum emission is very large. The intensity of the emission lines near 0.8 microns exceeds the ordinate scale by well over one order of magnitude.

Figure 15 is a similar run with argon, using approximately the same current and power input but with an increase in pressure to 10.2 atmospheres. The ratio of line to continuum emission has been greatly reduced while the continuum in the UV region has been enhanced.

Figure 16 is a third run with argon but with the pressure at 16.8 atmospheres, current at 135 amps, and 18,200 watts input power. Again the ratio of line to

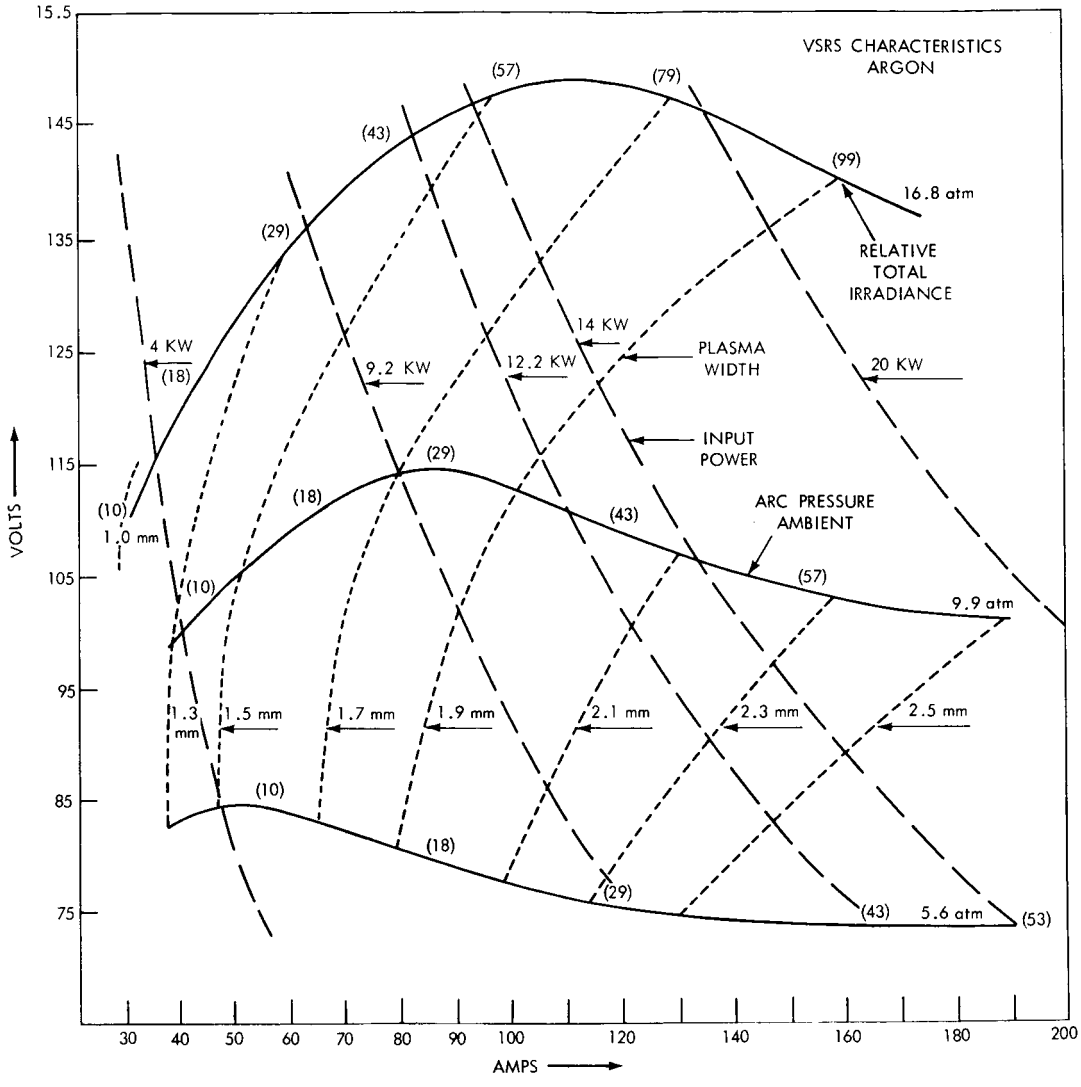

Figure 13—VSRS Operational Parameters

continuum emission has been further reduced, the UV content enhanced, and an appreciable degree of line broadening has become apparent.

The trend towards higher UV content and larger percentages of continuum energy with increased power and pressure is clearly indicated. Further investigations continue into the possible redistribution of spectral energy in order to achieve improved simulation.

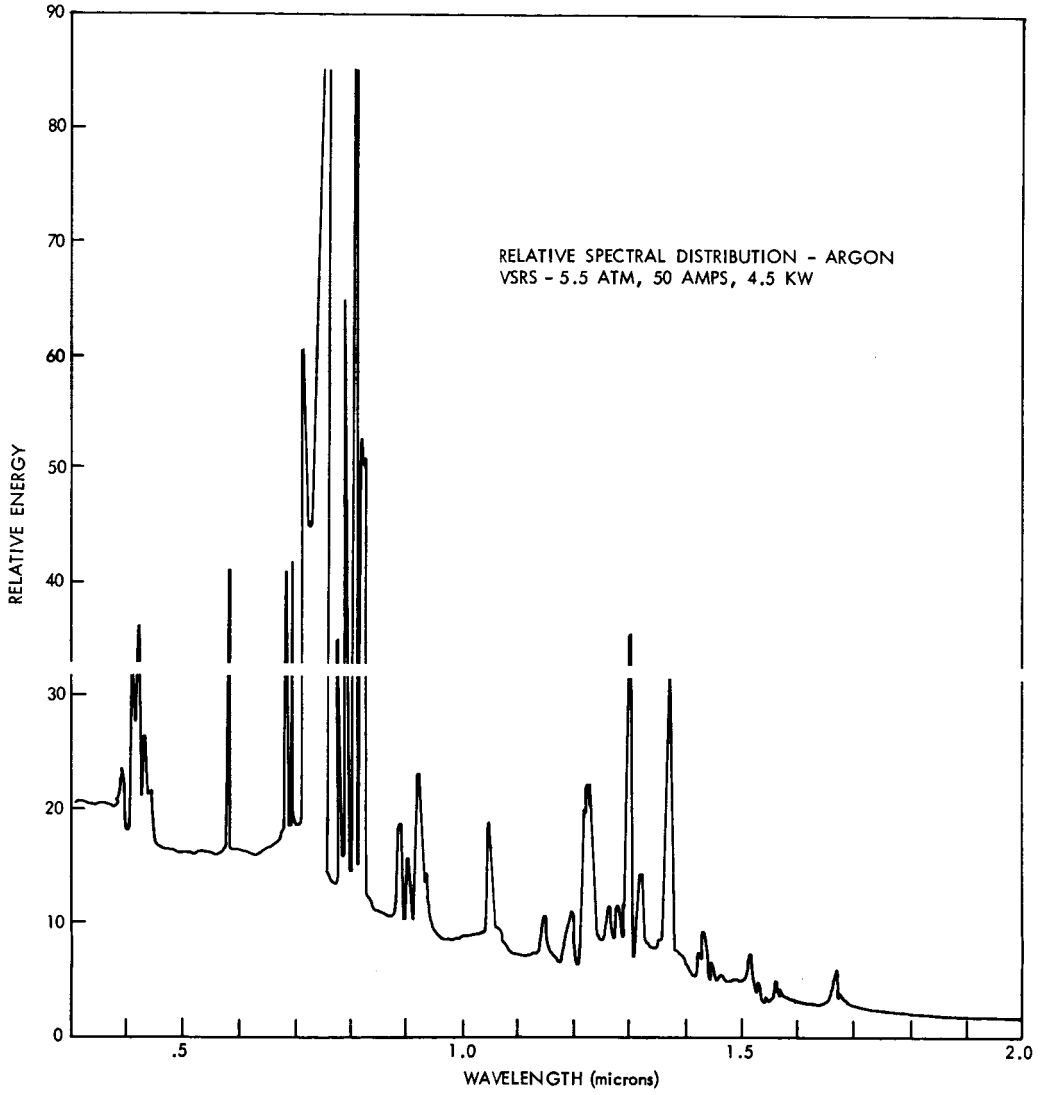

Figure 14—Spectral Distribution at 4.5 KW and 5.5 Atm., (Argon)

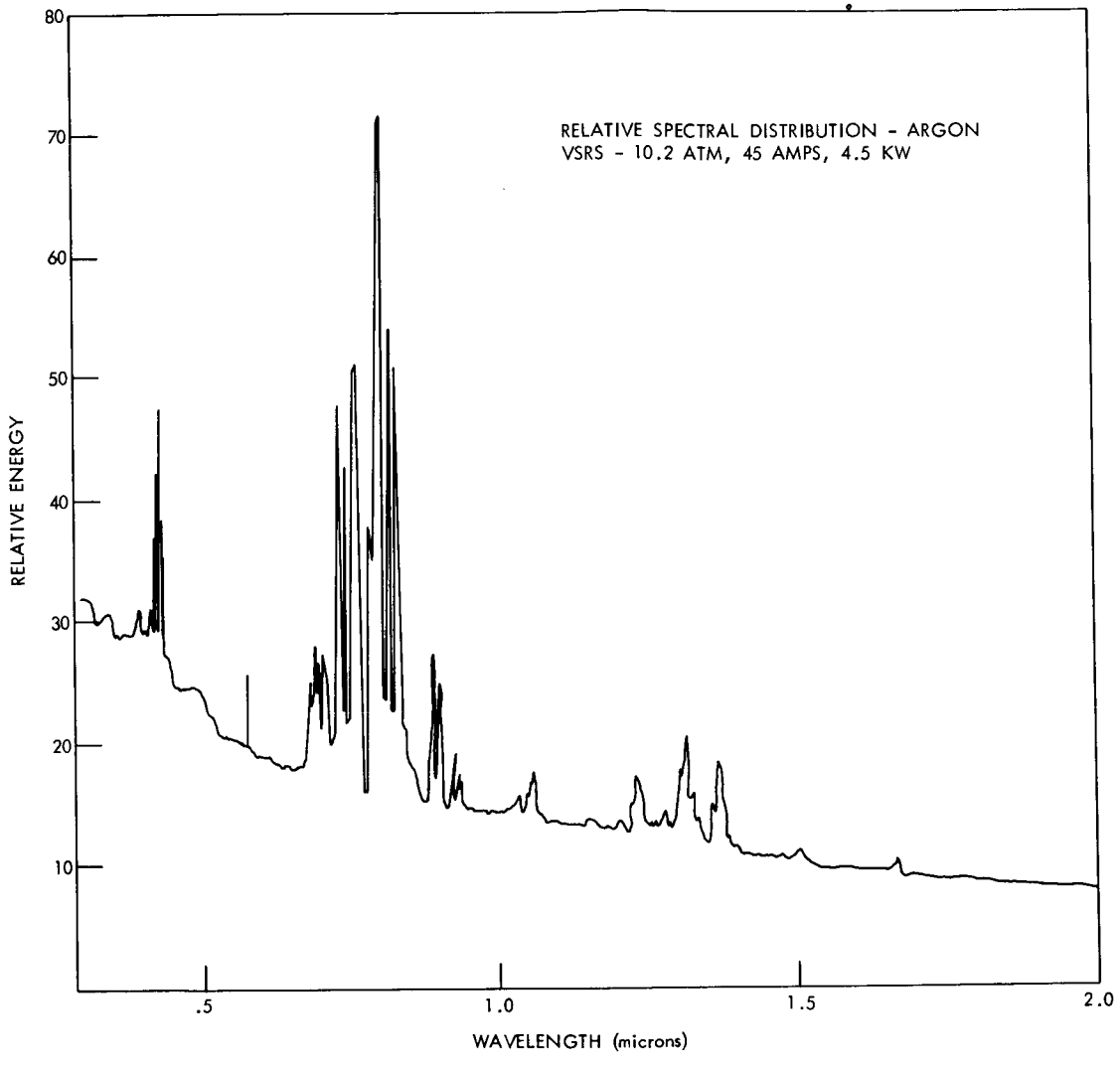

Figure 15—Spectral Distribution at 4.5 KW and 10.2 Atm., (Argon)

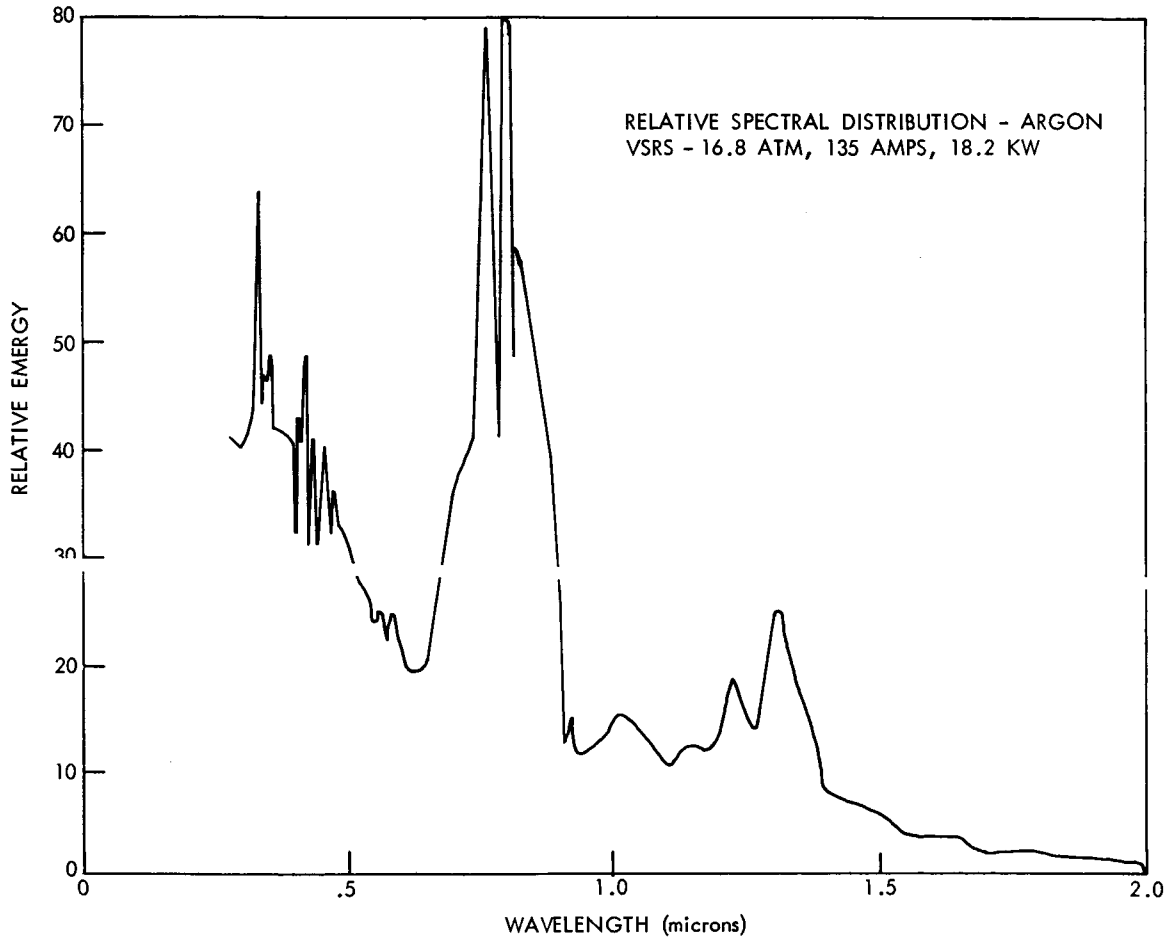

Figure 16—Spectral Distribution at 18.2 KW and 16.8 Atm., (Argon)

VI. Contractual Work (NASw-858)

Several interesting results of studies made at the Giannini Scientific Corporation are reproduced in Figures 17, 18 and 19. The relative distribution of UV and near IR emission shown in Figure 17, is somewhat different than that shown in Figure 16. Further verification is necessary. Figure 18 is a result of investigations with a number of solid additives. Figure 19 is the spectral distribution of the VSRS with xenon at 21,700 watts and 12.7 atmospheres.

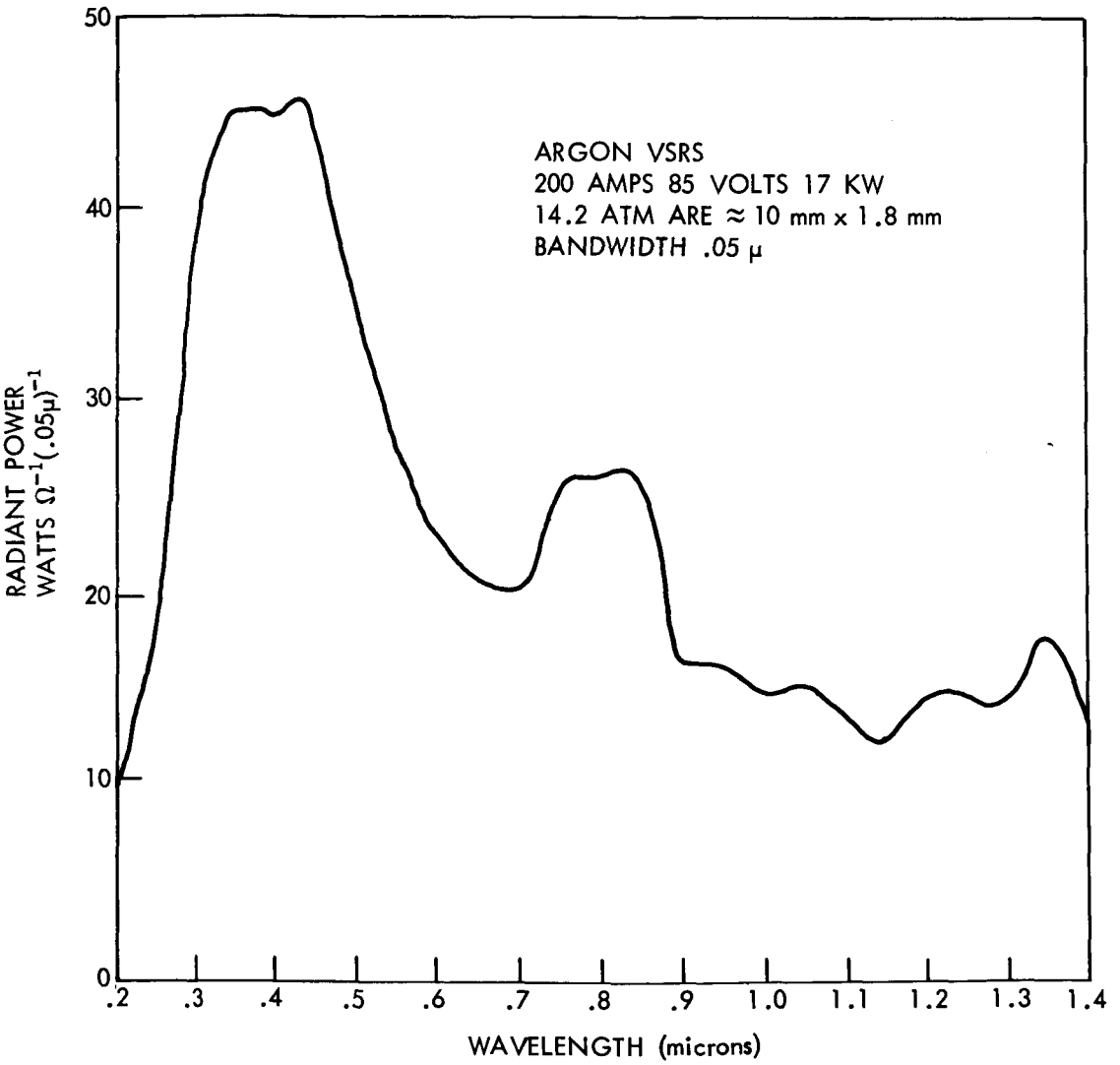

Figure 17—Spectral Distribution at 17 KW and 14.2 Atm., (Argon)

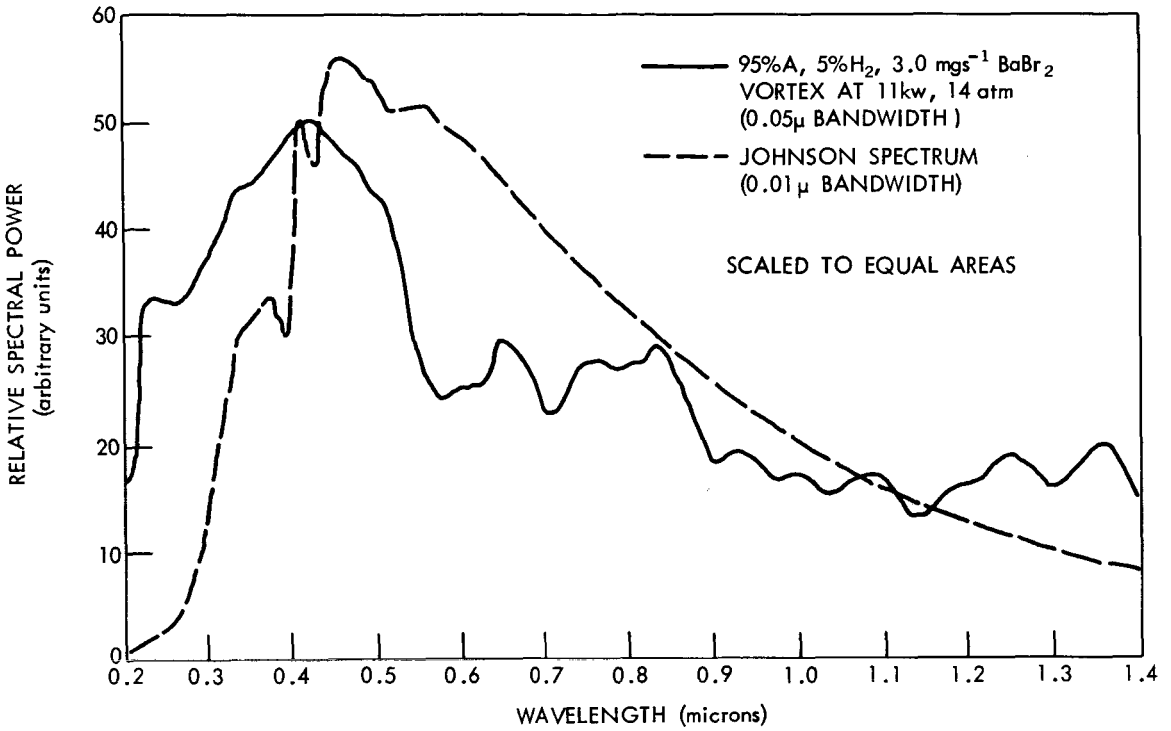

Figure 18—Spectral Distribution at 11 KW and 14 Atm., (95% A, 5% H_2, $BaBr_2$)

VII. VSRS Stability, Repeatability, and Lifetime

Short term stability over several hours was of the order of ±2%. Investigations of repeatability and long term stability have not as yet been made. The lifetime appears to be quite satisfactory as can be seen from the small amount of electrode damage following 100 hours of non-continuous operation.

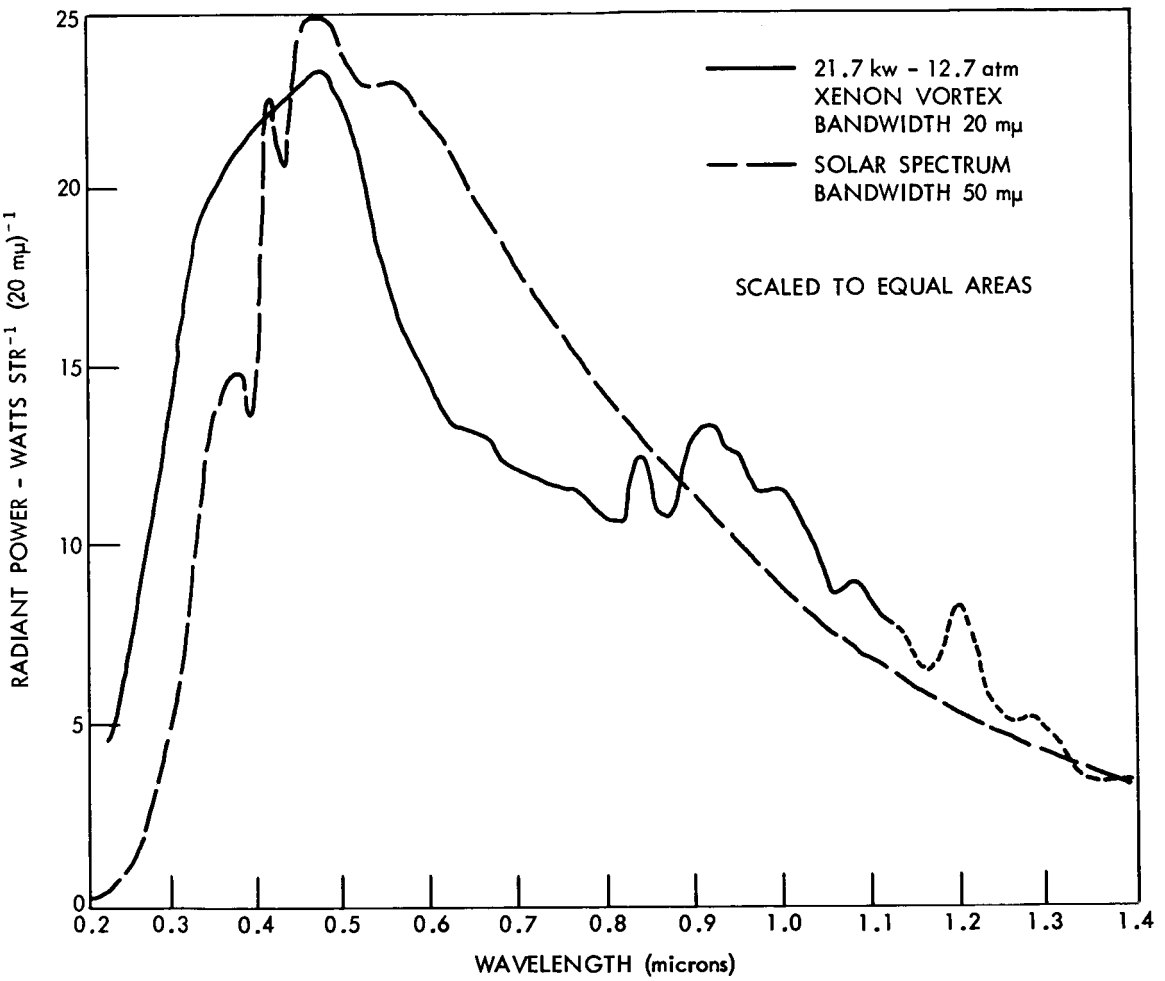

Figure 19—Spectral Distribution at 21.7 KW and 12.7 Atm., (Xenon)

ULTRAVIOLET MEASUREMENTS OF SEVERAL LIGHT SOURCES

James J. Webb

Radiometry Group

Thermal Systems Branch

Spacecraft Tech. Div.

ULTRAVIOLET MEASUREMENTS OF SEVERAL LIGHT SOURCES

James J. Webb

Radiometry Group

Thermal Systems Branch

Spacecraft Tech. Div.

ABSTRACT

Information concerning the ultraviolet energy content of light sources is particularly useful in the degradation studies of various materials and coatings, as well as in solar simulation research and development. This report describes a method for measuring the UV content (between 2400 and 3600 Angstroms) of four commonly used high intensity sources. The errors inherent in such measurements are examined and accounted for, and it is believed that the final irradiance results are accurate to within a 7% RMS error. In an effort to determine how aging effects the UV content, a 2500 watt xenon lamp was run for nearly 1500 hours. Periodic samplings of its irradiance were made to ascertain its variations with time. No decrease in ultraviolet irradiance was noted for 650 hours.

ULTRAVIOLET MEASUREMENTS OF SEVERAL LIGHT SOURCES

Information concerning the ultraviolet content of various light sources is desirable in studies of the degradation of different materials and coatings, as well as in solar simulation research. The purpose of this report is to examine four commonly used lamps as to their energy content and characteristics in the near UV region.

The lamps tested were: A 500 watt mercury vapor lamp; a 1000 watt mercury-xenon arc lamp; a 2500 watt mercury-xenon arc lamp (all manufactured by Hanovia); and, a 2500 watt xenon arc lamp (manufactured by Osram).

Two energy detectors were employed: An Eppley 30 junction bismuth-silver thermopile with a response time of 10 seconds; and, a Hilger-Watts model FT-1 thermopile with a response time of approximately 5 milliseconds. Thermopiles were chosen over other possible detectors because their sensitivities were purported to be relatively high and constant, their response is fairly linear over a wide range (.2 microns to 5 microns), and they are comparatively easy to operate. To a first approximation, their response is independent of the spectral characteristics of the source.[1] Both thermopiles were covered with quartz windows and were operated at atmospheric pressure.

The lamps were mounted in a special housing designed specifically for this purpose. The housing is a rectangular-shaped metal box, set on end, and painted with a dull black finish on the inside. The front cover has a suitable opening through which the light passes. (This was removed during the 500 watt lamp

---

[1] Final Report of the Goddard Summer Workshop Program in Measurement and Simulation of the Space Environment. 1963, p. A-53.

test to allow for the lamp's elongated shape.) The detector was mounted rigidly on one end of a lathe bed and lined up with the opening in the housing. The output was fed directly to a Keithley model 150 AR microvoltmeter, designed for low-level measurements of this type. On the source end of the lathe bed, a removable shield was mounted so that readings could be made with and without incident light on the thermopiles. In this way, the effects of spurious light were minimized. All the lamps were run at their rated values of current and voltage by means of appropriate power supplies. The detectors were placed at two measured distances from the source, 100 cm. and 150 cm., in order to check for water and carbon dioxide absorption. Figure 1 shows the test arrangement used.

In order to obtain energy values in the UV region only, Eppley high-pass filters were used. The two filters were Corning types 9-54 and 0-52, having nominal 50% cut-off wavelengths of 2400 and 3600 angstroms, respectively. The cut-offs were 2340 and 3575 angstroms, as determined by measurements made with the McPherson Instrumentation.

Before the actual test was run, the two thermopiles were calibrated using a standard of total irradiance obtained from the National Bureau of Standards.

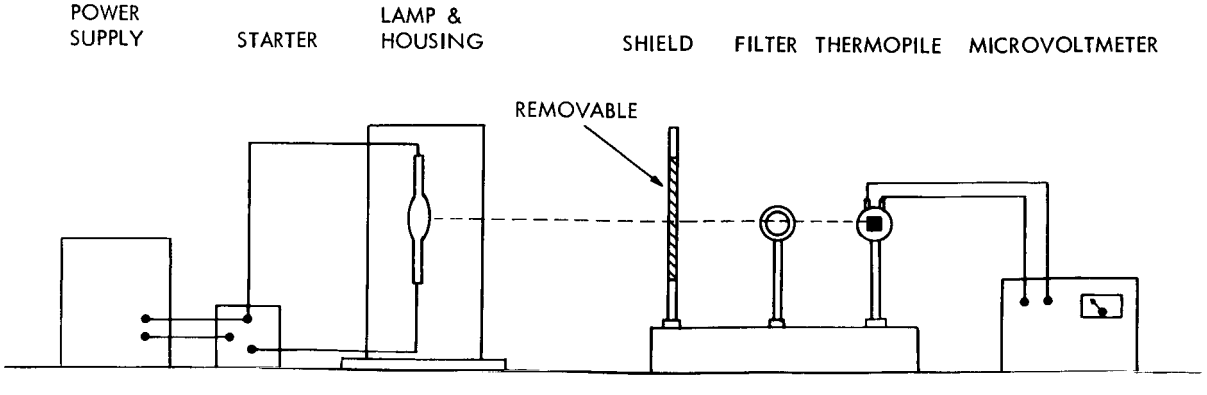

Figure 1—Test Configuration

Irradiance at a particular distance was calculated using the inverse square law ($J = Hd^2$). Readings were obtained with the Keithley meter at this distance, and sensitivities with an accuracy of approximately 3% were thus obtained in microvolts/watt/cm^2.

The raw test data were recorded by taking several readings (generally 10, but sometimes less when repeatability was good) at each distance with and without the filters. The readings were averaged to obtain a value in microvolts for each position, and the energy in watts/cm^2 was calculated.

In order to determine some degree of accuracy and justify the data reduction, a statistical analysis was attempted. Although the experiment was not set up in such a manner as to permit a rigorous analysis, nevertheless some conclusions were possible.

Since a major criterion for any statistical test is randomness[2], the first step was to determine whether or not the samples were drawn at random from their populations. This was done by means of a "run test for randomness"[3,4]. Some difficulty was encountered here, in that only about 40% of the data were able to be so tested. The trouble resulted from the fact that the sample sizes were too small. However, in all cases where a sufficient number of readings were recorded, the null hypothesis of randomness at the 5% level of significance was accepted. (It should be noted that the data that could not be tested were generally grouped closer than the tested data. The error was in not planning on using

---

[2]Crow, Davis, and Maxfield. Statistics Manual, Dover, p. 83-4.

[3]Ibid.

[4]See appendix for explanation of all statistical tests.

statistics until the data taking was completed. Otherwise, enough points could have been recorded.)

If the assumption is made that the rest of the data is also random, then another test may be applied in an effort to determine whether or not there is a significant difference between the thermopiles. The test used is known as the "sign test"[5] for paired observations. This is a quick and simple way of deciding whether a set of paired readings shows a significant mean difference between pair members. The sign test was chosen over other similar ones because it does not depend on a known distribution. In all cases, no significant difference was found (at the 5% level) between the performances of the two thermopiles. Because of this it was felt justifiable to combine the results of the two detectors and obtain single energy values.

Before tabulating any results, however, it is necessary to determine what correction factors might be applied to yield more accurate data.

Several errors inherently present in the system need to be accounted for. These include: 1) inaccuracies of the Keithley microvoltmeter (2%); 2) electrical noise of the detectors and meter; 3) H_2O and CO_2 absorption; 4) variations in lamp radiances due to power supply fluctuations; 5) errors of filter and detector placement; 6) temperature changes of the detectors; 7) losses due to transmissions of the filters and quartz windows; and finally 8) losses due to multiple reflections between the quartz windows and filters.

Assuming that the discrepancies of the Keithley meter and the power supply variations occurred in a random fashion, then the manner in which the data were recorded — several readings and an average — would minimize these effects.

[5]Ibid., p. 56.

The noise levels of the meter and detectors appeared to be well below the signal levels. The Johnson noise was down in the nanovolt range. The H_2O and CO_2 absorptions were roughly checked by taking measurements at two different distances, as mentioned previously. The radiant intensity was found to be the same for each distance within 3%, thus indicating no measurable absorption. The detectors were initially placed by using a meter stick. These points were then carefully marked. While this might yield on initial error of ± 1 cm., it was nevertheless consistent since the detectors were always returned to these marked positions. The positioning of the filters did not appear to be too critical. A tilt of approximately 5-10° from the center line was allowable before any noticeable drop in output occurred. The same was true of the detectors, though not separately. The total tilt cannot exceed the 10° figure. The Eppley thermopile was temperature compensated, and both detectors were allowed to approach equilibrium before any measurements were made. Thus, the only corrections that appeared to be necessary were for the transmission losses and multiple reflection losses.

In order to determine the transmissions of the filters and also the 50% cut-off wavelengths, a McPherson monochromator with an estimated accuracy of 2% was used. With appropriate energy sources and detectors, transmission curves were obtained for each filter. The 9-54 was found to have a 93% transmission and a cut-off wavelength of 2340 angstroms. The 0-52 had a 92% transmission and a cut-off of 3575 angstroms. These cut-off wavelengths are accurate within ± 5 angstroms. Figure 2 shows the transmissions of these filters.

The multiple reflection losses were corrected by applying a 1% correction factor given by Eppley Laboratories.

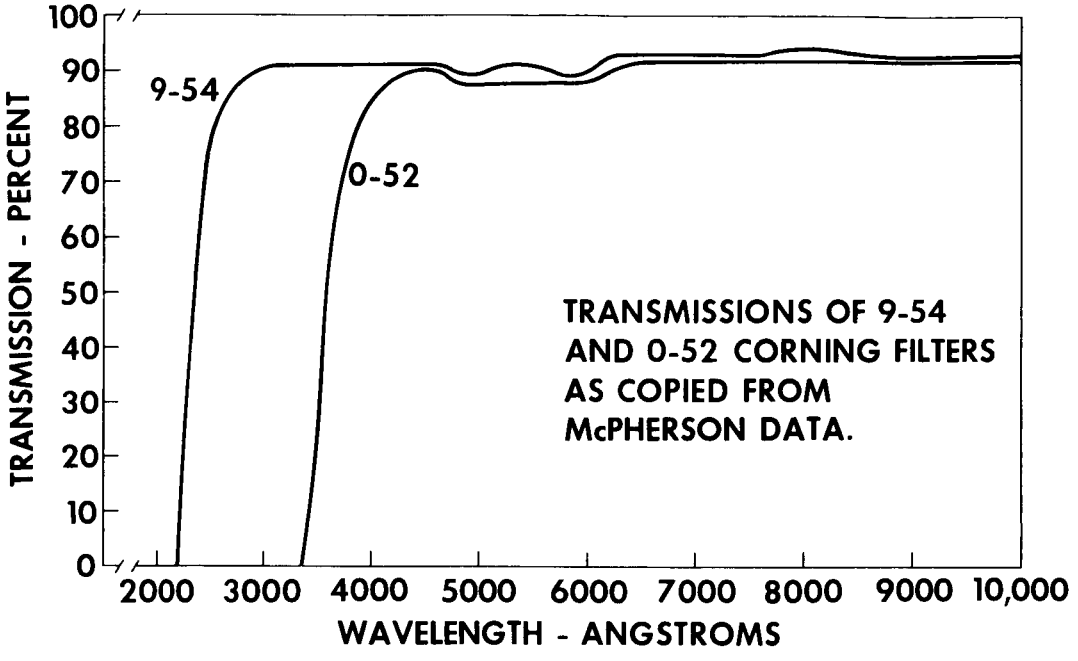

Figure 2—Spectral Transmission of Filters

Thus, it was apparent that in order to obtain values of the total incident energy, all that was needed was to specify some confidence limits on the measured data. No corrections were needed. This was done by assuming a Student's t distribution and calculating 90% confidence limits.[6] This distribution was used because the number of samples was so small. The total energy values are shown in Table I. It is possible that this is not an accurate set of values due to quartz absorption in the far infrared. However, this data was not the primary intent of the paper.

The UV energy values are shown in Table II. These values were determined by applying the appropriate correction factors to the data taken with the filters and then subtracting the two. The confidence limits were calculated as before.

---

[6]Monroney, M. J. Facts From Figures, p. 243. Pelicon Publishing Co.

TABLE I: TOTAL ENERGY RESULTS

I. 2500 WATT Xe:		
A. 100 cm.	21.7± .3	MILLIWATTS/cm^2
B. 150 cm.	9.88± .09	MILLIWATTS/cm^2
II. 2500 WATT Hg-Xe:		
A. 100 cm.	20.6± .3	MILLIWATTS/cm^2
B. 150 cm.	9.26± .16	MILLIWATTS/cm^2
*III. 1000 WATT Hg-Xe:		
A. 100 cm.	9.91± .13	MILLIWATTS/cm^2
B. 150 cm.	4.28± .08	MILLIWATTS/cm^2
IV. 500 WATT Hg:		
A. 100 cm.	3.36± .08	MILLIWATTS/cm^2
B. 150 cm	1.47± .01	MILLIWATTS/cm^2

*EPPLEY ONLY

TABLE II: UV ENERGY (2340-3575Å)

I. 2500 WATT Hg-Xe:		
A. 100 cm.	3.2± .5	MILLIWATTS/cm^2
B. 150 cm.	1.43± .28	MILLIWATTS/cm^2
II. 2500 WATT Xe:		
A. 100 cm.	1.45± .4	MILLIWATTS/cm^2
B. 150 cm.	0.68± .10	MILLIWATTS/cm^2
*III. 1000 WATT Hg-Xe:		
A. 100 cm.	1.23± .21	MILLIWATTS/cm^2
B. 150 cm.	0.73± .13	MILLIWATTS/cm^2
IV. 500 WATT Hg:		
A. 100 cm.	0.75± .11	MILLIWATTS/cm^2
B. 150 cm.	0.31± .05	MILLIWATTS/cm^2

*EPPLEY ONLY

In examining these results, it is apparent that the spread of data is somewhat large in a few cases. This is due primarily to the fact that, as mentioned before, not enough raw data points were taken in some instances, which forced the statistics to expand the tolerances. Another way of determining the accurracy is to sum the % errors in the system and calculate an overall RMS error. When this was done, a figure of approximately 7% RMS was obtained.

In conjunction with this test, an attempt was made to determine what effects aging might have on the UV output of the lamps. As it was not practical to age all four lamp types, a 2500 watt xenon was chosen since it is the type used in the A-1200 Solar Simulator.

The lamp was set up as before, but with a blower on the housing to roughly match the airflow environment of the simulator lamps. The lamp was allowed to run continuously until it reached approximately 1000 hours. After that, it was turned off on week-ends to prevent it from burning out unattended and also to more closely match the simulator operation. Measurements were made with the Eppley thermopile with and without the filters, and the uncorrected irradiance values are plotted as shown in Figure 3. It was not necessary to correct these readings since deviations from the initial output were of interest.

After running for nearly 1400 hours, a jumping of the arc from one spot to another on the anode was very noticeable. From the severity of the movements, it seemed reasonable to assume that the jumping began sometime before the 1400 hour mark and gradually increased. This could explain the rippling effect in the graph beyond the 1130 mark. No explanation can be given for the three low readings, other than to assume that they were due to the instrumentation and supporting equipment (possibly the power supply). The test was terminated at 1460 hours,

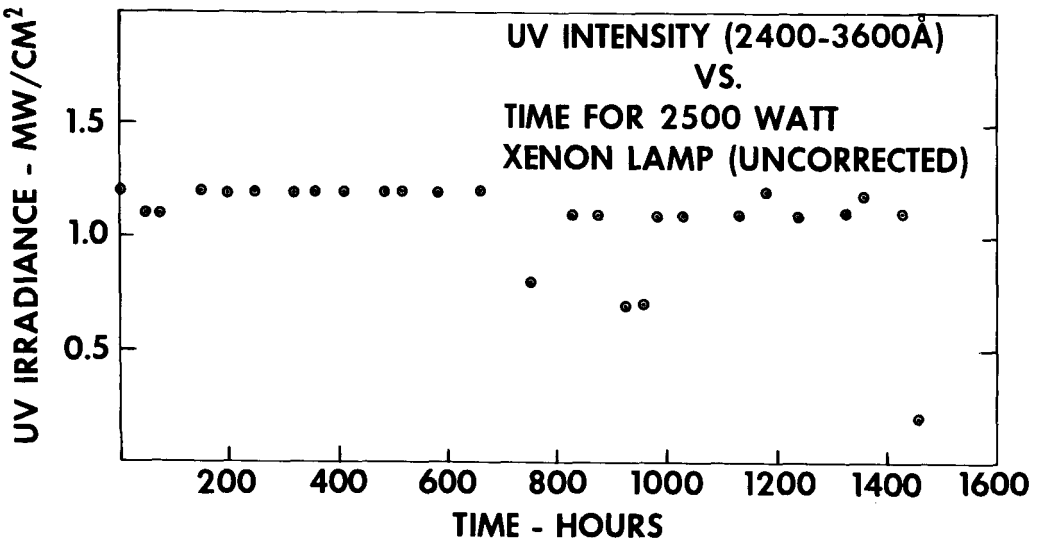

Figure 3—UV intensity vs. age for Xenon Lamp

when the UV output fell to about 1/6 of its original value. Examination of the lamp then revealed a badly pitted and corroded anode, as well as a cloudiness of the bulb, especially at the top and bottom (a characteristic of leakage).

APPENDIX

I. Randomness test

Randomness is checked by ordering a set of readings according to size, finding the median, and determining how many values are above and below the median. These two results are used with a table to determine whether or not the null hypothesis of randomness can be accepted at various levels of significance.

II. Sign test for paired observations

Two sets of values, A and B, are recorded and compared one by one. The number of times A is greater than B and the number of times B is greater than A are noted. These two numbers are used with a table to determine whether or not the performances of the two items (in this case thermopiles) are different at various levels of significance.

III. Student's test for 90% confidence limits

Used for small samples, the test yields a ± value around a mean. It can be determined for any level of significance. The equation used is

$$\bar{x} \pm \frac{t\sigma}{\sqrt{n}}$$

where $\bar{x}$ = the mean

t comes from tables (different for each level)

σ = standard deviation corrected for by Bessel's correction factor (n-1/n).

n = number of samples

SPECTRAL RESPONSE MEASUREMENTS AND CALIBRATION SYSTEM FOR SPECTRAL IRRADIANCE DETECTORS

by

William Gdula

Radiometry Group

Thermal Systems Branch

Spacecraft Technology Division

SPECTRAL RESPONSE MEASUREMENTS AND CALIBRATION SYSTEM FOR SPECTRAL IRRADIANCE DETECTORS

by

William Gdula*

Radiometry Group

Thermal Systems Branch

Spacecraft Technology Division

ABSTRACT

Instrumentation to measure the spectral response characteristics of irradiance detectors is discussed. The basic calibration system is composed of a high resolution 1 meter grating monochromator and synchronous detecting amplifier. Representative calibration data of solar cells used as detectors is presented. Modifications being made will make possible accurate measurements of transmission and reflectance properties of narrowband and neutral density filters.

*Taag Designs, Inc., employee at GSFC.
Contract # NAS5-2382

SPECTRAL RESPONSE MEASUREMENTS AND CALIBRATION SYSTEM FOR SPECTRAL IRRADIANCE DETECTORS

I. INTRODUCTION

Primary considerations were to develop a highly accurate system for spectral response calibration of solar cells and detectors. The well known problems of absolute standards and black body detectors were encountered along with the inherent difficulties in making solar cell measurements. The system is primarily designed for measuring the properties of solar cells but most types of detectors can be readily calibrated. During the course of the measurements, significant improvements were found to be necessary and will be briefly described. The effort of detector calibration and improvements in accuracy will be a continual effort in view of the basic need for improvements in radiometric procedure.

II. SOLAR CELL THEORY AND EXPERIMENTAL DATA

(A) Spectral Response Characteristics

In order to effectively use the solar cell as a detector it is necessary to consider the fundamental energy conversion process involved. For a general analysis, the solar cell, when used as an irradiance detector can be evaluated as a large-area, P/N junction current generator.

When photon flux incident on the cell surface is absorbed within the bulk material, an energy transformation results and is characterized by the generation of electron-hole pairs. Each photon absorbed creates one minority carrier. These minority carriers, electrons for "p" type material and holes for "n" type are capable of being collected by virtue of the internal electrostatic field in the junction region of the solar cell and a net current flow can be delivered into

an external load. The probability that the generated carriers are collected is highly dependent upon the junction and bulk properties of the solar cell and the energy level of the incident photons.

The ratio of the total number of collected carriers to the photon flux density absorbed within the solar cell is defined as the absolute quantum yield. Absolute spectral response characteristics are derived by simply converting the eV energy of the monochromatic photon flux density to equal μW energy units. For a given monochromatic photon flux density the absolute current output of the cell is given by

$$i_{(\lambda)} = \int_0^D \left[1 - R_{(\lambda)}\right] N_0 \, e^{-\alpha(\lambda)x} \, k(x) \, dx \qquad (1)$$

where N_0 = photon flux

$R_{(\lambda)}$ = surface reflection coefficient

$k(x)$ = collection efficiency parameter

$\alpha_{(\lambda)}$ = optical absorption coefficient

D = cell thickness.

Figure 1 shows a normalized spectral response of a silicon solar cell uncorrected for surface reflection and electrode area losses. The absolute quantum yield of the same cell is shown in Figure 2. Wide variations in the reflectance properties of the S_iO coatings has made it necessary to measure the surface reflectance of the cells in order to evaluate the bulk properties. Surface reflectance data for S_iO coatings as a function of optical thickness is

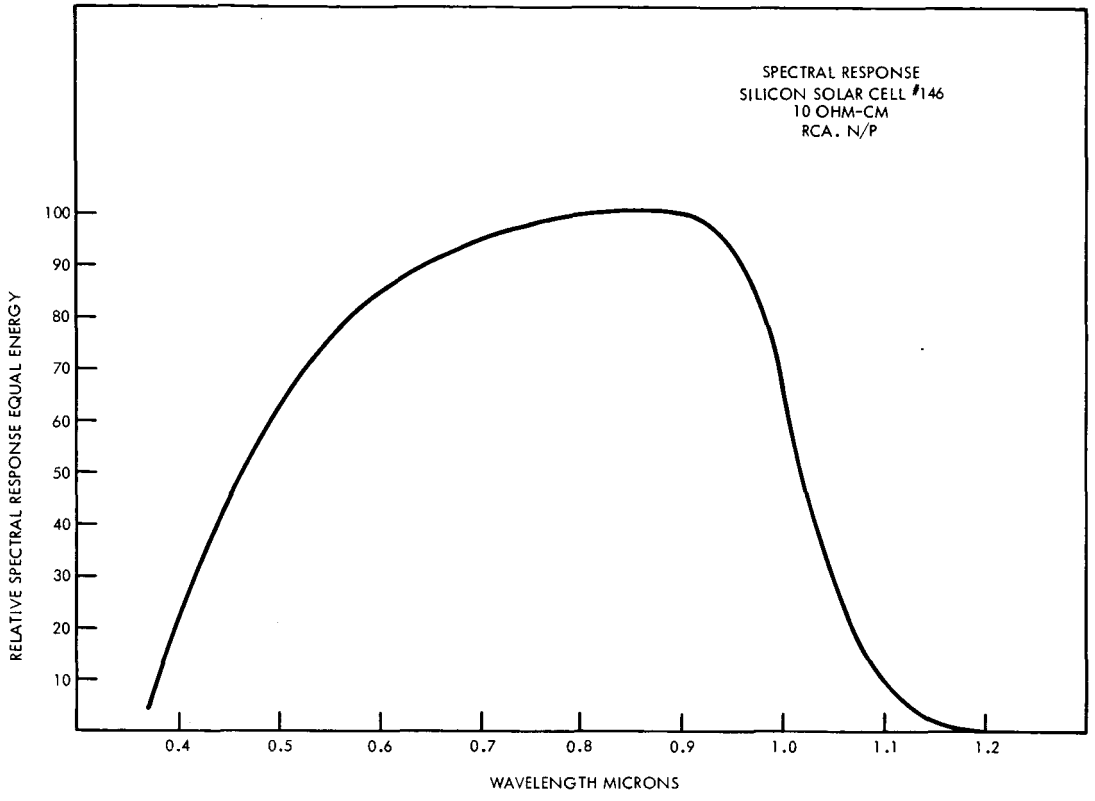

Figure 1 — Relative Spectral Response Silicon Solar Cell

shown in Figure 3. The monochromatic cell output of this solar cell is decreased by 16% at 5000A° as a result of surface losses. When the cell is exposed to air mass zero spectral irradiance conditions the total surface energy loss is approximately 18%. The total solar cell current output, given by

$$I_{sc} = \int_0^{\lambda_g} \int_0^{D} \left[1 - R_{(\lambda)}\right] N_0 \, \bar{e}^{\alpha (\lambda)^x} \, k(x) \, dx \, d\lambda \qquad (2)$$

would be 34 milliamps. The infra-red wavelength, λ_g is determined by the bandgap of the material and is 1.18 microns for a silicon solar cell. Graphic

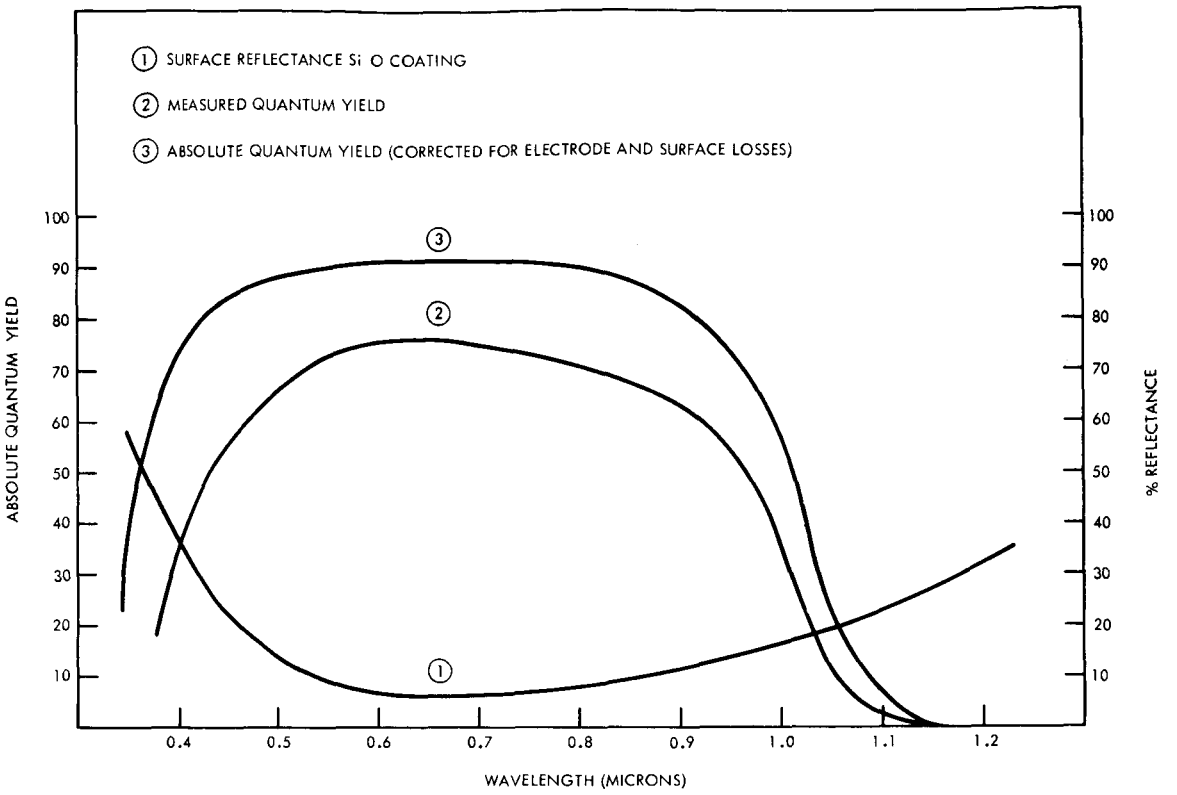

Figure 2 — Absolute Quantum Yield

relationships between the response regions of the cell in relation to the air mass zero spectral irradiance conditions are shown in Figure 4. It is readily apparent that the silicon solar cell when used as a detector is only capable of measuring energy from 3800A° to 11,000A°. Erroneous conclusions can result when comparing solar data taken with different solar simulation sources.

(B) Solar Cell Diode Properties

When the free carriers generated in the solar cell are collected and delivered to an external load, the cell can be effectively described as a P/N junction biased in the forward direction. An equivalent circuit shown in Figure 5 and the ideal diode equation can adequately describe the current-voltage characteristics of the junction when photon energy is absorbed in the cell.

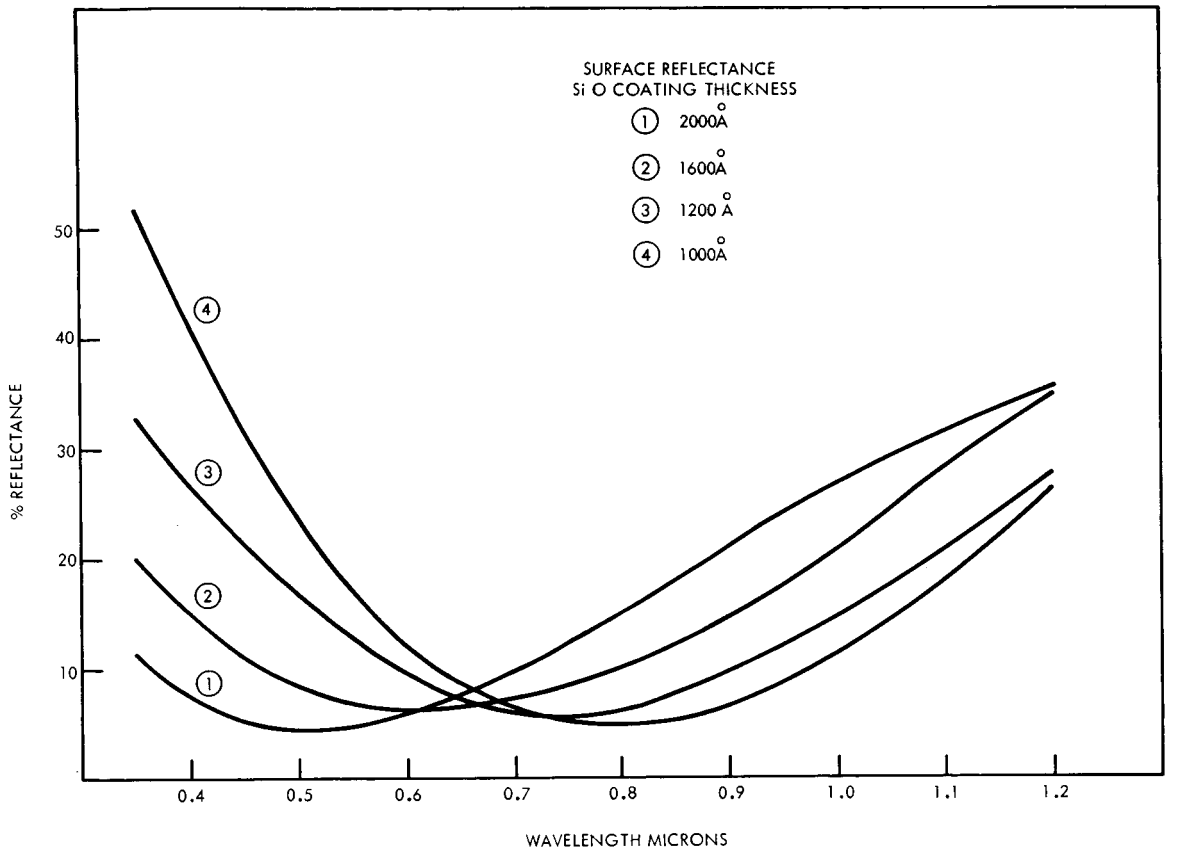

Figure 3 — Surface Reflectance with S_1O Coating

The open-circuit voltage, V_0, derived from the ideal diode equation is

$$V_0 = \frac{AkT}{e} \ell n \left(\frac{I_L}{I_0} + 1 \right) \tag{3}$$

Assuming the thermally generated I_0 component is independent of the voltage across the cell, V_0 is an approximate logarithmic function of the photon flux

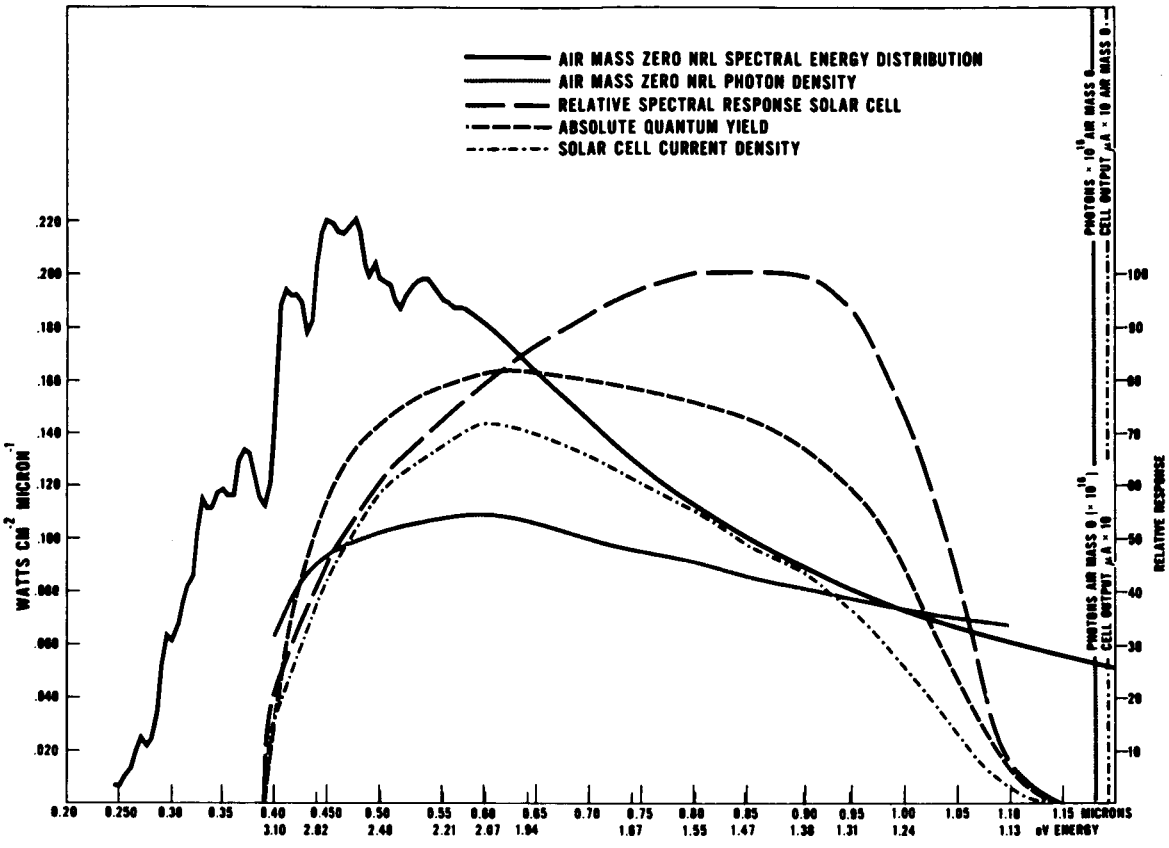

Figure 4 — Solar Irradiance Data and Solar Cell Quantum Yield

density incident on the cell. Since

$$\frac{I_L}{I_0} \gg 1$$

and neglecting the series resistance which is not significant for low resistivity material, the open circuit voltage can then be written as

$$V_0 = \frac{AkT}{e} \ell n \frac{I_L}{I_0} \qquad (4)$$

$$(3)\quad I_L = I_S - \frac{V}{R_{SHUNT}} - I_O e^{\frac{q}{AkT}(V-IR_s)}$$

WHERE:

I_S = GENERATED CURRENT
I_L = LOAD CURRENT
I_O = REVERSE SATURATION CURRENT
$\lambda = \frac{q}{kT}$
A = EMPIRICAL PARAMETER

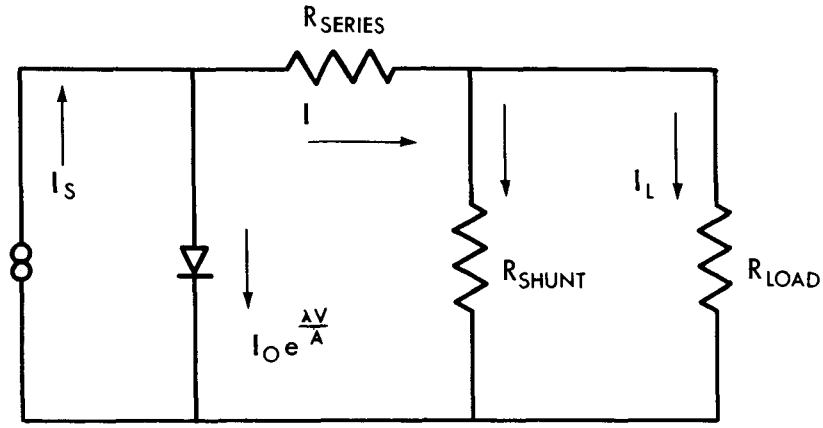

SOLAR CELL EQUIVALENT CIRCUIT

Figure 5 — Solar Cell Equivalent Circuit and Diode Equation

Experimental data of the open circuit voltage is shown in Figure 6 where V_0 is plotted as a function of relative intensity units. At low generation levels the open circuit voltage however is not a logarithmic function primarily because of the large junction area of the solar cell. Large junction areas have soft reverse-bias characteristics as shown in Figure 7. The thermally generated reverse saturation current I_0 thus becomes a complicated function, primarily of the bandgap, bulk properties, and the voltage across the junction. As a practical consequence of this property, the solar cell, when used as a linear detector should be operating into a low impedance as possible to prevent a non-linear output.

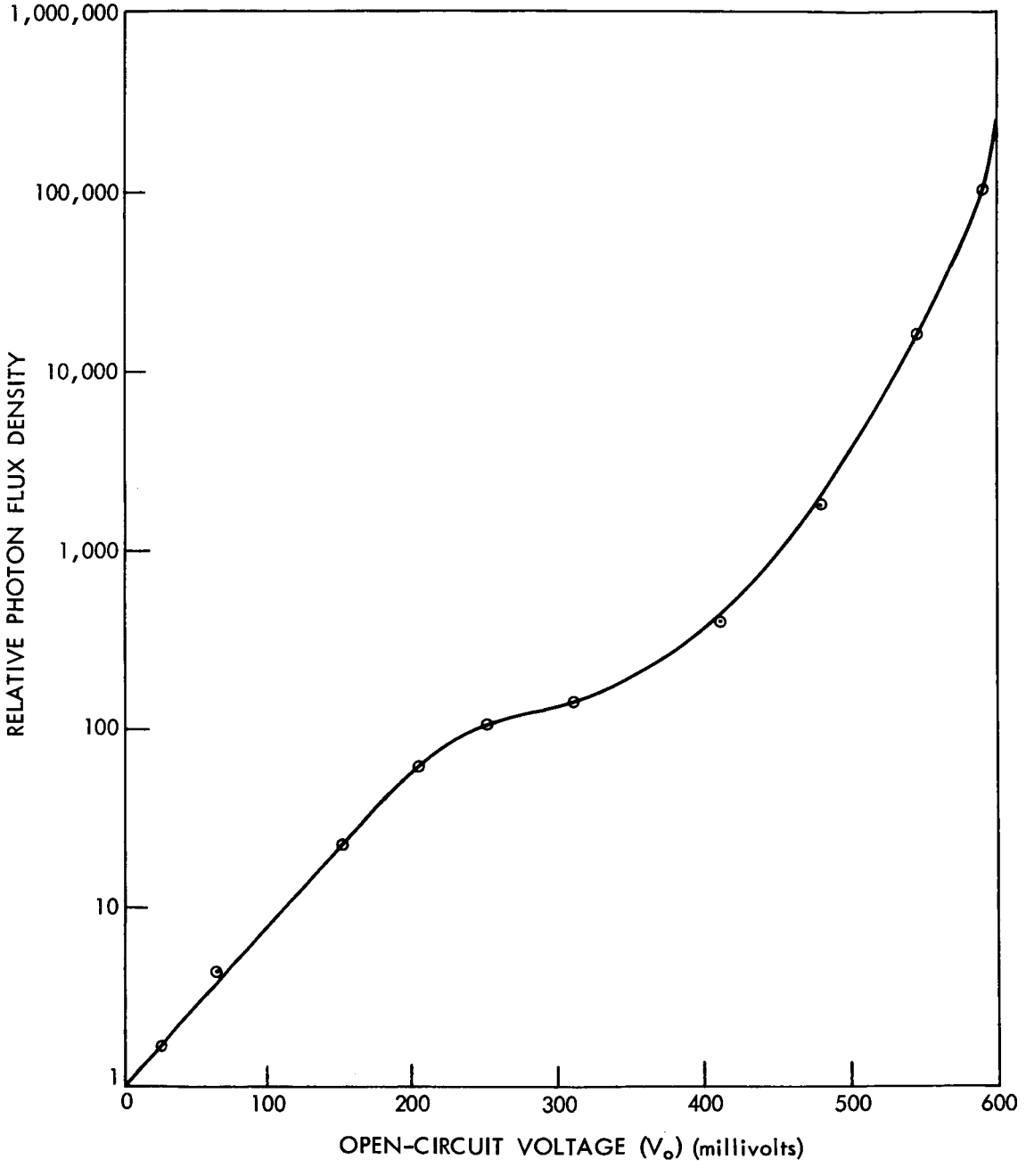

Figure 6 — Photovoltaic Voltage as a Function of Photon Flux Density

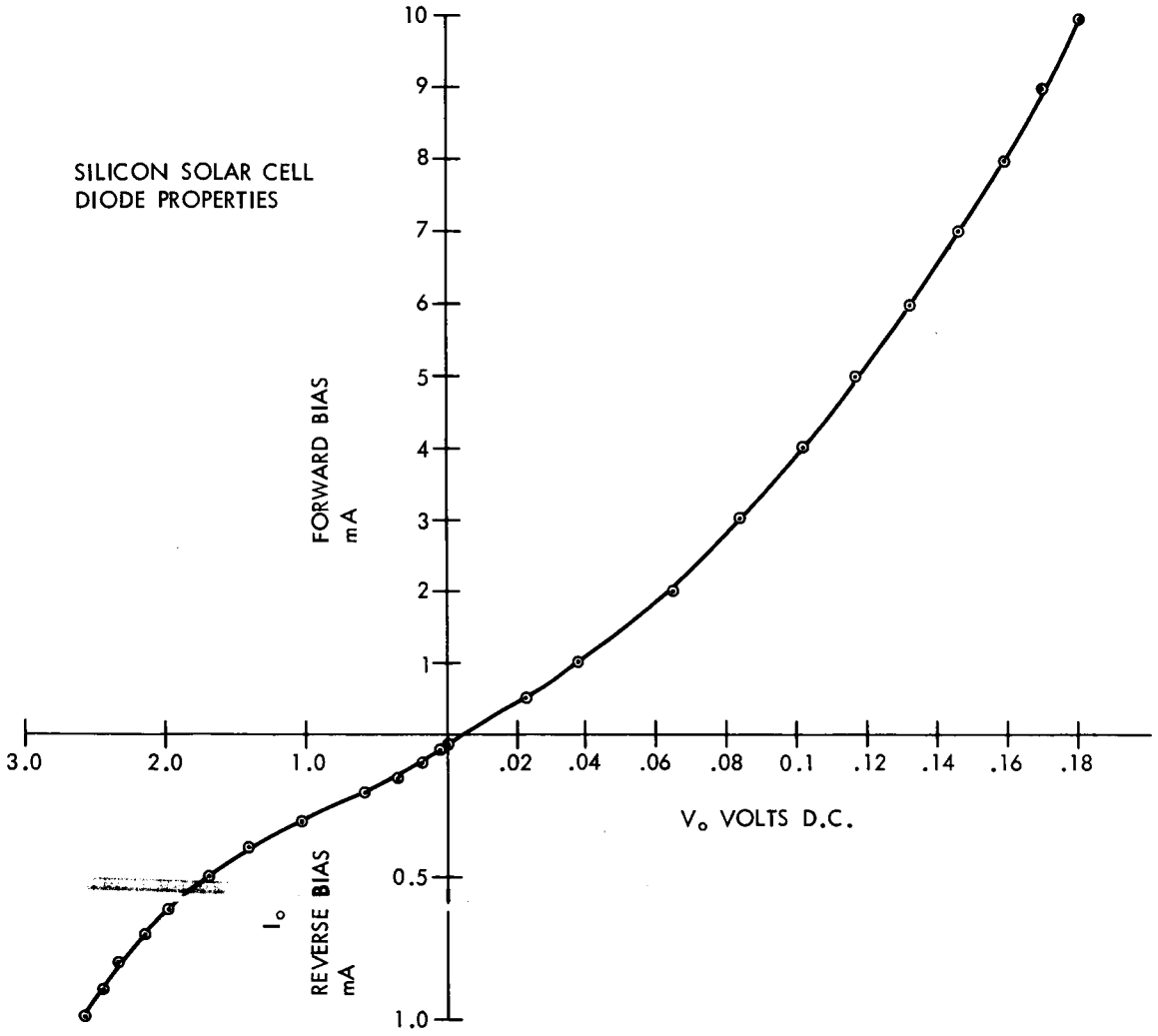

Figure 7 — Silicon Solar Cell Diode Properties

Under true short-circuit conditions the voltage across the junction is a few millivolts and the solar cell acts as a low-impedance current generator. The short-circuit current is proportional to the level of intensity as demonstrated in Figure 8. These measurements were made at monochromatic low injection levels to investigate the possibility of a non-linear spectral response. The cell output is linear over a three decade range. Linearity with a xenon source is shown in Figure 9.

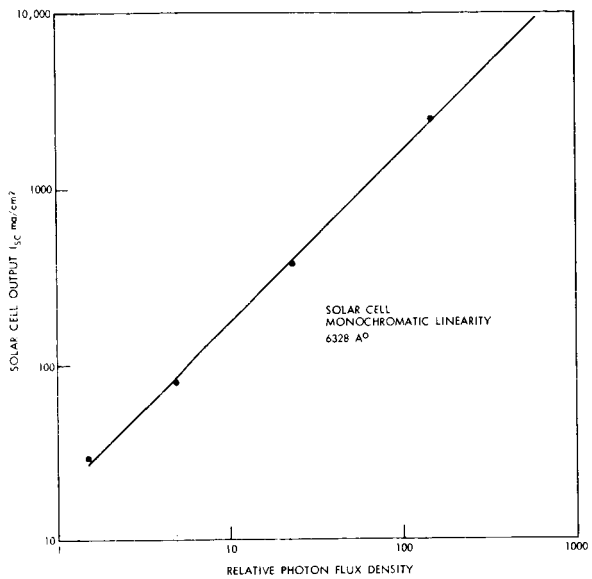

Figure 8 — Solar Cell Linearity with a Monochromatic Source

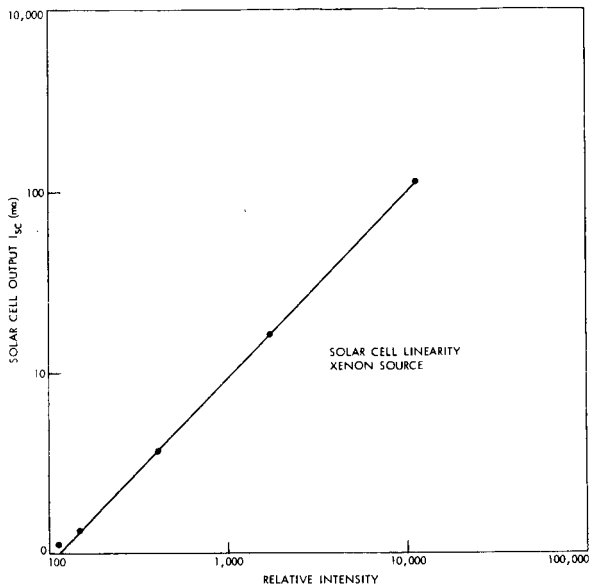

Figure 9 — Solar Cell I_{sc} Linearity with a Xenon Source

(C) Temperature Dependence of the Solar Cell Current and Voltage

The operating characteristics of the solar cell are sensitive to any change in temperature conditions and constant temperature operating conditions are required for repeatable measurements. The temperature dependence of the photovoltaic voltage of a silicon 10-ohm-cm cell is shown in Figure 10. Linearity in the temperature dependence is definite over a $|200°C|$ range and the coefficient for this particular cell is 2.3 mv/°C. The open-circuit voltage approaches the theoretical bandgap value of 1.18 volts at the low temperatures.

The monochromatic short circuit current is also temperature dependent and this dependence shown in Figure 11 presents several interesting observations. For this particular solar cell the temperature coefficient is .89μ A/°C and remains independent of wavelength from 6000A° to 10,000A° which isn't

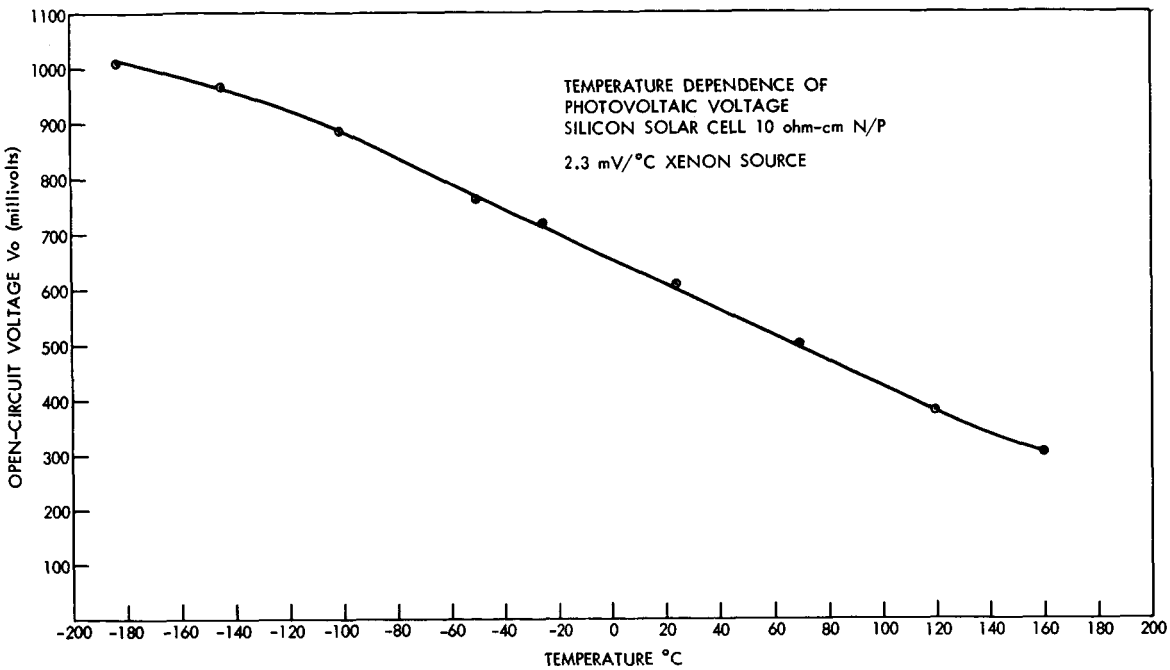

Figure 10 — Temperature Dependence of the Photovoltaic Voltage

to be expected. As seen in Figure 12 it takes 130 microns of silicon to absorb all of the energy at 10,000A° while only 10 microns will absorb energy at 6000A° This means that the effective "diffusion length" of the free carriers generated with 10,000A° energy is at least 10 times larger than the free carriers created by the 6000A° energy. Since the degradation of the monochromatic short-circuit current within this temperature range is independent of wavelength, this implies that the effective diffusion length has not degraded as a result of the increased temperature and the decrease in monochromatic current output is a direct result of the change in collection efficiency at the junction region.

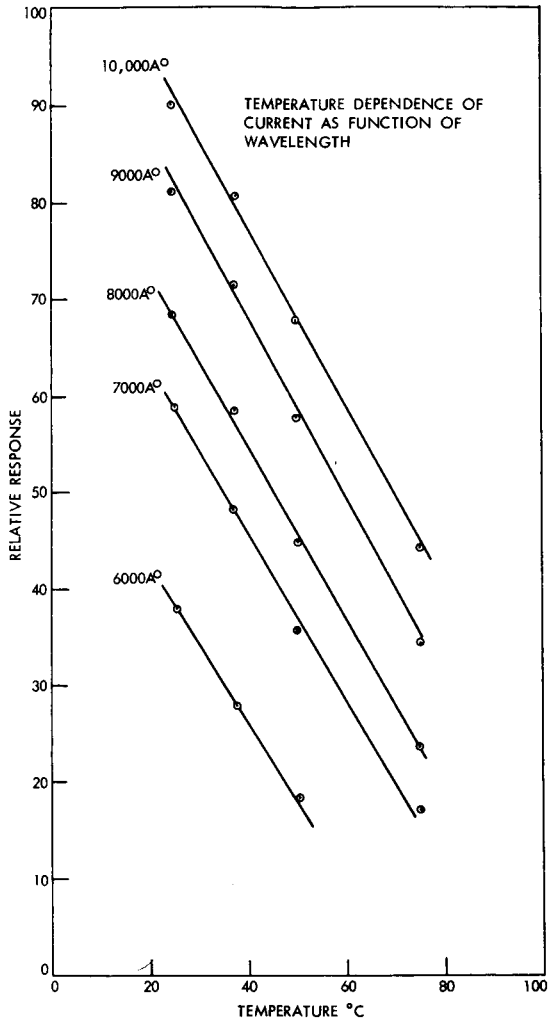

Figure 11 — Temperature Dependence of Monochromatic Current

III INSTRUMENTATION FOR QUANTUM YIELD MEASUREMENTS

In order to have the capabilities of high resolution with a maximum transmission efficiency, a grating monochromator was selected as the basic unit for the spectral response and quantum yield measurements; the monochromator shown in Figure 13 is a 1 meter Czerny-Turner model made by McPherson

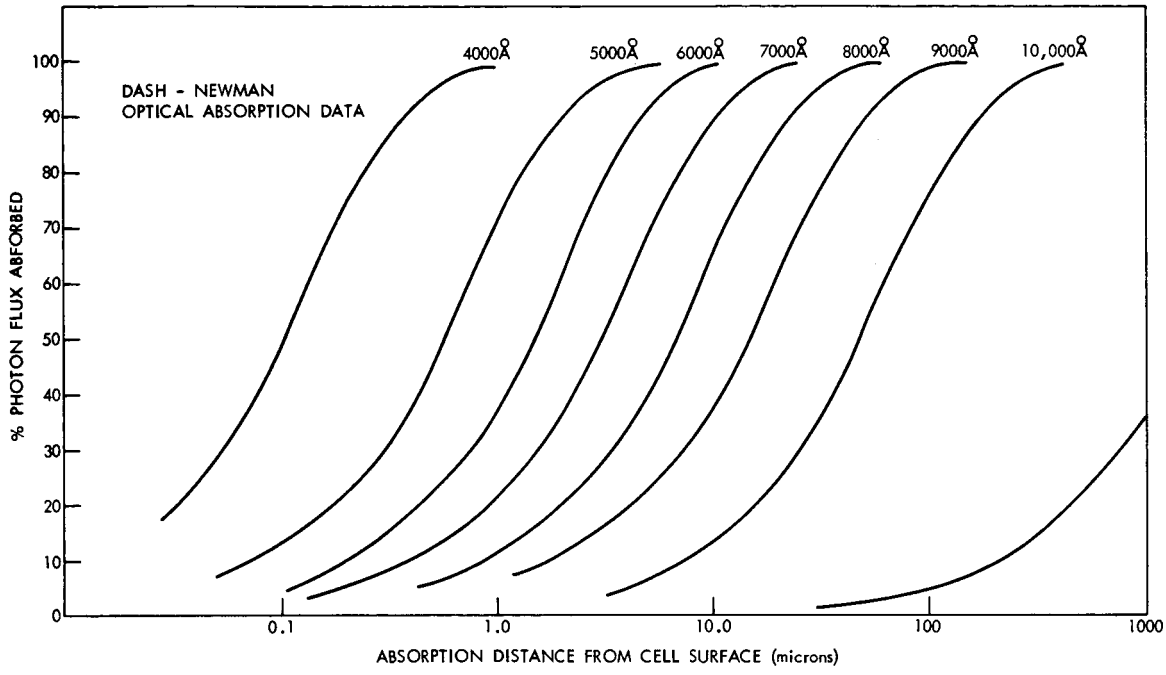

Figure 12 — Photon Absorption in Silicon Solar Cell

Instruments. The instrument uses a 10 cm x 10 cm B&L grating blazed at 5000A° with [illegible] giving a maximum resolution of 0.3A°. The monochromator is capable of being scanned from 1800A° to 26,000A° with scanning rates varying from 0.5A° to 2000A° per minute.

A detector housing assembly located at the exit slit contains a beam-splitting, oscillating, reflecting-wedge which alternately applies the monochromatic beam at a 6.66 cps rate from the detector to be calibrated to a calibrated thermopile. When solar cells are calibrated the cell output channel is referenced to a calibrated thermocouple; a ratio of the two signal levels is derived by an automatic gain control method and a relative spectral response, equal energy, is obtained. This response is plotted on an x-y recorder as a function of wavelength; the wavelength, x-base, is derived from a pot on the wavelength shaft of

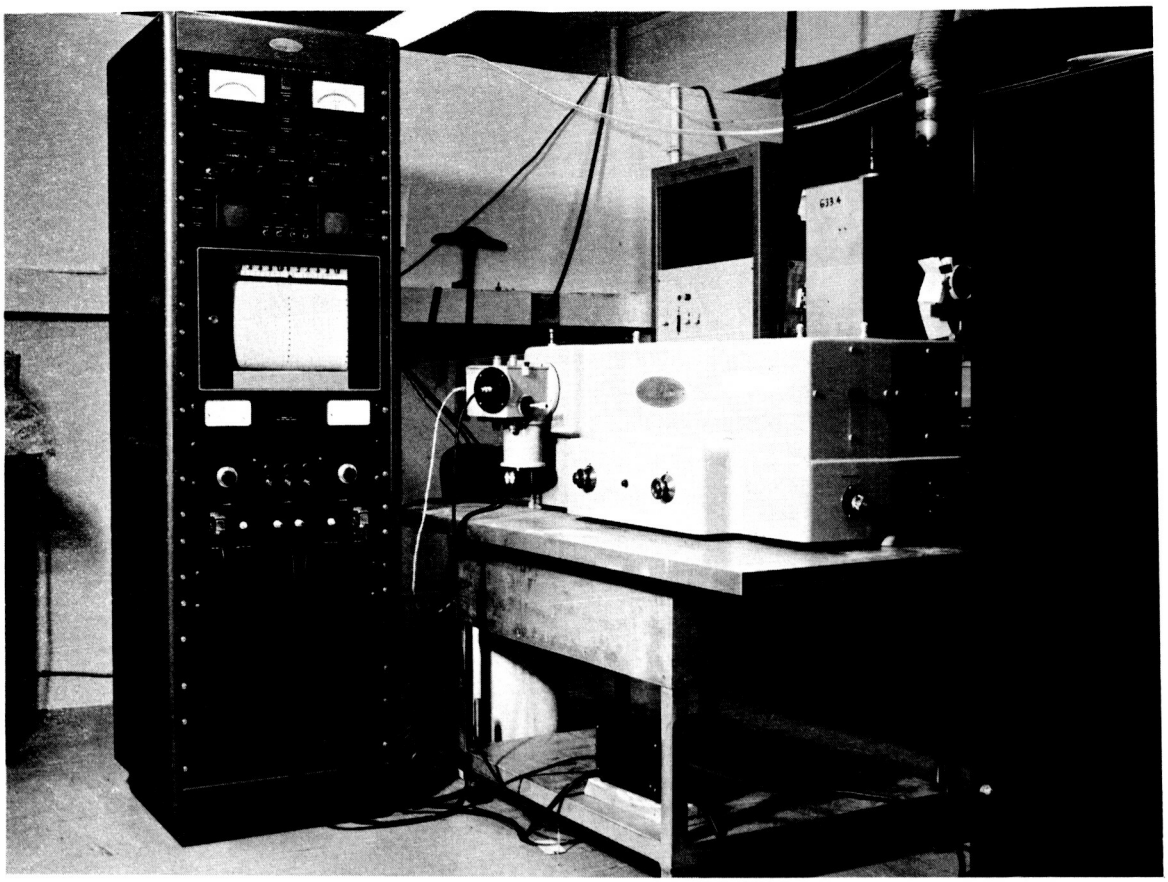

Figure 13 — McPherson Grating Monochromator

the monochromator. During the measurement procedure it was found that surface reflectance properties, which have to be made separately, could be done at the same time the quantum yield is being measured. A reflectance assembly, composed of a revised beam-splitting arrangement and a Gier-Dunkle integrating sphere will measure surface reflectance losses. The photon flux density incident on the cell surface can then be corrected for the surface reflectance losses and this will enable an absolute quantum yield measurement to be made.

The three low-level outputs, solar cell or detector, reference thermopile, and the thermopile measuring the surface reflectance energy will be stored on a magnetic tape recorder along with wavelength information derived from a shaft encoder on the grating monochromator. All ratioing and scaling required will be programmed for computer calculations. A general layout of the spectral response calibration system is shown in Figure 14.

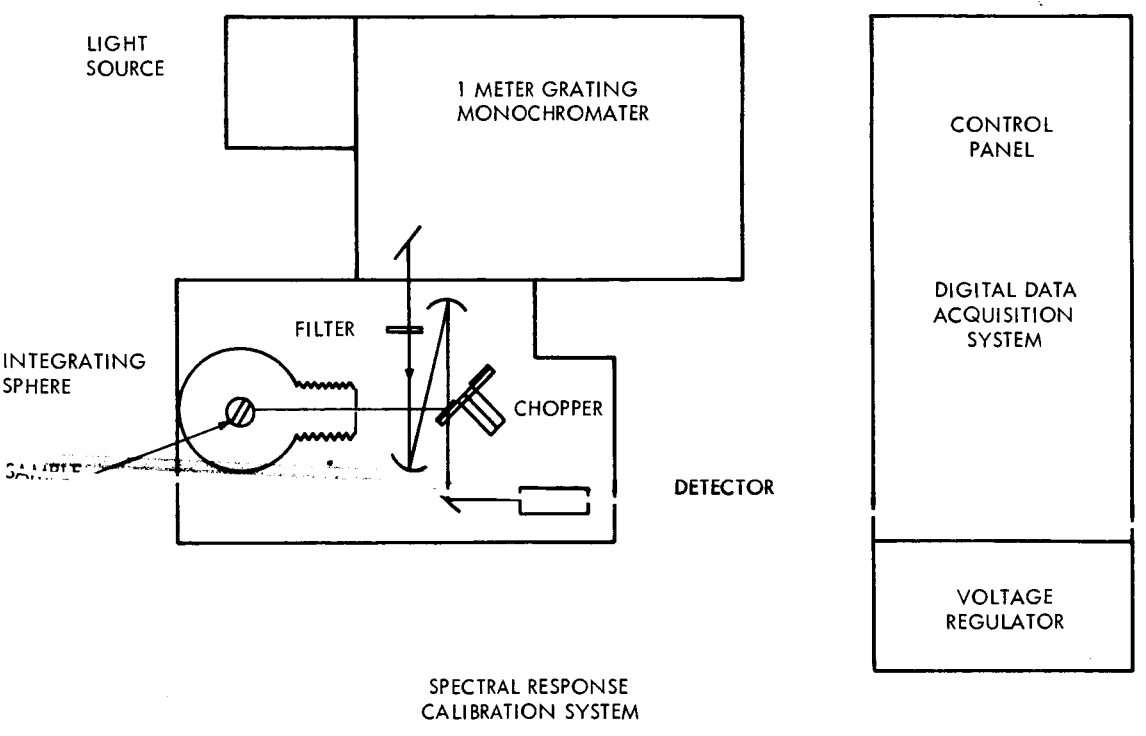

Figure 14 — Spectral Response Calibration System

IV SUMMARY

Solar cells are widely used as detectors for measuring and monitoring the performance features of solar simulations. The simplicity in measuring the output and general ruggedness are attractive features; however for quantitative analysis, the narrow range of the response region, 3800A° to 11,000A° and the temperature dependence of the operating characteristics dictate judicious care in data interpretation.